

**The function of *Tbx2* and *Tbx3* in regulation
of morphogenesis and sensory cell differentiation
in the murine inner ear**

Von der Naturwissenschaftlichen Fakultät
der Gottfried Wilhelm Leibniz Universität Hannover

zur Erlangung des Grades
Doktorin der Naturwissenschaften (Dr. rer. nat.)

genehmigte Dissertation

von

Marina Kaiser, M.Sc.

2022

Referent: Prof. Dr. rer. nat. Andreas Kispert
Korreferentin: Prof. Dr. rer. nat. Doris Steinemann
Korreferent: Prof. Dr. rer. nat. Hans Gerd Nothwang
Tag der Promotion: 25.11.2021



Angefertigt am
Institut für Molekularbiologie
der Medizinischen Hochschule Hannover
unter der Betreuung von
Prof. Dr. rer. nat. Andreas Kispert

Meiner Mama

The following publication and manuscript contributed to this thesis:

1. **Kaiser, M.**, Wojahn, I., Rudat, C., Lüdtke, T. H., Christoffels, V. M., Moon, A., Kispert, A. and Trowe, M.-O. (2021). Regulation of otocyst patterning by *Tbx2* and *Tbx3* is required for inner ear morphogenesis in the mouse. *Development* 148.
<https://doi.org/10.1242/dev.195651>

2. **Kaiser, M.**, Lüdtke, T. H., Christoffels, V. M., Kispert, A. and Trowe, M.-O. TBX2 specifies and maintains inner hair and supporting cell fate in the Organ of Corti.
Under review in *Nature*

Abstract

The mammalian inner ear is an asymmetric sensory organ that consists of the dorsal vestibular organ (sense of balance) and the ventral cochlea (acoustic sense). Clusters of mechanosensitive hair cells convert mechanical stimuli into electrical impulses and transmit them to the brain by sensory neurons of the vestibular and cochlear ganglia. The sensory epithelium of the cochlea, the organ of Corti, contains sound-receiving inner hair cells (IHCs) and sound-amplifying outer hair cells (OHCs).

All epithelial and neuronal components of the inner ear derive from the otic placode which forms a simple sphere (otocyst) upon invagination. Morphogenesis of the otocysts into a complex 3-dimensional labyrinth, and the precise spatial and temporal differentiation of neurosensory cells is controlled by a complex interplay of dynamic signalling and regionalized transcription factor activities.

The aim of this thesis was the characterization of the cellular and molecular functions of the two T-box transcription factor genes *Tbx2* and *Tbx3* in the early morphogenesis of the otocyst and in the development of the organ of Corti.

Analysis of conditional loss-of-function mutants demonstrated that *Tbx2* and *Tbx3* are individually and combinatorially required for the morphogenesis of the vestibular and cochlear components of the inner ear by patterning the early otocyst. TBX2 restricts the neurogenic domain to the anterior-ventral aspect of the otic epithelium by repressing *Fgf8* and maintaining *Tbx1* expression in the posterior-ventral otocyst.

Conditional inactivation of *Tbx2* in prosensory cells prior to the onset of differentiation, caused a complete conversion of IHCs to OHCs, whereas *Tbx2* misexpression led to an increased number of IHCs at the expense of OHCs. Similar changes were observed in the underlying supporting cells. Transcriptional profiling and RNA *in situ* hybridization analyses suggest that TBX2 regulates the specification of inner hair and supporting cells by repressing *Fgfr3*-mediated signalling. Hair cell-specific inactivation or misexpression of *Tbx2* shortly after birth caused a cell-autonomous transdifferentiation of hair cells.

The results of this thesis provide new insights into the cellular and molecular control of otic neurogenesis and sensory cell diversification identifying TBX2 as a crucial regulator of these processes. This insight might be useful for future regenerative efforts concerning hair cell loss in human patients.

Keyword: *Tbx2*, *Tbx3*, inner ear, morphogenesis, neurogenesis, hair cell diversification

Zusammenfassung

Das Innenohr der Säugetiere besteht aus dem dorsalen Vestibularorgan (Gleichgewichtssinn) und der ventralen Cochlea (Hörsinn). Gruppen von mechanosensitiven Haarzellen wandeln in beiden Teilorganen mechanische Reize in elektrische Impulse um und leiten diese über die Neurone des cochleären und vestibulären Ganglions an das Gehirn weiter. Das sensorische Epithel der Cochlea, das Corti-Organ, enthält Ton-empfangende innere Haarzellen und Ton-verstärkende äußere Haarzellen.

Alle epithelialen und neuronalen Komponenten des Innenohrs stammen von einer otischen Plakode ab, aus der sich durch Einstülpung eine einfache Sphäre (Otozyste) bildet. Die Umwandlung der Otozyste in ein komplexes 3-dimensionales Labyrinth und die präzise räumliche und zeitliche Differenzierung der neurosensorischen Zellen wird durch ein Zusammenspiel aus dynamischen und regional-beschränkten Aktivitäten von Signal- und Transkriptionsfaktoren kontrolliert.

Das Ziel dieser Arbeit war die Charakterisierung der zellulären und molekularen Funktionen der T-Box Transkriptionsfaktorgene *Tbx2* und *Tbx3* in der frühen Morphogenese der Otozyste und in der Entwicklung des Corti-Organs.

Die Analyse konditioneller Verlustmutanten zeigte, dass *Tbx2* und *Tbx3*, sowohl einzeln als auch zusammen, für die Morphogenese der vestibulären und cochleären Anteile des Innenohrs benötigt werden, indem sie die Musterung der frühen Otozyste beeinflussen. TBX2 beschränkt die neurogene Domäne auf die anterior-ventrale Otozyste, indem es die posterior-ventrale Expression von *Fgf8* hemmt und die von *Tbx1* aufrechterhält.

Die konditionelle Inaktivierung von *Tbx2* in prosensorischen Zellen, vor dem Beginn der Differenzierung, führt zu einer kompletten Umwandlung von inneren in äußere Haarzellen, während die Misexpression von *Tbx2* in einer zunehmenden Anzahl von inneren beim gleichzeitigen Verlust von äußeren Haarzellen resultierte. Ähnliche Veränderungen konnten in den darunterliegenden Stützzellen beobachtet werden. Expressionsanalysen deuten darauf hin, dass TBX2 die Spezifizierung der inneren Haar- und Stützzellen reguliert, indem es die *Fgfr3*-vermittelte Signalaktivität hemmt. Die Haarzell-spezifische Inaktivierung oder Misexpression von *Tbx2*, kurz nach der Geburt, führt zu einer zellautonomen Transdifferenzierung von Haarzellen.

Die Ergebnisse dieser Arbeit geben neue Einblicke in die zelluläre und molekulare Kontrolle der otischen Neurogenese und der Diversifizierung sensorischer Zellen, indem es TBX2 als einen zentralen Regulator dieser Prozesse identifiziert. Diese Einblicke könnten für zukünftige regenerative Therapien bei Haarzellverlust in Patienten relevant sein.

Schlagwörter: *Tbx2*, *Tbx3*, Innenohr, Morphogenese, Neurogenese, Diversifizierung der Haarzellen

Contents

ABSTRACT	IV
ZUSAMMENFASSUNG	V
CONTENTS	VI
INTRODUCTION	1
ANATOMY AND FUNCTION OF THE INNER EAR	1
THE VESTIBULAR ORGAN IS RESPONSIBLE FOR THE SENSE OF BALANCE	2
THE COCHLEAR DUCT AND DETECTION OF SOUND	3
PATTERNING AND MORPHOGENESIS OF THE INNER EAR	4
EXTRINSIC SIGNALS ESTABLISH THE AXIAL PATTERNING OF THE DEVELOPING OTOCYST	5
PROGRESSION OF INNER EAR MORPHOGENESIS	7
GENETIC REGULATION OF INNER EAR MORPHOGENESIS	8
REGULATION OF CELL FATE DECISIONS IN INNER EAR DEVELOPMENT	9
PROGRESSION AND REGULATION OF OTIC NEUROGENESIS	9
DIFFERENTIATION OF HAIR AND SUPPORTING CELLS IN THE ORGAN OF CORTI	10
REGULATION OF HAIR AND SUPPORTING CELL DIVERSIFICATION IN THE ORGAN OF CORTI	11
THE FUNCTION OF <i>Tbx2</i> AND <i>Tbx3</i> IN EMBRYONIC DEVELOPMENT AND DISEASE	12
AIMS OF THE THESIS	14
PART 1 – <i>Tbx2</i> AND <i>Tbx3</i> IN PATTERNING OF THE OTOCYST	16
REGULATION OF OTOCYST PATTERNING BY <i>Tbx2</i> AND <i>Tbx3</i> IS REQUIRED FOR INNER EAR MORPHOGENESIS IN THE MOUSE	16
PART 2 – <i>Tbx2</i> IN HAIR AND SUPPORTING CELL DIFFERENTIATION	47
TBX2 SPECIFIES AND MAINTAINS INNER HAIR AND SUPPORTING CELL FATE IN THE ORGAN OF CORTI	47

CONCLUDING REMARKS AND FUTURE PERSPECTIVES	68
NEW INSIGHTS INTO THE REGULATORY NETWORK PROMOTING OTIC NEUROGENESIS	68
<i>Tbx2</i> IS A CRUCIAL REGULATOR OF INNER HAIR AND SUPPORTING CELL IDENTITY	69
THE THERAPEUTIC POTENTIAL OF <i>TBX2</i>	71
REFERENCES	72
ACKNOWLEDGEMENT	78
APPENDIX	79
CURRICULUM VITAE	79
LIST OF PUBLICATIONS	80

Introduction

Hearing plays an essential role in linguistic and cognitive development, verbal communication, education and social integration. Therefore, hearing impairment often leads to social isolation. Moreover, hearing loss is associated with increased risk of dementia, thus affecting human health in an even broader context¹.

According to the World Health Organization (WHO), hearing impairment affects over 5% of the world's population and this number is estimated to almost double by 2050². This deficit is mainly caused by the degeneration of sensory hair cells and/or their innervating neurons due to hereditary defects, aging or environmental factors such as exposure to loud noises, viral infections, ototoxic drugs and traumas^{3–6}. Since mature mammalian hair cells and neurons cannot be regenerated their progressive loss leads to deafness^{7,8}.

So far, the options for treatment of acoustic deficits are limited to electronic devices, such as hearing aids and cochlear implants. Although these devices are beneficial, they are not suitable for each and every patient and are less efficient under noisy conditions. Moreover, they do not address the origin of the sensory deficit and cannot restore normal hearing^{9,10}. Therefore, alternative treatment strategies are required such as cell-based therapies, or gene- or drug-induced tissue regeneration. However, these therapeutic approaches demand detailed knowledge about the regulators of cell fate decisions in the development of the inner ear.

Anatomy and function of the inner ear

The inner ear is a sensory organ that consists of interconnected fluid-filled ducts and chambers that together form a membranous labyrinth (Fig. 1A). It is enclosed by the hardest bone in the human body, the temporal bone, emphasizing the importance of this sensory organ. The inner ear is a mediator of two distinct sensory perceptions and therefore can be subdivided into two functionally different subunits: the ventral cochlea and the dorsal vestibular organ. Herein, specialized epithelial domains (neuroepithelia or sensory end organs) comprised of mechano-sensitive hair cells and underlying supporting cells mediate the two senses. The apical surface of hair cells harbours “hair-like” stereocilia embedded into gelatinous membranes. Specific stimuli induce the deflection of stereocilia and the subsequent release of excitatory neurotransmitters at the basal side of the sensory cells. This in turn leads to excitation of afferent bipolar neurons of the VIIIth cranial nerve and subsequent processing of these neuronal signals by the brain.

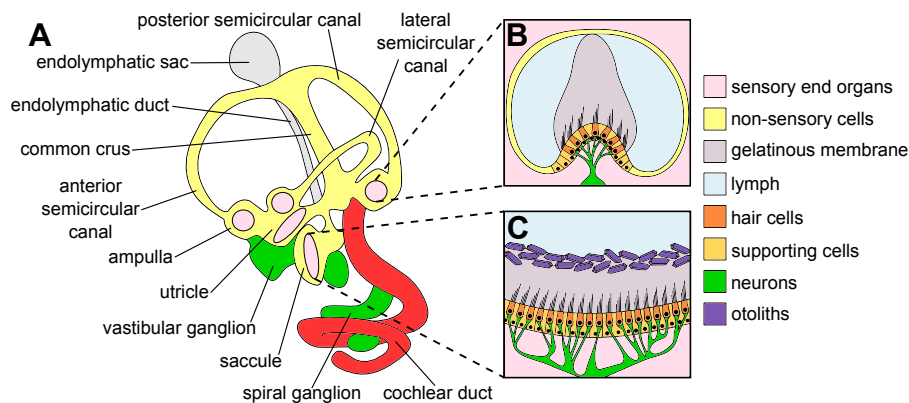


Fig. 1. Scheme of the membranous inner ear labyrinth and the sensory epithelia of the vestibular organ in mice. A, The murine inner ear consists of the dorsal vestibular organ (yellow) and the ventral cochlear duct (red). B, *Crista ampullaris* is the

sensory end organ of a semicircular canal. It consists of hair cells and intercalated supporting cells. Hair cell stereocilia and kinocilia are embedded into the gelatinous capula which spans the lumen of the ampulla. C, *Macula sacculi* is the sensory end organ of the saccule. Stereocilia and kinocilia of macular hair cells are embedded into a gelatinous membrane covered with otoliths (calcium carbonate crystals).

The vestibular organ is responsible for the sense of balance

The utricle (*utriculus*), one of the two vestibular sacs, is the central part of the vestibular labyrinth from which the three semicircular canals and the endolymphatic duct arise. The semicircular canals are arranged perpendicularly to each other and are dilated at one end forming the ampulla. The fusion area of the two vertical semicircular canals (anterior and posterior) forms the common crus (*crus commune*) while the lateral canal remains separated. The saccule (*sacculus*), the second vestibular sac, is joint to the utricle by the utriculosaccular duct (*ductus utriculosaccularis*) and to the base of the cochlear duct by the *ductus reuniens* (Fig. 1A)¹¹.

The sensory end organs of the semicircular canals, the *cristae ampullaris*, reside within the ampullae and consist of vestibular hair and intercalated supporting cells (Fig. 1B). Hair cell stereocilia and one long kinocilium are embedded into the gelatinous capula which spans the lumen of the ampulla. Angular rotation of the head sets the fluid contained within the canals in motion, resulting in the deflection of the capula and the subsequent bending of hair cell stereocilia.

Mechano-sensitive hair cells of the utricle and the saccule reside within the maculae (*macula utriculi* and *macula sacculi*) which are also oriented perpendicularly to each other (Fig. 1C). Here, hair cell stereocilia and kinocilia are embedded into a gelatinous membrane covered with otoliths (calcium carbonate crystals). Horizontal and vertical changes of the body position exert shear forces onto the otolith-membrane leading to the bending of hair cell stereocilia. Therefore, macular hair cells exert the detection of linear acceleration and gravity.

The cochlear duct and detection of sound

The auditory part of the inner ear is a coiled structure, named the cochlea (Fig. 2A). It consists of three distinct compartments: *scala vestibuli*, *scala tympani* and *scala media* (Fig. 2B, C). The first two compartments are filled with the perilymph (similar to extracellular fluid). They merge at the blind ending apex of the cochlea and connect with the middle ear through the oval and the round window, respectively.

The blind-ending, triangular *scala media* (cochlear duct) is located in between these two other scalae and is filled with the endolymph (similar to intracellular fluid) (Fig. 2C). The roof of the cochlear duct is formed by the vestibular membrane (Reissner's membrane) that is adjoined to the *scala vestibuli*. The floor contains the basilar membrane and forms a separation to the *scala tympani*. The lateral wall of the cochlear duct contains the *stria vascularis*, a special epithelium essential for production of the endolymph¹¹.

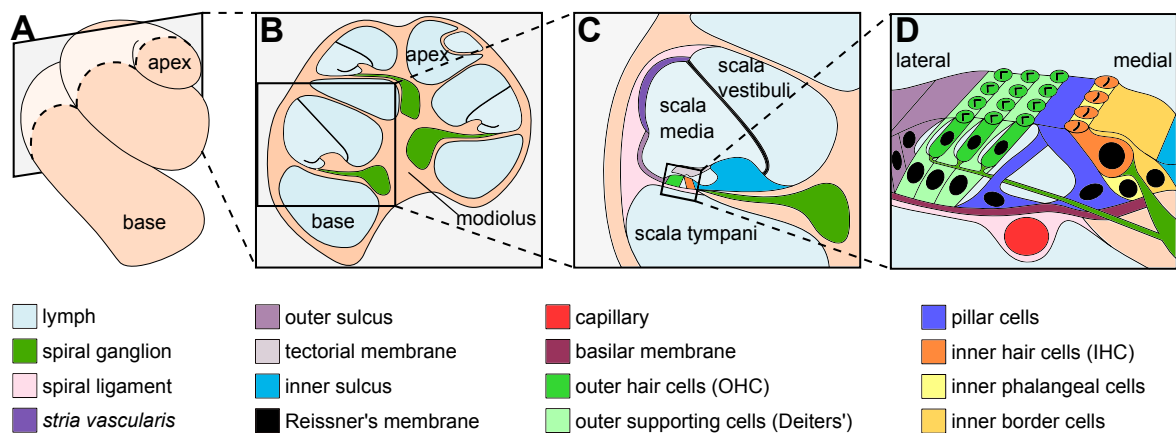


Fig. 2. Graphical depiction of the anatomy of the mature murine cochlea. **A**, The basal part of the cochlea is oriented towards the vestibular organ (base), while the apical part is a blind ending (apex). **B**, Cross-section through the cochlea as indicated in (A). The cochlea coils around the bony modiolus. **C**, The cochlea consists of three different compartments: *scala vestibuli*, *scala media* and *scala tympani*. The *Scala media* (cochlear duct) is a triangular duct which adjoins to the *scala vestibuli* by the Reissner's membrane and to the *scala tympani* by the basilar membrane. The third wall contains the *stria vascularis* which produces the endolymph. **D**, The sensory epithelium of the cochlear duct, the organ of Corti, is laterally flanked by cells of the outer sulcus and medially by cells of the inner sulcus. The organ of Corti consists of two functionally different compartments: 1) outer hair and supporting cells (green), 2) inner hair and supporting cells (orange). In between, mechanically stiff pillar cells form the tunnel of Corti.

The cochlear duct harbours the acoustic neurosensory epithelium, the organ of Corti, which resides on the elastic basilar membrane and is covered by the gelatinous tectorial membrane (Fig. 2C, D). Medially, it is flanked by cells of the inner sulcus, and laterally, by cells of the outer sulcus. The organ of Corti consists of precisely arranged sensory hair cells and various types of underlying sensory cells which are organized in rows, spanning the whole length of

the cochlear duct. Radially, the organ of Corti can be subdivided into two functionally distinct compartments which are separated by the tunnel of Corti that is formed by mechanically stiff pillar cells¹² (Fig. 2D). The inner (medial) sound-receiving compartment contains inner hair cells (IHCs) and inner supporting cells (ISCs) (inner phalangeal cells and inner border cells). The outer (lateral) sound-amplifying compartment consists of outer hair cells (OHCs) and outer supporting cells (OSCs) (Deiters' cells).

Around 95% of afferent neurons are associated with the bigger, flask-shaped IHCs, the primary transducers of the acoustic information. Sound-induced vibrations of the basilar membrane lead to the deflection of IHC stereocilia and subsequent excitement of auditory neurons that transmit sound information to the brain. The cylindrically shaped OHCs are signal amplifiers. In response to the bending of their stereocilia through shearing forces a motor protein (prestin) is activated in the lateral membrane of OHCs leading to changes of the cell length, a process known as somatic electromotility¹³. OHC motility is required for modulation of sound-induced vibration of the basilar membrane and improvement of acoustic sensibility.

In addition to radial patterning, hair cell morphology and physiology, especially that of OHCs, is adapted to the perception of different frequencies and therefore varies along the tonotopic (base-to-apex) axis of the cochlear duct. Shorter hair cells at the base are specialized in the detection of high frequencies, whereas longer and more flexible hair cells at the apex perceive lower frequencies¹⁴.

Patterning and morphogenesis of the inner ear

The inner ear derives from the otic placode, a thickening of the surface ectoderm adjacent to the hindbrain at the level of rhombomeres 5 and 6. In mice, it emerges at embryonic day (E) 8.5, invaginates into the underlying mesenchyme and forms a fluid-filled sphere (otocyst) by E9.5^{15–17}. The subsequent transformation of a simple sphere into a complex asymmetric labyrinth depends on a series of spatially and temporarily restricted morphogenetic events such as proliferation, apoptosis and epithelial remodelling^{18–24}. Thereby, the establishment of regional identity in the developing otocyst is controlled by a refined network of signalling molecules produced by surrounding tissues, such as ectoderm, mesoderm, neural tube and notochord^{25–33}. This extrinsic information is translated into asymmetric gene expression within the otic epithelium that progressively establishes axial polarisation and determination of lineage-restricted compartments in the developing otocyst.

Extrinsic signals establish the axial patterning of the developing otocyst

From the timepoint of otic placode induction, the otic epithelium receives patterning information from surrounding tissues resulting in axial polarization of the otocyst. Retinoic acid (RA) signalling plays a major role in the establishment of the anterior-posterior (A/P) polarity (Fig. 3A). At E8.5, the paraxial mesoderm provides the source of RA at the level of rhombomeres 5 and 6 through expression of the RA synthesizing enzyme *ALDH1A2*^{25,34}. It is counteracted by the RA degrading enzyme *CYP26C1* which is expressed in the ectoderm anterior to the invaginating otic placode, thereby restricting RA signalling to the posterior otic epithelium. Transient activity of RA signalling is required and sufficient to induce *Tbx1* expression in the posterior half of the invaginating placode which mainly gives rise to the non-sensory components of the inner ear^{25,35,36}. The anterior aspect (*Lfng*, *Fgf10*, *Neurog1*, *Neurod1*) contains neuronal and sensory precursors demonstrating that the A/P polarization of the developing otocyst is strongly associated with the neurosensory development^{36–43}.

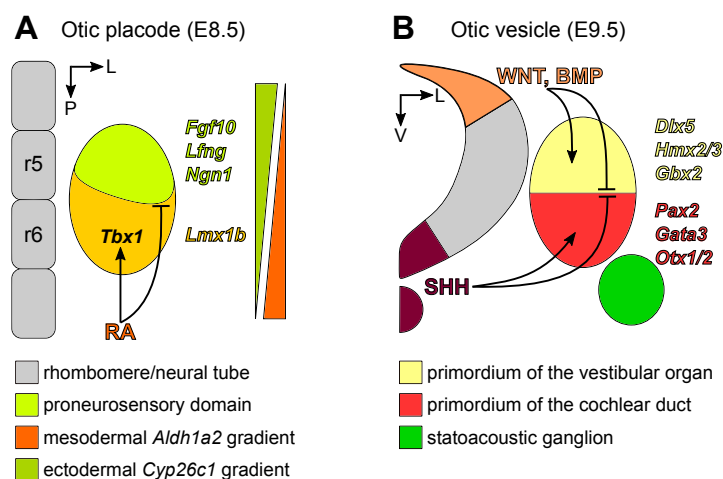


Fig. 3. Anterior-posterior and dorso-ventral patterning of the otic epithelium in chicken and mice. A, Specification of the anterior-posterior axis through retinoic acid (RA) signalling. Mesoderm-derived RA signalling is restricted to the posterior half of the otic placode by an opposing gradient of *Cyp26c1* expressed in the anterior ectoderm. RA induces *Tbx1* expression in the posterior otic placode,

while the anterior domain is marked by expression of proneurosensory genes. **B,** Signals from the neural tube and the notochord regulate the dorso-ventral polarization of the otocyst. WNTs and BMPs from the dorsal neural tube induce the expression of genes in the dorsal otocyst which gives rise to the vestibular structures. SHH secreted by the floor plate of the neural tube and the underlying notochord promotes the expression of genes in the ventral otocyst mediating cochlear morphogenesis. L, lateral; P, posterior; r, rhombomere; V, ventral.

Polarisation of the developing otocyst along the dorso-ventral (D/V) axis is the driving force for the development of dorsal vestibular and ventral cochlear structures. The dorsal half of the otocyst is marked by *Dlx5*, *Gbx2*, *Hmx2/3* and *Wnt2b* expression, while the ventral otocyst displays the expression of *Pax2*, *Otx1/2*, *Gata3* and *Gli1* (Fig. 3B). Rotation and tissue ablation experiments in chicken embryos and analysis of several mouse mutants

demonstrated that signals from the neural tube and the notochord are the major inducers of D/V polarity^{26–33}.

The ventral half of the otocyst responds to sonic hedgehog (SHH) secreted by the floor plate of the neural tube and the underlying notochord^{44–47}. Expression of ventral genes such as *Pax2*, *Otx2*, *Gata3* is lost, while the dorsal *Dlx5* expression is ventrally expanded in *Shh*-deficient otocysts^{32,47}. In contrast, ectopic expression of *Shh* (*ShhP1*) in the dorsal otocyst leads to complete absence of vestibular structures, dorsal expansion of *Pax2* and downregulation of *Dlx5* expression^{31,32}. Hence, SHH signalling is required and sufficient to induce ventral identity in the developing otocyst.

The effect of SHH signalling is opposed by WNT ligands secreted by the dorsal neural tube³¹. Double-inactivation of *Wnt1* and *Wnt3a* in the dorsal neural tube or mechanical removal of this tissue compartment leads to a complete loss of dorsal *Dlx5* and dorso-medial *Gbx2* expression while ventrally expressed *Gli1* and *Pax2* are expanded into the dorsal otocyst. In contrast, forced activation of WNT signalling by LiCl leads to ventral expansion of *Dlx5* and *Gbx2* expression demonstrating that WNT signalling induces dorsal otic fate.

Since dorso-lateral *Hmx3* expression was unchanged upon manipulation of WNT signalling an additional factor must be involved in regulation of dorsal identity in the developing otocyst³¹. Bone morphogenic proteins (BMPs) are secreted by the dorsal neural tube while *Bmp4* is expressed in the dorsal surface ectoderm and in the dorsal otocyst^{37,48,49}. Inactivation of BMP4 signalling results in disturbed formation of vestibular structures in mice and chicken^{50,51}. Overexpression of *Noggin*, a BMP antagonist, in the head mesenchyme adjacent to the chick otocyst or conditional deletion of *Bmp4* in murine otocysts results in loss of *Dlx5* and *Hmx3* expression in the dorso-lateral but not in the dorso-medial otic epithelium whereas ventro-lateral *Otx2* expression is expanded dorsally^{50,52}. In contrast, *Dlx5* and *Hmx3* are expanded ventrally, while *Otx2* expression is lost upon overexpression of *Bmp4*. Therefore, WNT and BMP signalling promote dorso-medial and dorso-lateral identity in the developing otocyst, respectively.

Another signalling pathway implicated in D/V patterning of the otocyst is fibroblast growth factor (FGF) signalling⁵³. The most promising candidates *Fgf3* and *Fgf10* are expressed in the neural tube and the ventral otocyst while their receptor *Fgfr2* is expressed in the dorsal otic epithelium^{53–56}. Inner ears of *Fgf3*- and *Fgfr2*-null mutants consist only of cystic cavities and chambers while loss of *Fgf10* leads to malformation of semicircular canals^{53,55,57,58}. Extrinsic and intrinsic expression of FGF ligands makes it difficult to discriminate between the different functions of FGF signalling in inner ear development. However, analysis of

kreisler mutants, which are characterized by molecular defects in the rhombomeres 3-7, displayed a specific loss of *Fgf3* expression in the neural tube but not in the otocyst^{28,59}. McKay et al. proposed that *Fgf3* deficiency is the main cause of inner ear defects in *kreisler* mutants²⁸. Expression analysis revealed a patterning defect in the otic epithelium of these mutants: *Fgf3* expression is shifted from the ventro-lateral to the ventro-medial domain of the otocyst, dorso-medial *Gbx2* and *Wnt2b* expression is lost, the ventro-lateral expression of *Otx2* is expanded medially while *Dlx5* expression is unchanged^{28,60}. Recently, it was shown that double-inactivation of *Fgf3* and *Fgf10* in the otic epithelium has no effect on *Gbx2* expression but disturbs inner ear morphogenesis⁵⁶. Together these results argue for a function of extrinsic FGFs in medial-lateral (M/L) patterning of the otocyst and of intrinsic FGFs in regulation of morphogenesis.

As a result of axial polarization spatially restricted gene expression promotes the morphogenetic development at confined sites of the otocyst.

Progression of inner ear morphogenesis

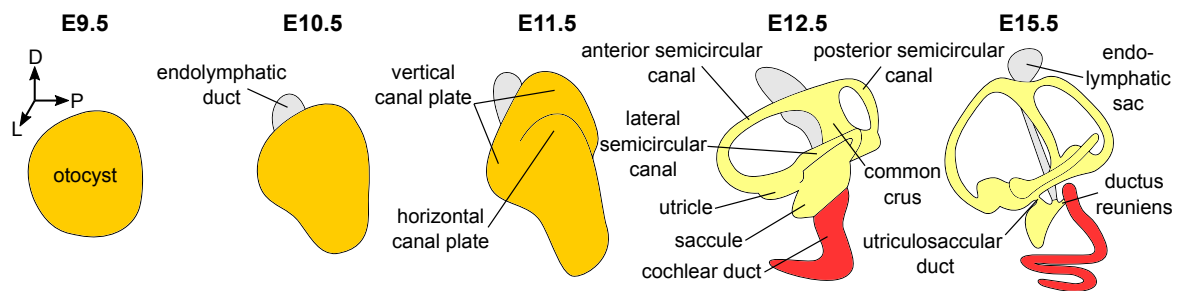


Figure 4. Graphical depiction of inner ear morphogenesis from a simple otocyst to an asymmetrical labyrinth in mice. Shown are the morphological changes between embryonic day (E) 9.5 and E15.5. In the course of morphogenesis, the dorsal aspect of the otocyst (orange) transforms into the vestibular organ (yellow) while its ventral part gives rise to the cochlear duct (red). For better visualisation the respective schemes are not depicted at the right scale. D, dorsal; L, lateral; P, posterior.

The main morphological structures of the murine inner ear are formed within a short period of time, between E10.5 and E13.5³⁷. The following morphogenetic changes mainly include further growth and refinement of the membranous labyrinth (Fig. 4).

The first morphological event is represented by the evagination of the endolymphatic duct from the dorso-medial aspect of the otocyst starting at E10.5. Thereafter, the endolymphatic duct elongates dorsally and forms the endolymphatic sac at its distal end.

Morphogenetic development of the semicircular canals begins around E11.5 with the evagination of two epithelial outpocketings: the vertical and horizontal canal plates. The opposing epithelial layers in central regions of these plates converge, intercalate and form

transient structures also known as fusion plates (two in the vertical and one in the horizontal canal plate)^{37,61}. Removal of fusion plate cells occurs through apoptosis in chicken and through recruitment into the forming tubular canals in mice^{21,62}. Through these remodelling processes, the vertical canal plate gives rise to the anterior and posterior semicircular canals as well as the connecting common crus, while the horizontal canal plate develops into the lateral semicircular canal³⁷.

At E11.5, the posterior-ventro-medial aspect of the otocyst evaginates, elongates and curves anterior-medially forming a hook-like structure. Further elongation and posterior-lateral coiling gives rise to the cochlear duct. Elongation of the cochlear duct is mainly mediated by epithelial remodelling also known as convergent extension^{63–65}. Around E17.5, the cochlear duct reaches its final 1.75 turns in mice³⁷.

Utricle and saccule appear ventrally from the developing semicircular canals around E12.5. The saccule presents as an expansion of the cochlear duct at this stage. At E15.5, utricle and saccule become clearly separated by the utriculosaccular duct, and saccule and the cochlear duct by the *ductus reuniens*.

Genetic regulation of inner ear morphogenesis

The proper progression of inner ear morphogenesis critically depends on precisely confined gene expression⁶⁶. Therefore, the inactivation of just one of the patterning genes might result in severe inner ear malformations.

For example, inactivation of dorsally expressed *Dlx5* results in disturbed semicircular canal formation while the growth of the endolymphatic and cochlear ducts is mainly unaffected^{67,68}. Similar defects can be observed in *Hmx2* and *Hmx3* mutants^{69,70}. These transcription factors are expressed in the dorso-lateral aspect of the otocyst. *Gbx2* is expressed in the dorso-medial otocyst and the membranous labyrinth of mice deficient for this gene is dilated while the endolymphatic duct is completely missing⁷¹. Inactivation of *Fgf10* and *Bmp4* leads to defects in the formation of cristae and their associated semicircular canals^{50,58,72}. *Otx1* and *Otx2* are both expressed in the ventro-lateral aspect of the otocyst. In *Otx1/2*-deficient inner ears the lateral semicircular canal is absent and the cochlear duct is severely shortened⁷³. *Pax2* is expressed mainly in the ventro-medial otic epithelium and its inactivation results in severe hypoplasia of the cochlear duct^{74,75}. Systemic or conditional inactivation of posteriorly expressed *Tbx1* results in cystic inner ears without recognizable vestibular and cochlear structures^{41,76–79}. Similar to *Tbx1*, *Lmx1a* is mainly expressed in the posterior otocyst^{35,40,80}. Inner ears of *Lmx1a* loss-of-function mutants fail to develop the

semicircular canals and the endolymphatic duct, while the cochlear duct is severely shortened^{80,81}.

Regulation of cell fate decisions in inner ear development

The otic placode gives rise to three different cell lineages in the developing inner ear: 1) proneuronal precursors that differentiate into neurons of the statoacoustic ganglion (SAG, the primordium of the cochlear and vestibular ganglia), 2) cells of the pro-sensory lineage that become hair and supporting cells of the sensory end organs, and 3) non-sensory cells which form the ducts and chambers of the inner ear⁸².

Progression and regulation of otic neurogenesis

Early in inner ear development, at around E9.0, the neurogenic domain is established in the ventral aspect of the otocyst and is then rapidly restricted to the anterior-ventral otic epithelium until E10.5^{36,79}. Within this domain a subset of cells commits to the proneural lineage. These neuronal progenitors (neuroblasts) subsequently delaminate from the otic epithelium, migrate into the adjacent periotic mesenchyme and proliferate to expand the pool of neuronal progenitors (Fig. 5A). During the formation of the SAG maturing neuroblasts continue to differentiate, exit the cell cycle and form protrusions/axons to provide innervation of the sensory areas of the developing inner ear.

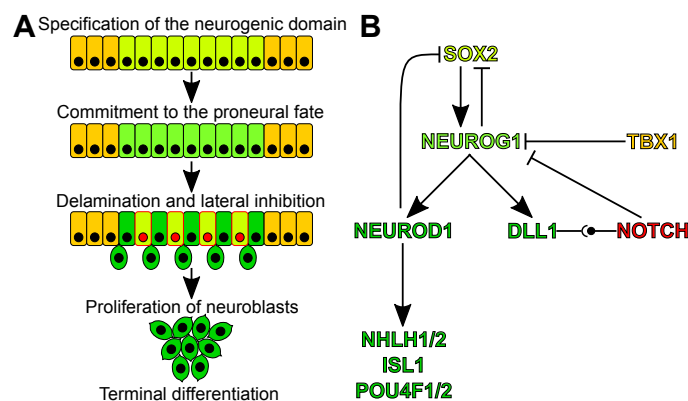


Figure 5. Progression and regulation of otic neurogenesis in mice and chicken. **A**, Scheme showing the main steps of otic neurogenesis. **B**, Depiction of the regulatory network involved in the progression of otic neurogenesis. SOX2 promotes neuronal fate in the otic epithelium (light green) and induces *Neurog1* expression in neuronal precursors (green) within the neurogenic domain. NEUROG1 induces the expression of *Neurod1* to promotes neuroblast differentiation and delamination as well as of *Dll1* to limit the number of neuronal precursors through Notch-mediated lateral inhibition (red). TBX1 restricts the neurogenic domain by repression of proneuronal genes.

NEUROG1 induces the expression of *Neurod1* to promotes neuroblast differentiation and delamination as well as of *Dll1* to limit the number of neuronal precursors through Notch-mediated lateral inhibition (red). TBX1 restricts the neurogenic domain by repression of proneuronal genes.

Otic neurogenesis is regulated by a cascade of transcription factors that promote specific steps in SAG development. SOX2 is required for specification of the neurogenic domain and activates the proneural basic helix-loop-helix (bHLH) transcription factor NEUROGENIN1 (NEUROG1)^{83–86}. Inactivation of *Sox2* leads to a complete loss of NEUROG1-positive

neuroblasts while ectopic expression of *Neurog1* is observed upon misexpression of *Sox2*^{83,87}. NEUROG1 is a potent inducer of the otic neurogenic program that is required and sufficient for the subsequent activation of another bHLH transcription factor gene, namely *Neurod1*^{83,88}. Misexpression of *Sox2* in the chicken otic placode demonstrated that SOX2 has to be downregulated to enable *Neurod1* expression⁸³. This downregulation is mediated by NEUROG1 and later by NEUROD1⁸³. *Neurod1* is required for delamination and survival of otic neuroblasts⁸⁹. Shortly before *Neurod1* expression, NEUROG1 activates *delta-like 1* (*Dll1*) in neuronal precursors⁸⁸. The Notch ligand DLL1 limits the number of neuronal precursors through activation of Notch signalling in neighbouring cells and subsequent downregulation of proneural bHLH genes. This process is known as Notch-dependent lateral inhibition. Accordingly, genetic inactivation of *Dll1* or pharmacological inhibition of Notch signalling results in increased volume of the SAG^{90,91}. In contrast, inactivation of either *Neurog1* or *Neurod1* results in a severe hypoplasia or agenesis of the SAG^{87–89}. Upon delamination, neuroblasts activate the expression of further transcription factor genes such as *Nhlh1/2*, *Isl1* and *Pou4f1*, and terminally differentiate^{88,92,93}.

Restriction of the neurogenic domain to the anterior-ventral aspect of the otocyst is regulated by the T-Box transcription factor TBX1. Inactivation of *Tbx1* results in posterior expansion of the *Neurog1-Dll1-Neurod1* domain and a severely increased size of the SAG^{36,76,78}. In contrast, the expression domain of *Neurog1* as well as *Neurod1* is strongly reduced upon (anterior) misexpression of *TBX1*³⁶.

In addition to neuroblasts, the neurogenic domain gives rise to prosensory cells of the *macula utriculi* and the *macula sacculi*⁹⁴. The sensory domains of the three cristae and the organ of Corti derive from the *Tbx1*-expressing region^{78,95}.

Differentiation of hair and supporting cells in the organ of Corti

The organ of Corti is a highly organized cell mosaic formed by diverse cell types with different anatomical, physiological and molecular features. In general, one can distinguish two types of mechanosensitive hair cells (inner hair cells (IHCs) and outer hair cells (OHCs)) and at least five types of non-sensory supporting cells (Deiters' cells, inner and outer pillar cells, inner phalangeal cells and inner border cells) (Fig. 2D).

Development of these cell types can be subdivided into three main phases: 1) prosensory specification, 2) cell cycle exit and 3) differentiation (Fig. 6A).

Prosensory specification is mediated by the transcription factor SOX2 that is expressed in the floor of the outgrowing cochlear duct^{96,97}. SOX2-positive prosensory progenitors then

express the cell cycle inhibitor *Cdkn1b* (*p27^{kip1}*) in a temporal gradient from the apex towards the base of the cochlear duct from E12.5 until E14.5^{98,99}. Thus, the final number of hair and supporting cells is determined early in embryonic development. Differentiation of postmitotic progenitors occurs in an opposing base-to-apex and medial-to-lateral wave^{100–103}. The hair cell fate is determined by the bHLH transcription factor ATOH1 that regulates hair cell differentiation and survival and represses *Sox2* expression^{96,100,104–107}.

Differentiation of supporting cells is regulated by Notch-mediated lateral inhibition. ATOH1-positive hair cells express the Notch ligands DLL1 and JAGGED2 (JAG2) which bind to the NOTCH1 receptor on neighbouring cells^{90,101,108–110}. Activation of Notch signalling stimulates the expression of transcriptional repressors such as HES1, HES5 and HEY2, which subsequently inhibit *Atoh1* expression, thereby promoting supporting cell fate^{101,111–114}. This leads to maintenance of *Sox2* expression in supporting cells as opposed to hair cells (Fig. 6B).

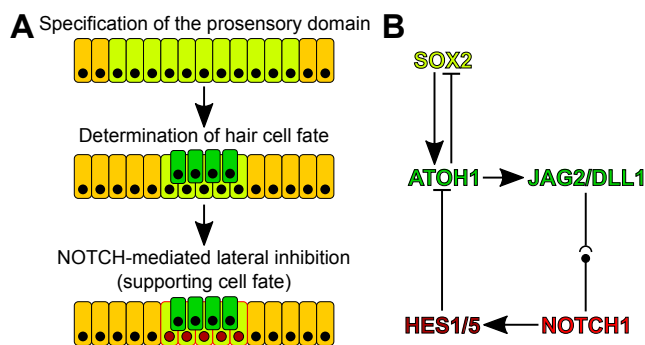


Figure 6. Progression and regulation of hair and supporting cell differentiation in the organ of Corti in mice. **A**, Scheme showing the main steps of hair and supporting cell differentiation. **B**, Depiction of the regulatory network involved in the prosensory cell differentiation. SOX2 specifies prosensory cells (light green) and induces hair cell differentiation (dark green) through activation of *Atoh1* expression. ATOH1-positive hair cells express the ligands DLL1 and JAGGED2 (JAG2) which bind to NOTCH1 on adjacent cells. Activation of Notch signalling (red) induces the expression of HES1/5 and subsequent repression of *Atoh1* promoting supporting cell fate.

(dark green) through activation of *Atoh1* expression. ATOH1-positive hair cells express the ligands DLL1 and JAGGED2 (JAG2) which bind to NOTCH1 on adjacent cells. Activation of Notch signalling (red) induces the expression of HES1/5 and subsequent repression of *Atoh1* promoting supporting cell fate.

Regulation of hair and supporting cell diversification in the organ of Corti

While the establishment of hair vs supporting cell fate is well characterized on the molecular level, only little is known about the regulatory mechanisms involved in the diversification of hair and supporting cells.

FGF signalling plays a role in differentiation of pillar cells and Deiters' cells. From the onset of differentiation *fibroblast growth factor receptor 3* (*Fgfr3*) is expressed in a subset of prosensory cells that give rise to OHCs, Deiters' cells and pillar cells^{115–117}. In the course of differentiation its expression is downregulated in OHCs but maintained in supporting cells. The FGFR3 ligand FGF8 is expressed in IHCs, and therefore, in close proximity to developing pillar cells^{115,116}. In contrast, the more laterally localized supporting cells are

exposed to the FGF antagonist sprouty2 (SPRY2)¹¹⁸. Inactivation of *Spry2* or constitutive activation of *Fgfr3* leads to transformation of Deiters' cells into pillar cells^{118–121}. Contrary, *Fgfr3* or *Fgf8* deficiency disrupts pillar cell development^{116,122,123}. Hence, FGFR3-positive supporting cells that receive strong FGF signals differentiate into pillar cells while exposure to weak FGF signalling promotes Deiters' cell differentiation. In collaboration with NOTCH signalling, FGFR3-mediated signalling induces the expression of *Hey2* in pillar cells¹¹². HEY2 maintains pillar cell fate and prevents their transdifferentiation into ATOH1-positive hair cells.

Recently, two transcription factors were identified that regulate OHC differentiation at different developmental stages, demonstrating that hair cell differentiation is a gradual process. *Insm1* is transiently expressed in OHCs from E15.5 to P2¹²⁴. Constitutive inactivation of this zinc-finger transcription factor gene leads to transdifferentiation of a subset of OHCs into IHC-like cells¹²⁵. OHC-specific expression of Helios (IKZF2) is initiated at P4¹²⁶. Disturbed function of this zinc-finger transcription factor leads to hearing impairment through downregulation of specific OHC markers such as prestin. In contrast, forced expression of *Ikzf2* activates a subset of OHC-specific genes in IHCs.

To date, the molecular regulators involved in progression of inner hair and supporting cell differentiation are unknown.

The function of *Tbx2* and *Tbx3* in embryonic development and disease

The T-box (*Tbx*) gene family codes for evolutionary conserved transcription factors that regulate a variety of developmental processes in all classes of metazoa. T-box proteins share a common DNA-binding domain (the name giving T-box) that recognizes a specific DNA motif with the core sequence AGGTGTGA. Based on sequence conservation, the 18 members of the vertebrate T-box gene family have been grouped into five subfamilies: *Brachyury*, *Tbx1*, *Tbx2*, *Tbx6* and *Tbr1*. Mutations of human orthologues underlie congenital diseases but also cause acquired syndromes such as cancer^{127–129}.

Two members of the *Tbx1*-subfamily, *Tbx1* and *Tbx18*, have previously been implicated in inner ear development. *Tbx18* is required for otic fibrocyte differentiation and formation of the stria vascularis¹³⁰. *Tbx1* has tissue-specific functions. In the epithelium, it restricts the neurogenic domain to the anterior-ventral otocyst and is required for the development of the stria vascularis^{36,78,131}. In the otic mesenchyme, TBX1 promotes morphogenesis of the semicircular canals and the cochlear duct^{78,132}.

Two other members of the T-box gene family, *Tbx2* and *Tbx3*, were shown to be expressed in the otic placode and/or otocyst indicating that they might present additional regulators of inner ear development^{133–136}. *Tbx2* and *Tbx3* belong to the *Tbx2*-subfamily and share more than 90% of their amino acid residues within the T-box domain¹³⁷. Both proteins act as potent transcriptional repressors that negatively regulate the expression of common and individual target genes such as *Cdkn1a*, *Cdkn1b* and *Cdkn2a* (cell cycle inhibitors), *Cdh1* and *Flrt3* (cell adhesion)^{138–143}. Homozygous deletion of *Tbx2* or *Tbx3* results in embryonic lethality in mice likely due to defects in yolk sac and heart development^{144,145}. In humans, haploinsufficiency of *TBX3* causes the ulnar-mammary syndrome that is characterized by abnormalities of mammary glands, upper limbs and genitals¹⁴⁶. Loss-of-function variants of *TBX2* are associated with cardiovascular defects, cleft palate, hypoplasia of the thymus and skeletal anomalies¹⁴⁷. Microdeletions of chromosome 17 that encompass several genes including *TBX2* has been associated with sensorineural hearing loss, arguing for a possible role of this T-box gene in inner ear function^{148,149}.

Aims of the thesis

TBX2 and TBX3 regulate the development of various organs during embryogenesis such as heart, limb, lung, ureter and eye^{139,144,150–153}. Initial analyses performed in our lab prior to this work revealed that these two T-box genes are also critical for murine inner ear development^{154–156}. Expression of *Tbx2* and *Tbx3* was found to be restricted to specific domains in the developing otic epithelium in a partially overlapping manner and early conditional inactivation of these genes severely impaired inner ear morphogenesis. Furthermore, *Tbx2* was differentially expressed in the inner compartment of the developing organ of Corti and its early inactivation or misexpression in the otic epithelium resulted in anomalies of hair and supporting cell arrangement^{154,156}. The precise phenotypic changes associated with loss and gain of these two genes and their specific cellular and molecular function in the murine inner ear development remained unknown.

The aim of this thesis was therefore twofold:

1. Analysis of the cellular and molecular function of *Tbx2* and/or *Tbx3* in the early morphogenesis of the otocyst,
2. Analysis of the cellular and molecular function of *Tbx2* in the development of the sensory epithelium in the cochlea.

In the first subproject, the individual and combined function of *Tbx2* and *Tbx3* in early inner ear development was to be investigated by a conditional gene inactivation approach using the *Pax2-cre*-line which specifically recombines in the otic epithelium at the placode stages. The morphological, histological and cellular changes of the mutant inner ears were to be examined. To characterize the molecular changes associated with loss of the two genes in the otic placode, transcriptional profiling by microarray experiments was to be performed and the candidate genes validated by RNA *in situ* hybridization for changes of their spatial expression patterns. A special focus was to be given on the characterization of changes in the spatial extent of neurogenesis in the otic vesicle of conditional double mutant embryos.

In the second subproject, the spatial and temporal expression of *Tbx2*/TBX2 in the organ of Corti was to be analysed in development and homeostasis using RNA *in situ* hybridization and (co)-immunofluorescence analyses in comparison to cell type-specific proteins at different developmental stages. The requirement of *Tbx2* in specification and/or maintenance of sensory cell identity was to be investigated by conditional inactivation of this T-box gene at different developmental stages using two tamoxifen-inducible *Cre*-lines: *Sox2^{creERT2}* (prosensory domain), *Atoh1-CreERT2* (hair cells)^{157,158}. Moreover, the

sufficiency of *Tbx2* to confer cell-type specific changes in the developing and mature organ of Corti was to be investigated by conditional misexpression experiments using an *Hprt^{TBX2}*-line and the mentioned tamoxifen-inducible *CreERT2*-driver lines (*Sox2^{creERT2}* and *Atoh1-CreER^{T2}*). Importantly, transcriptional profiling experiments were to be used to identify mediators and/or targets of TBX2 activity in cell-type differentiation in the organ of Corti.

Part 1 – *Tbx2* and *Tbx3* in patterning of the otocyst

Regulation of otocyst patterning by *Tbx2* and *Tbx3* is required for inner ear morphogenesis in the mouse

Marina Kaiser¹, Irina Wojahn¹, Carsten Rudat¹, Timo H. Lüdtkke¹, Vincent M. Christoffels², Anne Moon^{3,4}, Andreas Kispert¹ and Mark-Oliver Trowe^{1,*}

¹Institute for Molecular Biology, Medizinische Hochschule Hannover, 30625 Hannover, Germany.

²Department of Anatomy, Embryology and Physiology, Academic Medical Center, University of Amsterdam, 1105 AZ Amsterdam, The Netherlands.

³Department of Molecular and Functional Genomics, Weis Center for Research, Geisinger Clinic, Danville, PA 17822, USA. ⁴Department of Human Genetics, University of Utah School of Medicine, Salt Lake City, UT 84112, USA.

*Author for correspondence (trowe.mark-oliver@mh-hannover.de)

KEY WORDS: Otic vesicle, Cochlea, *Tbx1*, Otic neurogenesis, Morphogenesis, FGF

Type of authorship:	First author
Type of article:	Research article
Share of the work:	75%
Contribution:	(co)-planned, and performed experiments, analysed data, prepared figures, assisted in writing the manuscript
Journal:	<i>Development</i>
Impact factor:	6.868 (2020)
Number of citations:	1
Date of publication:	15.04.2021
DOI:	10.1242/dev.195651

Note that the supplementary tables of this paper are not included in the printed version of this thesis! They are included on the accompanied compact disc.

Permission

13.8.2021

<https://marketplace.copyright.com/rs-ui-web/mp/license/65a2da33-a958-4968-8cf9-44ee344a057e/71434342-5b02-4235-aec7-9412f1ebc2d5>


This is a License Agreement between Marina Kaiser ("User") and Copyright Clearance Center, Inc. ("CCC") on behalf of the Rightsholder identified in the order details below. The license consists of the order details, the CCC Terms and Conditions below, and any Rightsholder Terms and Conditions which are included below.

All payments must be made in full to CCC in accordance with the CCC Terms and Conditions below.

Order Date	12-Aug-2021	Type of Use	Republish in a thesis/dissertation
Order License ID	1140144-1	Publisher	COMPANY OF BIOLOGISTS,
ISSN	1477-9129	Portion	Chapter/article

LICENSED CONTENT

Publication Title	Development	Rightsholder	The Company of Biologists Ltd.
Article Title	Regulation of otocyst patterning by Tbx2 and Tbx3 is required for inner ear morphogenesis in the mouse	Publication Type	e-Journal
		Start Page	dev.195651
		Issue	8
Author/Editor	Company of Biologists.	Volume	148
Date	01/01/1987	URL	http://dev.biologists.org/
Language	English		
Country	United Kingdom of Great Britain and Northern Ireland		

REQUEST DETAILS

Portion Type	Chapter/article	Rights Requested	Main product
Page range(s)	all	Distribution	Worldwide
Total number of pages	28	Translation	Original language of publication
Format (select all that apply)	Print, Electronic	Copies for the disabled?	No
Who will republish the content?	Author of requested content	Minor editing privileges?	No
Duration of Use	Life of current edition	Incidental promotional use?	No
Lifetime Unit Quantity	Up to 499	Currency	EUR

NEW WORK DETAILS

Title	The function of Tbx2 and Tbx3 in regulation of morphogenesis and sensory cell differentiation in the murine inner ear	Institution name	Gottfried Wilhelm Leibniz Universität Hannover
		Expected presentation date	2021-08-19
Instructor name	Prof. Dr. rer. nat. Andreas Kispert		

ADDITIONAL DETAILS

Order reference number	N/A	The requesting person / organization to appear on the license	Marina Kaiser
------------------------	-----	---------------------------------------------------------------	---------------

<https://marketplace.copyright.com/rs-ui-web/mp/license/65a2da33-a958-4968-8cf9-44ee344a057e/71434342-5b02-4235-aec7-9412f1ebc2d5>

1

13.8.2021

<https://marketplace.copyright.com/rs-ui-web/mp/license/65a2da33-a958-4968-8cf9-44ee344a057e/71434342-5b02-4235-aec7-9412f1ebc2d5>

REUSE CONTENT DETAILS

Title, description or numeric reference of the portion(s)	Regulation of otocyst patterning by Tbx2 and Tbx3 is required for inner ear morphogenesis in the mouse	Title of the article/chapter the portion is from	Regulation of otocyst patterning by Tbx2 and Tbx3 is required for inner ear morphogenesis in the mouse
Editor of portion(s)	Kaiser, Marina; Wojahn, Irina; Rudat, Carsten; Lüdtkke, Timo H.; Christoffels, Vincent M.; Moon, Anne; Kispert, Andreas; Trowe, Mark-Oliver	Author of portion(s)	Kaiser, Marina; Wojahn, Irina; Rudat, Carsten; Lüdtkke, Timo H.; Christoffels, Vincent M.; Moon, Anne; Kispert, Andreas; Trowe, Mark-Oliver
Volume of serial or monograph	148	Issue, if republishing an article from a serial	8
Page or page range of portion	dev.195651	Publication date of portion	2021-04-23

RESEARCH ARTICLE

Regulation of otocyst patterning by *Tbx2* and *Tbx3* is required for inner ear morphogenesis in the mouse

Marina Kaiser¹, Irina Wojahn¹, Carsten Rudat¹, Timo H. Lüdtkke¹, Vincent M. Christoffels², Anne Moon^{3,4}, Andreas Kispert¹ and Mark-Oliver Trowe^{1,*}

ABSTRACT

All epithelial components of the inner ear, including sensory hair cells and innervating afferent neurons, arise by patterning and differentiation of epithelial progenitors residing in a simple sphere, the otocyst. Here, we identify the transcriptional repressors TBX2 and TBX3 as novel regulators of these processes in the mouse. Ablation of *Tbx2* from the otocyst led to cochlear hypoplasia, whereas loss of *Tbx3* was associated with vestibular malformations. The loss of function of both genes (*Tbx2/3cDKO*) prevented inner ear morphogenesis at midgestation, resulting in indiscernible cochlear and vestibular structures at birth. Morphogenetic impairment occurred concomitantly with increased apoptosis in ventral and lateral regions of *Tbx2/3cDKO* otocysts around E10.5. Expression analyses revealed partly disturbed regionalisation, and a posterior-ventral expansion of the neurogenic domain in *Tbx2/3cDKO* otocysts at this stage. We provide evidence that repression of FGF signalling by TBX2 is important to restrict neurogenesis to the anterior-ventral otocyst and implicate another T-box factor, TBX1, as a crucial mediator in this regulatory network.

KEY WORDS: Otic vesicle, Cochlea, *Tbx1*, Otic neurogenesis, Morphogenesis, FGF

INTRODUCTION

The mammalian inner ear is a highly asymmetric sensory organ that is characterised by an elaborated system of fluid-filled epithelial ducts and chambers. Ventro-medially in this membranous labyrinth lies the spirally coiled cochlear duct, which is essential for the perception of sound. Dorso-laterally resides the vestibular organ, in which anterior, posterior and lateral semicircular canals and two membranous sacs, the saccule and the utricle, mediate the perception of angular and linear acceleration, as well as of gravity. In both the cochlea and the vestibular organ, sensory stimuli are converted into electrical impulses by clusters of mechanosensitive hair cells and are transmitted to the brain by sensory neurons of the cochlear and the vestibular ganglia.

Hair cells, their supporting cells, non-sensory epithelial cells as well as sensory neurons of the inner ear all derive from a common

precursor tissue, the otic placode, which in mice is established in the ectoderm lateral to the hindbrain around embryonic day (E) 8.5 (reviewed by Wu and Sandell, 2016). This epithelial patch invaginates and pinches off the surrounding ectoderm to form at E9.5 an epithelial sphere, the otocyst. Within the next 8 days, localised changes of cell shapes, cell migration, proliferation and apoptosis drive morphogenesis of the semicircular canals and the endolymphatic duct from the dorsal and dorso-medial aspect of the otocyst, respectively; of utricle and saccule from the intermediate part; and of the cochlear duct from the posterior-ventral region (Alsina and Whitfield, 2017; Martin and Swanson, 1993; Morsli et al., 1998; Nishikori et al., 1999).

Around E9.0, epithelial cells in the ventral otocyst initiate a neurosensory differentiation programme. From this neurogenic domain, which is rapidly restricted to the anterior subregion of the otocyst until E10.5, neuroblasts delaminate and coalesce to form the statoacoustic ganglion (SAG), which later subdivides and innervates the auditory and vestibular inner ear components (Carney and Silver, 1983; Ma et al., 1998; Raft et al., 2004). Remaining cells of the proneurosensory domain, as well as cells of the neighbouring prosensory domain, segregate to different regions of the inner ear where they eventually differentiate into mechanosensitive hair cells and supporting cells of the vestibular and cochlear sensory patches (reviewed by Raft and Groves, 2015; Wu and Sandell, 2016).

Spatially confined morphogenetic and neurosensory differentiation programmes rely on prior patterning of the otocyst along three perpendicular axes. WNTs and BMPs from the dorsal hindbrain, and SHH from the basal plate of the hindbrain and the underlying notochord provide asymmetric cues to generate opposing signalling gradients along the dorso-ventral and medio-lateral axes of the otocyst (Hatch et al., 2007; Ohta et al., 2016; Pirvola et al., 2000; Riccomagno et al., 2002, 2005). Combinatorial signalling activities confer regionalised expression of transcription factors that regulate distinct morphogenetic programmes in subregions of the otocyst (reviewed by Ohta and Schoenwolf, 2018). Polarisation along the anterior-posterior axis is triggered by retinoic acid (RA) from paraxial mesoderm at the posterior edge of the forming otocyst (Bok et al., 2011). In the posterior otocyst, high levels of RA induce the expression of the T-box transcription factor TBX1, which suppresses neurogenesis (Bok et al., 2011; Raft et al., 2004). Commitment to the neuronal lineage within the anterior-ventral otocyst is regulated by the basic helix-loop-helix (bHLH) transcription factor NEUROG1, which acts upstream of NEUROD1 and DLL1 (Ma et al., 2000, 1998). DLL1 limits the number of neuronal precursors by NOTCH-dependent lateral inhibition (Brooker et al., 2006; Daudet et al., 2007), and NEUROD1 controls the subsequent delamination and differentiation of neuroblasts (Kim, 2013; Kim et al., 2001; Liu et al., 2000).

TBX2 and TBX3 are two closely related members of a T-box transcription factor subfamily that is distinct from that of TBX1

¹Institute for Molecular Biology, Medizinische Hochschule Hannover, 30625 Hannover, Germany. ²Department of Anatomy, Embryology and Physiology, Academic Medical Center, University of Amsterdam, 1105 AZ Amsterdam, The Netherlands. ³Department of Molecular and Functional Genomics, Weis Center for Research, Geisinger Clinic, Danville, PA 17822, USA. ⁴Department of Human Genetics, University of Utah School of Medicine, Salt Lake City, UT 84112, USA.

*Author for correspondence (trowe.mark-oliver@mh-hannover.de)

© M.K., 0000-0003-4193-8524; T.H.L., 0000-0002-4689-114X; M.-O.T., 0000-0002-0011-461X

Handling Editor: Liz Robertson
Received 2 August 2020; Accepted 23 March 2021

(Agulnik et al., 1996). Both proteins are expressed at many sites of the developing vertebrate embryo, where they regulate diverse cellular processes in early organogenesis as transcriptional repressors (reviewed by Papaioannou, 2014). Based on previous reports that these genes are also expressed in the early mouse otocyst (Bollag et al., 1994; Mesbah et al., 2012), we used a conditional gene-targeting approach to analyse their function in murine inner ear development. Here, we show that *Tbx2* and *Tbx3* are individually and combinatorially required for inner ear morphogenesis. We trace the developmental onset of these changes to the early otocyst, and characterise the cellular and molecular alterations at this stage. We provide evidence for a role of TBX2 in the anterior-ventral restriction of otic neurogenesis by repressing FGF signalling and maintaining *Tbx1* expression in the posterior-ventral otocyst.

RESULTS

Tbx2 and *Tbx3* show spatially restricted but partially overlapping patterns of expression in early murine inner ear development

Previous work reported expression of *Tbx2* in the E8.5 otic placode (Barriónuevo et al., 2008), and of *Tbx2* and *Tbx3* in the E9.5 otocyst (Bollag et al., 1994; Mesbah et al., 2012). However, a spatially and temporally resolved profile of (co-)expression of the two genes in the early development of the murine inner ear was not reported. RNA *in situ* hybridisation analysis confirmed that *Tbx2* expression commences in the otic placode at E8.5 (Fig. 1A). At E9.5, *Tbx2* was expressed in the epithelium of the entire otocyst with exception of the dorsolateral quadrant (Fig. 1B). From E10.5 to E12.0, expression of *Tbx2* was found ventrally in the developing cochlear duct, dorso-medially in the endolymphatic duct and in the central region, the vestibule, but not in the dorso-lateral region, which gives rise to the vertical canal plate, the primordium of the posterior and anterior semicircular canals (Morsli et al., 1998). Otic expression of *Tbx3* started at E9.5 in the lateral otocyst (Fig. 1A,B). From E10.5 onwards, expression was confined to the lateral aspects of the developing vestibular system and ventro-medially to the epithelium of the cochlear duct. Three-dimensional (3D) reconstructions from serial sections confirmed unique expression of *Tbx2* in the developing endolymphatic duct and in the posterior aspect of the cochlear duct, and of *Tbx3* in the dorsal vestibular system whereas expression of the two genes largely overlapped in the central-lateral part of the developing vestibular system and in the anterior cochlear duct (Fig. 1C). Expression of TBX2 and TBX3 protein mirrored the patterns of the mRNA (Fig. 1D). Together, this analysis argues for both unique and combined functions of *Tbx2* and *Tbx3* in the development of specific subregions of the otocyst.

Individual and combined inactivation of *Tbx2* and *Tbx3* in the otic epithelium disrupts inner ear morphogenesis

To test the individual and combined function of *Tbx2* and *Tbx3* in inner ear development, we used a tissue-specific gene inactivation approach with a *Pax2-cre* transgenic line that mediates recombination in the otic epithelium from E8.5 onwards (Trowe et al., 2011) (Fig. S1A), and floxed alleles of *Tbx2* (*Tbx2^{fllox}*) (Wakker et al., 2010) and *Tbx3* (*Tbx3^{fllox}*) (Frank et al., 2013). Complete loss of TBX2 and TBX3 protein in the otic epithelium of *Pax2-cre/+;Tbx2^{fllox/fllox};Tbx3^{fllox/fllox}* (*Tbx2/3cDKO*) embryos at E9.5 and E10.5 confirmed the validity of this approach (Fig. S1B).

Mice with individual and combined inactivation of *Tbx2* and *Tbx3* presented in the expected Mendelian ratio at E18.5 (Table S1) allowing for the inspection of inner ear morphology by serial

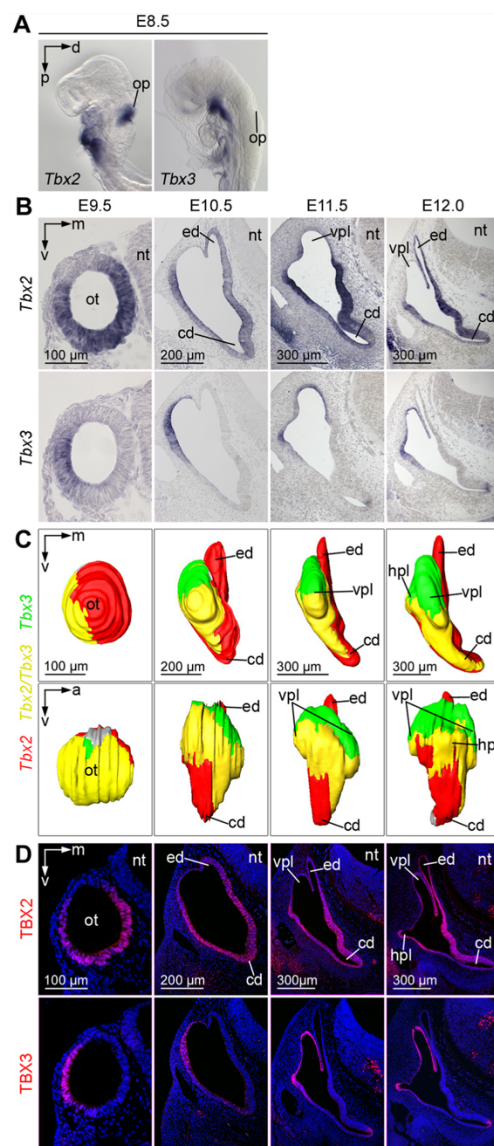


Fig. 1. *Tbx2* and *Tbx3* show spatially restricted but partially overlapping patterns of expression in early inner ear development. (A,B) RNA *in situ* hybridisation analysis of *Tbx2* and *Tbx3* expression in whole wild-type embryos at E8.5 (A) and on mid-transverse otocyst sections of E9.5 to E12.0 embryos (B). (C) 3D reconstructions of unique domains of *Tbx2* (red) and *Tbx3* (green) as well as overlapping expression (yellow) in the developing inner ear from E9.5 to E12.0. For this analysis, serial otocyst sections were alternately stained for *Tbx2* and *Tbx3* mRNA. Shown are anterior views (top) and lateral views (bottom) of the developing otocyst. (D) Immunofluorescence staining of TBX2 and TBX3 expression in mid-transverse sections of E9.5 to E12.0 otocysts. a, anterior; cd, cochlear duct; d, dorsal; ed, endolymphatic duct; hpl, horizontal canal plate; m, medial; nt, neural tube; op, otic placode; ot, otocyst; p, posterior; v, ventral; vpl, vertical canal plate.

histological sections and subsequent 3D reconstructions of the cavities of all mutant combinations at this stage (Fig. 2A, Fig. S2A). Embryos with an individual deletion of *Tbx2* (*Pax2-cre/+;Tbx2^{fllox/fllox}*,

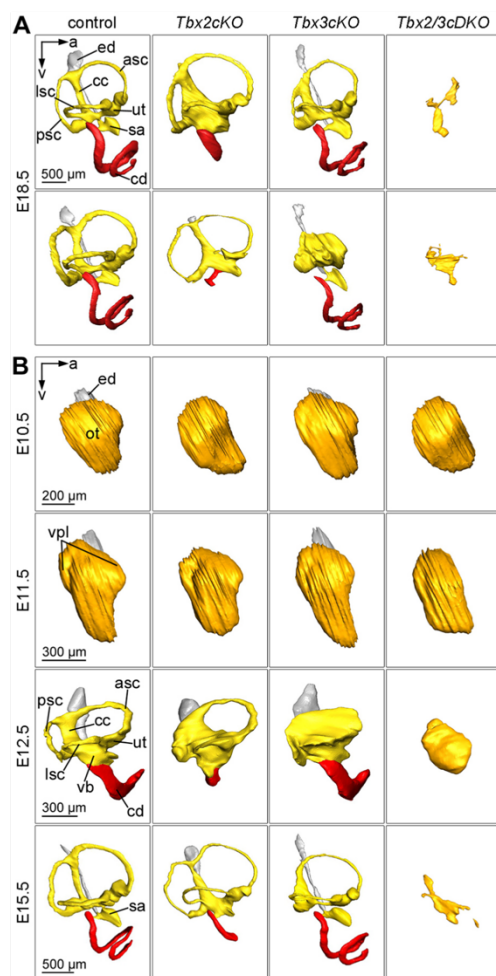


Fig. 2. Individual and combined loss of *Tbx2* and/or *Tbx3* in the otic epithelium severely affects inner ear morphology from E10.5 onwards. (A,B) 3D reconstructions derived from serial histologically stained sections of the cavities of the cochlear duct (red), the vestibular system (yellow) as well as the endolymphatic duct (grey). (A) Morphology of E18.5 inner ears in a lateral view. For each of the indicated genotypes, two specimens are shown to reflect the phenotypic range. (B) Inner ear morphogenesis between E10.5 and E15.5 in control and mutant embryos in a lateral view. a, anterior; asc, anterior semicircular canal; cc, crus commune; cd, cochlear duct; ed, endolymphatic duct; lsc, lateral semicircular canal; ot, otocyst; psc, posterior semicircular canal; sa, saccule; ut, utricle; v, ventral; vb, vestibule; vpl, vertical canal plate.

Tbx2cKO exhibited a severely shortened cochlear duct, a rudimentary endolymphatic duct, malformation of the vestibular system with dilation of the vestibule and crus commune, loss of the saccular cavity and variably truncated semicircular canals. In *Pax2-cre/+;Tbx3^{lox/flox}* (*Tbx3cKO*) embryos, the cochlear and endolymphatic ducts were established normally, but the vestibular system was variably hypo- or dysplastic. In *Tbx2/3cDKO* embryos, hypodysplasia of the cochlear and endolymphatic duct and of the vestibular system was strongly enhanced compared with single

mutants. The membranous labyrinth was severely reduced in size and collapsed. This shows that *Tbx2* is uniquely required for morphogenesis of the cochlea and the endolymphatic duct, whereas *Tbx2* and *Tbx3* redundantly regulate the formation of the vestibular system.

Morphological changes of the inner ear in *Tbx2*- and/or *Tbx3*-deficient embryos occur shortly after otocyst formation

To define both the onset and progression of these morphological defects, we analysed inner ear development from E9.5, when the otocyst is formed, to E15.5, when all epithelial ducts of the cochlea and vestibular system are established (Fig. 2B, Fig. S2B). In *Tbx2cKO* embryos, the first phenotypic changes were detected at E10.5 as a thickening of the otic epithelium in the ventro-lateral region of the otocyst (Fig. S2B, brackets). In 3D reconstructions, the protrusion of the endolymphatic duct at the dorso-medial side was much shorter than in controls. At subsequent stages, the endolymphatic duct remained short and did not separate from the vestibule. The cochlear duct underwent minimal elongation and no coiling. Formation of the posterior semicircular canal was delayed and separation of the vestibule and saccular cavity failed. Inner ears of *Tbx3cKO* embryos appeared normal until E11.5, but exhibited delayed semicircular canal morphogenesis at E12.5, and lacked the posterior semicircular canal at E15.5. In *Tbx2/3cDKO* inner ears, phenotypic changes started at E10.5, mirroring the findings in *Tbx2cKO* embryos. Unlike in *Tbx2cKO* embryos, the endolymphatic and the cochlear duct were absent at E11.5 and subsequent stages. The size and shape of the otocyst remained largely unchanged at E12.5. At E15.5, the cavity was collapsed. These findings point to onset of morphological changes in *Tbx2cKO* and *Tbx2/3cDKO* inner ears at E10.5, defining a requirement of *Tbx2* and *Tbx3* shortly after the otocyst has formed.

Tbx2/3cDKO embryos exhibit ectopic apoptosis in the dorso-lateral and ventral regions of the otocyst

We next investigated whether these morphological changes are preceded and/or accompanied by alterations in cell survival and/or proliferation in the otic epithelium. A bromodeoxyuridine (BrdU) incorporation assay revealed normal cell proliferation in four quadrants of *Tbx2/3cDKO* otocysts at E10.5 (Fig. 3A,B, Table S2). In contrast, terminal deoxynucleotidyl transferase dUTP nick end labelling (TUNEL) and anti-CASPASE-3 staining detected altered patterns of apoptosis (Fig. 3C, Fig. S3). A small cluster of apoptotic cells at the ventral-most tip of the otocyst was present in control and *Tbx3cKO* embryos at E10.5 but not in *Tbx2cKO* and *Tbx2/3cDKO* embryos (arrowheads in Fig. 3C). In the latter genotypes, ectopic programmed cell death occurred in the ventro-lateral and dorso-lateral region at this stage (arrows in Fig. 3C). At E11.5, *Tbx2cKO* and *Tbx2/3cDKO* embryos exhibited markedly increased apoptosis in the ventral-most area of the otocyst, and in cells and ganglion-like structures located in the adjacent periotic mesenchyme (arrows in Fig. 3C, Fig. S3).

Dorso-ventral and medio-lateral regionalisation of *Tbx2/3cDKO* otocysts is partly disturbed

To identify in an unbiased fashion molecular changes that correlate or even account for the observed cellular and morphological defects in *Tbx2/3cDKO* inner ears, we performed microarray-based transcriptional profiling using RNA from four independent pools of dissected otocysts of E10.5 *Tbx2/3cDKO* embryos and their Cre-negative littermates as controls. Using Qlucore Omics Explorer software, we found a total of 2860 differentially expressed genes

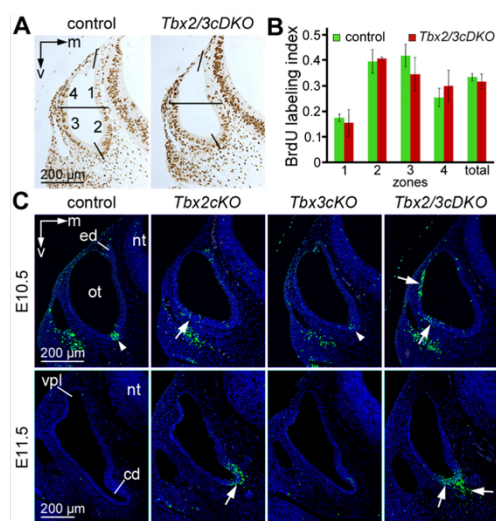


Fig. 3. Increased apoptosis in the otic epithelium upon individual and combined inactivation of *Tbx2* and *Tbx3* in this tissue. (A) Analysis of cell proliferation by the BrdU incorporation assay on transverse sections in the four indicated quadrants of E10.5 otocysts. (B) No significant differences in the proliferation rate are detected in *Tbx2/3cDKO* otic epithelium compared with control ($n=6$). Error bars represent s.d. For numbers, see Table S2. (C) Analysis of cell death by the TUNEL assay on transverse otocyst sections at E10.5 and E11.5. Arrowheads point to apoptotic cells at the ventral-most tip of the otocyst in control and *Tbx3cKO* embryos at E10.5. Arrows mark ectopic dorso-lateral and ventro-lateral clusters of apoptotic cells in *Tbx2cKO* and *Tbx2/3cDKO* otocysts at E10.5; and an ectopic apoptotic cell cluster in the ventral tip, the surrounding mesenchyme and ganglion-like structures in *Tbx2cKO* and *Tbx2/3cDKO* otocysts at E11.5. Nuclei are counterstained with DAPI. Stages and genotypes are as indicated. cd, cochlear duct; ed, endolymphatic duct; m, medial; nt, neural tube; ot, otocyst; v, ventral; vpl, vertical canal plate.

with $q < 0.05$ (Table S3); additional thresholds for signal intensity ($\text{INT} \geq 100$) and fold change ($\text{FC} \geq 2$) resulted in 234 robustly upregulated and 169 robustly downregulated genes in *Tbx2/3cDKO* otocysts (Fig. 4A, Tables S4 and S5).

Functional annotation using the DAVID software tool (david.ncifcrf.gov) revealed strongest enrichment of the gene ontology (GO) term 'inner ear morphogenesis' in the group of 169 genes with reduced expression (Fig. 4B, Table S6). Among the top 20 downregulated transcripts was the transcription factor gene *Otx1* (-5.4), which is required for lateral semicircular canal formation and cochlear morphogenesis (Morsli et al., 1999), and *Smpx* (-11.4), loss of which leads to hearing impairment in humans (Huebner et al., 2011) (Fig. 4C). Manual inspection of the list of downregulated genes uncovered additional regulators of inner ear morphogenesis, including *Otx2* (-4.9) (Miyazaki et al., 2006; Morsli et al., 1999), *Hmx2/3* ($-4.1/-3.1$) (Wang et al., 2001, 2004), *Gata2/3* ($-3.0/-2.2$) (Haugas et al., 2010; Lilleväli et al., 2006), *Gbx2* (-2.9) (Lin et al., 2005; Miyazaki et al., 2006), *Tbx1* (-2.7) (Raft et al., 2004; Vitelli et al., 2003), *Dlx5* (-2.3) (Robledo and Lufkin, 2006), *Fgf10* (-1.7) (Lilleväli et al., 2006; Pauley et al., 2003) and *Lmo4* (-1.6) (Deng et al., 2010) (Fig. 4D).

RNA *in situ* hybridisation analysis uncovered that regionalised expression of genes from the top 20 list as well as of further selected candidates was differentially affected in E10.5 *Tbx2/3cDKO* otocysts (Fig. 4E). Expression of *Smpx* and *Sstr1* in the dorso-

medial region was lost, and that of *Gbx2*, *Pax8* and *Wnt2b* was strongly reduced. *Aldh1a2* and *Hmx3* were no longer expressed in the dorso-lateral region, and *Gata3* and *Lmo4* were downregulated and their expression domain was smaller. The ventral expression limit of the lateral *Dlx5* domain was shifted dorsally. *Otx2* expression was completely abolished from the ventro-lateral region, and the expression domain of *Otx1* in the lateral otic epithelium was reduced. *Cldn22* was no longer transcribed in the ventral otocyst. *Gata3* expression in the ventral tip of the otocyst was reduced, and expression of *Gdf6*, *Fgf10* and *Tnni1* was not detected in this region. Other transcription factor genes implicated in dorso-ventral patterning of the otocyst (*Dach1*, *Eya1*, *Pax2*, *Six1*) (Ozaki et al., 2004; Torres et al., 1996; Xu et al., 1999; Zheng et al., 2003), were unchanged in the microarray and exhibited minor (*Pax2* was ventrally expanded) or no changes (*Dach1*, *Eya1*, *Six1*) in their expression pattern at E10.5 (Fig. 4F). Together, these findings indicate that the dorso-ventral and medio-lateral axes are established but that regionalised morphogenetic programmes along these axes are partly compromised upon combined loss of *Tbx2* and *Tbx3* in the otic epithelium.

Genes associated with neuronal differentiation are upregulated in *Tbx2/3cDKO* otocysts

As *Tbx2* and *Tbx3* encode transcriptional repressors (Brummelkamp et al., 2002; Carreira et al., 1998; Jacobs et al., 2000; Lingbeek et al., 2002), it is likely that the set of genes with increased expression in *Tbx2/3cDKO* otocysts (Table S5) better reflects their primary regulatory function. Functional annotation analysis of upregulated transcripts showed an enrichment of genes associated with the terms 'neurogenesis' and 'regionalisation' (Fig. 5A, Table S7). Many of these 'neuronal' genes are among the top 40 upregulated genes, including *En2* ($+17.1$), *Sox3* ($+5.2$), *Fgf8* ($+4.6$) and *Nefm* ($+4.3$) (Fig. 5B). Other highly upregulated neuronal genes were *Pou4f1* ($+3.1$), *Insm1* ($+2.3$), *Nhlh2* ($+2.2$) (Fig. 5C). Additional genes with known function or expression in otic neurogenesis were found among significantly upregulated genes that had a $\text{FC} < 2$, including the neurogenic marker genes *Dll1* ($+1.5$) and *Neurod1* ($+1.7$), *Heyl* ($+1.8$), *Nhlh1* ($+1.6$) and *Tubb3* ($+1.7$) (Jalali et al., 2011; Ma et al., 1998) (Fig. 5C, Table S3).

Using RNA *in situ* hybridisation analysis, we validated expression of the top 40 upregulated genes as well as of selected candidates for which we were able to obtain probes (Fig. 5D). Ten of the genes showed ectopic expression in *Tbx2/3cDKO* otocysts: *Cd83*, *En2*, *Lamc2*, *Papss2* and *Sox3* in the ventral region; *Cttn3* and *Kcns3* in the ventro-lateral region; and *Insm1*, *Prkaa2* and *Sowaha* in single cells in the ventral region as well as in the adjacent mesenchyme. Expression of *Nhlh2* in neuroblasts was unaffected. Dorso-lateral expression of *Ntn1* and medial expression of *Heyl* was expanded ventrally and ventro-laterally, respectively, in mutant otocysts. *Celf3*, *Dll3*, *Kcnmb2*, *Pou4f1* and *Tmeff2* were expressed in the SAG in both control and *Tbx2/3cDKO* embryos. Many of these genes (*Celf3*, *Dll3*, *Heyl*, *Insm1*, *Nhlh2*, *Pou4f1*, *Sox3*) were also transcribed in the neural tube, confirming their possible involvement in neurogenesis. Collectively, these results indicate that neurogenesis occurs ectopically in the ventral region of *Tbx2/3cDKO* otocysts.

The neurogenic domain is posteriorly expanded in *Tbx2*-deficient otocysts

In wild-type embryos, neurogenesis commences in the entire ventral aspect of the otocyst around E9.5 but becomes rapidly restricted to an anterior subregion at E10.5 (Raft et al., 2004). To judge whether

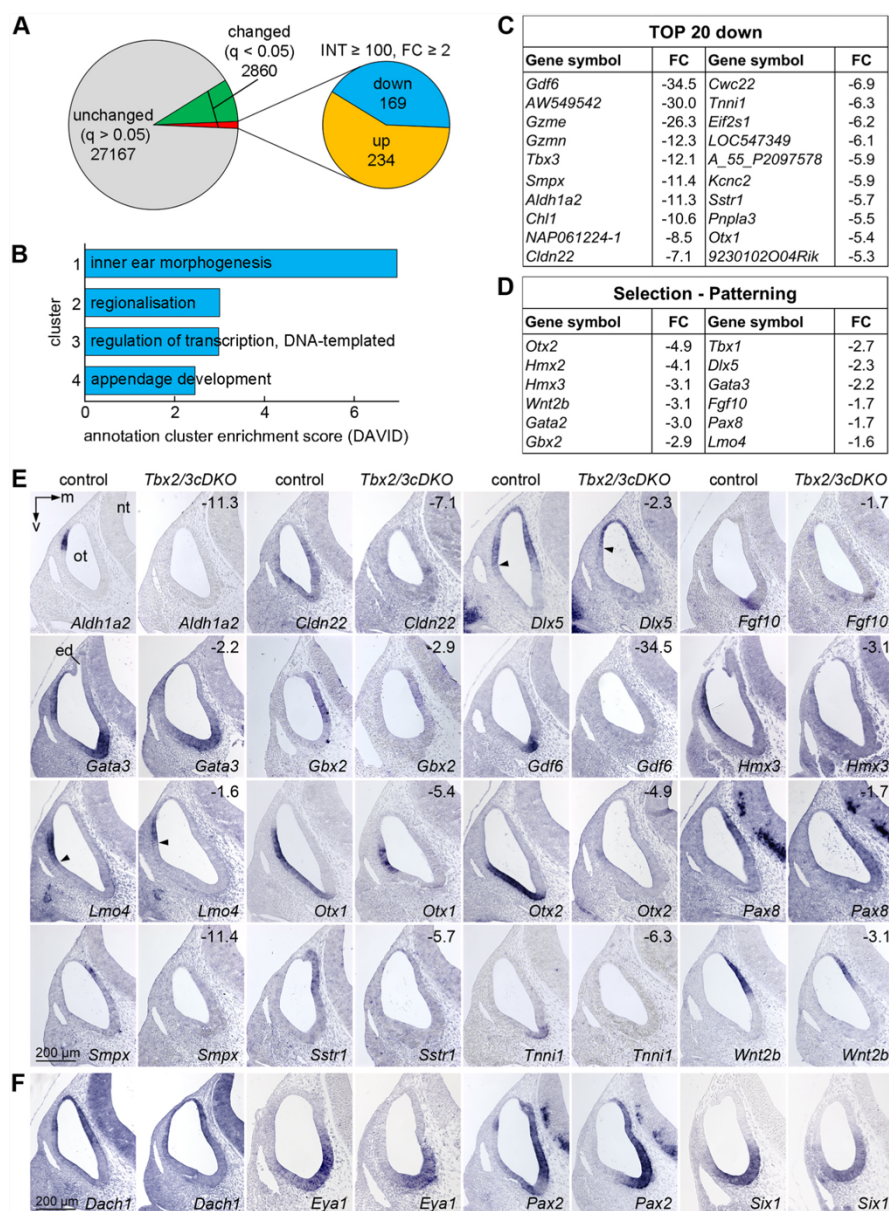


Fig. 4. *Tbx2/3cDKO* otocysts show defects in dorso-ventral and medio-lateral regionalisation at E10.5. (A) Pie-charts summarising the results from the microarray analysis of four independent otocyst pools from E10.5 *Tbx2/3cDKO* and control embryos. (B) Gene ontology (GO) enrichment analysis for downregulated genes. The top 4 scoring clusters are shown annotated with representative GO terms and cluster enrichment scores. (C,D) Tables of the top 20 (C) and selected (D) downregulated transcripts. Shown are average fold changes (FC) of RNA intensities between the pools. (E,F) Validation of the downregulated microarray candidates (E) and of selected dorsal and ventral markers (F) by RNA *in situ* hybridisation analysis on mid-transverse otocyst sections of control and *Tbx2/3cDKO* embryos. Arrowheads indicate the dorsal shift in *Dlx5* and *Lmo4* expression borders. Numbers in the mutant panels indicate the degree of downregulation. ed, endolymphatic duct; m, medial; nt, neural tube; ot, otocyst; v, ventral.

this regionalisation process is compromised in *Tbx2/3cDKO* embryos, we analysed the expression of genes involved in this programme on transverse sections along the anterior-posterior axis of the otocyst at E9.5 and E10.5. At E9.5, expression of the proneurosensory markers *Sox2* and *Lnfg*, and of the neurogenic

marker *Neurog1* in the ventral region along the anterior-posterior axis was unaffected as was the restriction of *Tbx1* to the posterior-lateral otocyst (Fig. S4).

At E10.5, *Neurog1* and its targets, *Dll1* and *Neurod1* (Ma et al., 1998) were found in the anterior ventro-lateral otocyst as well as in

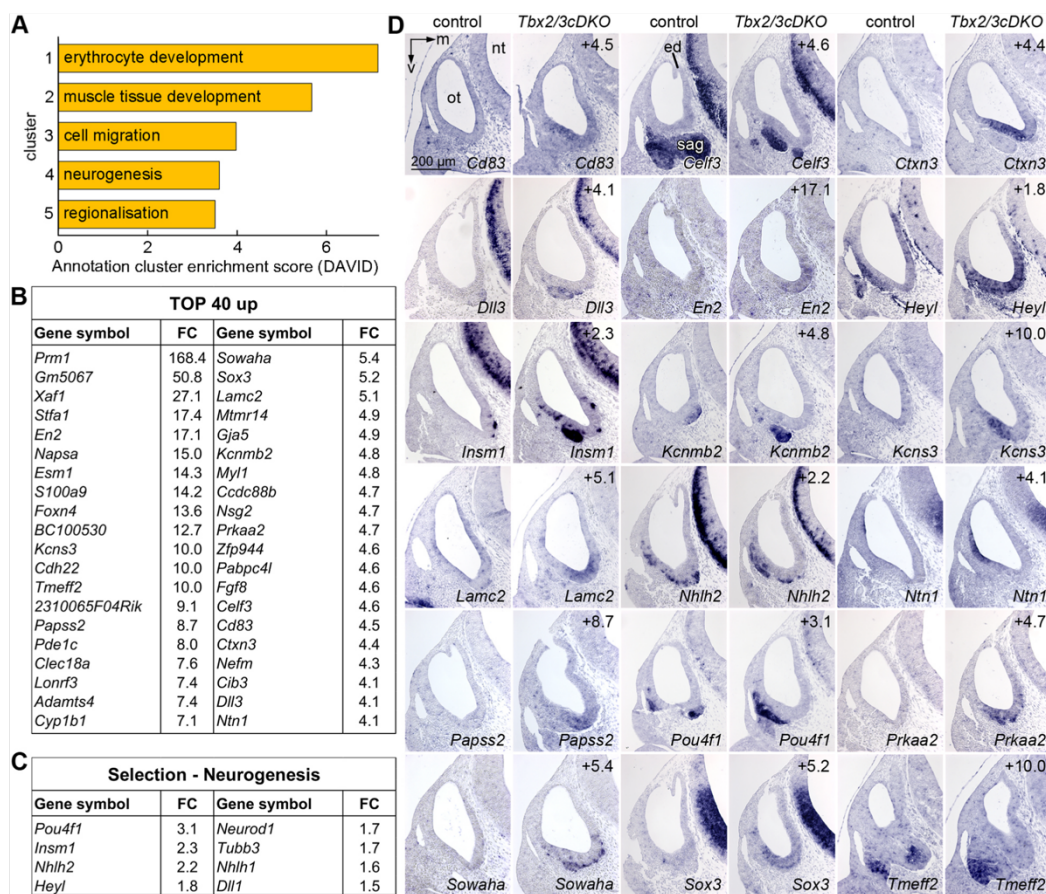


Fig. 5. Genes associated with neuronal development are upregulated in *Tbx2/3cDKO* otocysts. (A) Gene ontology (GO) enrichment analysis for upregulated genes. The top 5 scoring clusters are annotated with representative GO terms and cluster enrichment scores. (B,C) Tables of the top 40 (B) and selected (C) upregulated transcripts. Shown are average fold changes (FC) of RNA intensities between the pools. (D) Validation of upregulated microarray candidates by RNA *in situ* hybridisation analysis on mid-transverse otocyst sections shows ectopic expression of genes in the ventral region of *Tbx2/3cDKO* otocysts. Numbers in the mutant panels indicate the degree of upregulation. ed, endolymphatic duct; m, medial; nt, neural tube; ot, otocyst; sag, statoacoustic ganglion; v, ventral.

the periphery of the adjacent SAG in control embryos; *Nefm*, a gene transcribed in maturing neurons (Romand et al., 1990), was expressed in the centre of the SAG (Fig. 6A). In *Tbx2/3cDKO* otocysts, expression of *Neurog1*, *Dll1* and *Neurod1* was expanded posterior-ventrally into the non-neurogenic region of the otocyst, and was also observed in cells underneath the epithelium. Ectopic ganglion-like structures were found in the adjacent periotic mesenchyme (Fig. 6A, arrows), of which some were *Nefm* positive. 3D reconstructions confirmed posterior-ventral expansion of resident and delaminating neuroblasts (*Neurod1*) (Fig. 6B). However, only a subset of these ectopic neuroblasts managed to differentiate further (*Nefm*) as the slightly lateralised SAG was not expanded posteriorly (Fig. 6C). Importantly, posterior expansion of the neurogenic domain occurred in *Tbx2cKO* but not in the *Tbx3cKO* otocysts (Fig. S5), indicating that TBX2 accounts for the anterior restriction of the otic neurogenic programme after E9.5.

Tbx1, the major inhibitor of otic neurogenesis (Raft et al., 2004), was expressed in the entire otocyst except for the anterior-ventral neurogenic domain of control and *Tbx3cKO* embryos at E10.5. In

Tbx2cKO embryos, *Tbx1* expression was absent from the ventral aspect of the otocyst along the complete anterior-posterior axis. In *Tbx2/3cDKO* mutants, expression of *Tbx1* was additionally abolished from the anterior-dorsal otocyst (Fig. S6A, Fig. 6D). In *Tbx1*-deficient otocysts, expression of *Tbx2* expanded into a small anterior-dorsal region but was otherwise unaffected; *Tbx3* was lost in the posterior-medial region (Fig. S6B). Hence, ventral expression of *Tbx1* depends on *Tbx2* whereas *Tbx2/Tbx3* expression gets (minor) input from *Tbx1* function.

Ectopic FGF signalling contributes to the posterior expansion of the neurogenic domain in *Tbx2/3cDKO* otocysts at E10.5

Our transcriptional profiling revealed increased expression of *Fgf8* (+4.6) and of members of its synexpression group: FGF8 effectors *Etv1* (+1.5), *Etv4* (+1.6), *Etv5* (+1.5), and counter-regulators *Dusp6* (+1.8) and *Il17rd* (+1.4) in *Tbx2/3cDKO* otocysts (Fig. 5B, Table S3). Because FGF8 promotes commitment of otic epithelial cells to the neuronal lineage by inducing *Sox3* (increased 5-fold

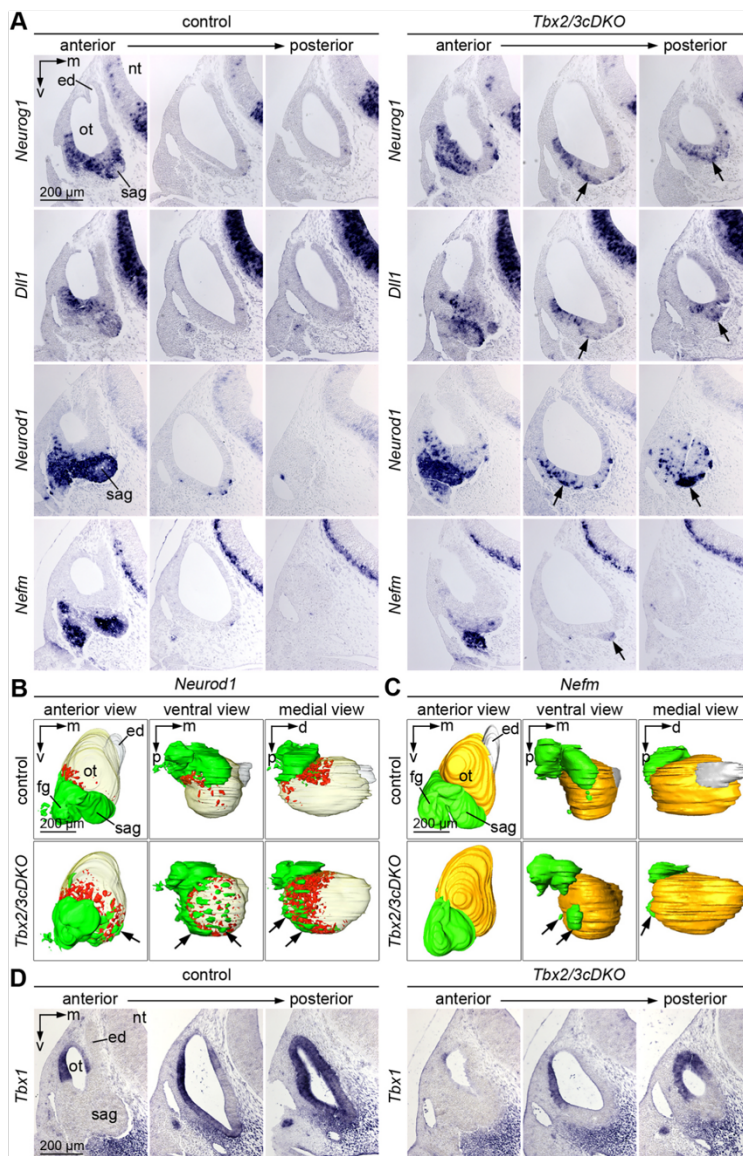


Fig. 6. The neurogenic domain is posteriorly expanded in *Tbx2/3cDKO* otocysts at E10.5. (A) RNA *in situ* hybridisation analysis of E10.5 control and *Tbx2/3cDKO* otocysts using three different section planes: anterior, mid-transverse, posterior. Expression of pro-neuronal genes (*Neurog1*, *Dll1*, *Neurod1*) is posterior-ventrally expanded in mutant otocysts; expression of *Nefm*, a marker of terminally differentiated neuronal cells, is unaltered. Ectopic ganglion-like structures are present adjacent to the posterior-ventral otocyst of mutant embryos (arrows). (B, C) Different views of 3D reconstructions of *Neurod1*⁺ cells in the otic epithelium (red) and in delaminated neuroblasts (green) in relation to the otocyst (translucent) (B), and of *Nefm* expression (green) in comparison with the otocyst (orange) (C). Arrows indicate ectopic ganglion-like structures adjacent to the posterior-ventral otocyst. (D) RNA *in situ* hybridisation analysis of *Tbx1* expression, which is downregulated in the posterior-ventral otocyst of *Tbx2/3cDKO* embryos. d, dorsal; ed, endolymphatic duct; fg, facial ganglion; m, medial; nt, neural tube; ot, otocyst; p, posterior; sag, statoacoustic ganglion; v, ventral.

here) and downstream *Neurod1* expression in the chick (Abelló et al., 2010), we wished to explore changes of the spatial pattern of *Fgf8* and *Sox3* (Fig. 7A). In control embryos, *Fgf8* was restricted to the periphery of the SAG in the anterior region; *Sox3* was not expressed. In *Tbx2/3cDKO* embryos, we detected ectopic expression of both genes in the ventral otocyst along the anterior-posterior axis. Importantly, this ectopic expression correlated with strongly enhanced FGF signalling, as indicated by ectopic posterior expression of *Etv4* and *Etv5*, bona fide target genes of this pathway (Raible and Brand, 2001). Notably, expression of another FGF ligand gene, *Fgf3*, which is confined to the anterior-lateral (neural) region of the otocyst (McKay et al., 1996), occurred ectopically in a dorso-medial position at the posterior region of the *Tbx2/3cDKO*

otocyst at this stage (Fig. 7A). Ectopic expression of *Fgf8*, *Etv4* and *Sox3* was also found in *Tbx2cKO* but not in *Tbx3cKO* otocysts at E10.5, implicating specifically TBX2 in the repression of *Fgf8* and FGF signalling (Fig. S7).

In *Tbx1KO* otocysts, *Fgf8* and *Sox3* were not ectopically expressed; the anterior-ventro-lateral expression of *Fgf3* was expanded posteriorly; and *Etv4* and *Etv5* expression occurred ectopically in the posterior-medial region (Fig. S8). These results suggest that loss of *Tbx1* in *Tbx2cKO* and *Tbx2/3cDKO* otocysts does not account for ectopic posterior-ventral activation of *Fgf8*/*Sox3* expression and FGF signalling.

Because signalling pathways are frequently interconnected in tissue patterning, we also analysed changes of the spatial activity of

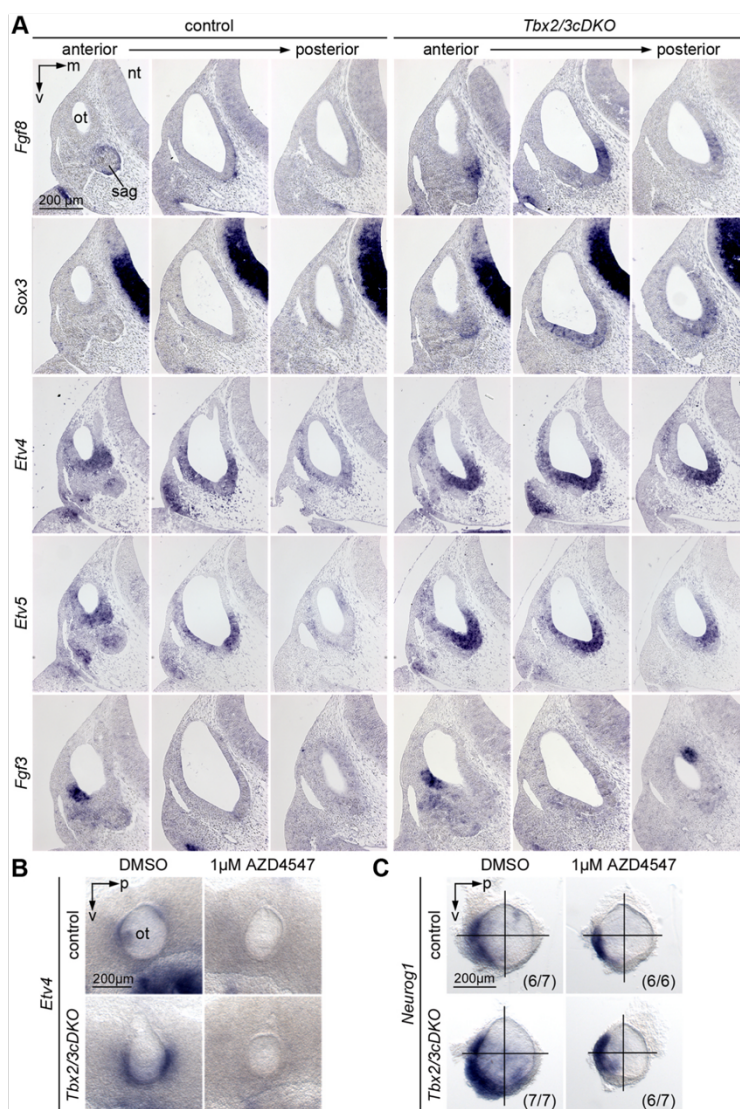


Fig. 7. Ectopic FGF signalling contributes to posterior-ventral expansion of *Neurog1* expression in *Tbx2/3cDKO* otocysts. (A,B) RNA *in situ* hybridisation analysis of expression of FGF ligand genes (*Fgf8*, *Fgf3*), target genes of FGF signalling (*Etv4*, *Etv5*) and of the proneural gene *Sox3* on transverse sections of E10.5 control and *Tbx2/3cDKO* otocysts at the anterior, mid-transverse and posterior region. (B,C) Right and left halves of embryonic heads were explanted from E9.5 control and *Tbx2/3cDKO* embryos and cultured for 24 h in the presence of 1 µM AZD4547, an FGF receptor inhibitor, or DMSO, the solvent. The explants were then analysed by whole-mount RNA *in situ* hybridisation using probes against *Etv4* (B) and *Neurog1* (C). For better visualisation, otocysts were dissected before documentation. Numbers in C indicate the fraction of analysed specimens showing the representative staining. m, medial; nt, neural tube; ot, otocyst; p, posterior; sag, statoacoustic ganglion; v, ventral.

other pathways important for otocyst patterning by RNA *in situ* hybridisation of known targets in E10.5 *Tbx2/3cDKO* otocysts (Fig. S9). *Id3*, target of BMP signalling (Hollnagel et al., 1999), was lost from the posterior-ventral and downregulated in the dorsal region. *Bmp4*, a ligand of this pathway, was ectopically expressed in the dorsolateral otocyst, but its expression was lost at ventro-medial sides in the posterior region. *Axin2*, a target of WNT signalling (Jho et al., 2002), was weakly expanded from the dorso-medial into the ventro-medial region whereas ventral expression of *Ptch1*, a target of SHH signalling (Ingham and McMahon, 2001), was slightly reduced in this region in *Tbx2/3cDKO* otocysts. *Rarb*, a target of RA signalling (Mendelsohn et al., 1991), was found neither in control nor in *Tbx2/3cDKO* otocysts.

At E9.5, expression of *Etv4* and *Etv5* indicated FGF signalling in the entire medial region of control otocysts. In *Tbx2/3cDKO*

otocysts, expression of both genes was enhanced and laterally expanded, correlating with ectopic *Fgf3* expression in this region. *Fgf8* expression was not detected at this stage (Fig. S10A). BMP, WNT, SHH and RA signalling were marginally affected (Fig. S10B). We conclude that ectopic neurogenesis in the posterior-ventral region of E10.5 *Tbx2*-deficient otocysts coincides with ectopic *Fgf8* expression and FGF signalling at this stage.

We used pharmacological inhibition to determine whether increased FGF signalling contributes to ectopic neurogenesis in *Tbx2/3cDKO* mutants (Fig. 7B,C). Halves of E9.5 embryo heads were cultured in the presence of the highly selective FGFR inhibitor AZD4547 (1 µM in DMSO) (Gavine et al., 2012; Gudernova et al., 2016), or with DMSO vehicle as a control. After 24 h of treatment, expression of *Etv4* was abolished in wild-type and *Tbx2/3cDKO* otocysts, validating the assay in this tissue (Fig. 7B). Upon

AZD4547 treatment, expression of *Neurog1* was restricted to the anterior-ventral domain in both control and *Tbx2/3cDKO* otocysts, suggesting that TBX2 restricts neurogenesis to the anterior-ventral otocyst after E9.5 by suppression of posterior-ventral FGF signalling (Fig. 7C).

DISCUSSION

***Tbx2* and *Tbx3* exert unique and redundant functions in early inner ear development**

The T-box transcription factors TBX2 and TBX3 regulate a diverse set of developmental programmes. Here, we have extended their functional analysis in mouse development and found that they are individually and combinatorially required for the formation of the cochlea and the vestibular organ. Our morphological analysis revealed strong hypoplasia of the cochlea and the endolymphatic duct combined with moderate vestibular defects in *Tbx2cKO* embryos, hypodysplasia of the semicircular canals in *Tbx3cKO* embryos and indiscernible cochlear and vestibular structures in *Tbx2/3cDKO* embryos shortly before birth. These morphological defects were preceded by markedly increased apoptosis in the ventral otocyst of *Tbx2cKO* and *Tbx2/Tbx3cDKO*, and in the dorsolateral domain of *Tbx2/3cDKO*, as well as by ectopic posterior-ventral neurogenesis in *Tbx2*-deficient otocysts. These individual and combined defects reflect the unique and overlapping sites of expression of the two genes in the early otocyst, i.e. of *Tbx2* in the dorsal-medial and ventral region, of *Tbx3* in the dorsal region, and of *Tbx2* and *Tbx3* in the central and ventro-medial region, from which the epithelial ducts and chambers of the membranous labyrinth arise in a region-specific manner. Similar to other developmental contexts (Aydoğdu et al., 2018; Lüdtke et al., 2016; Mesbah et al., 2012; Singh et al., 2012; Zirzow et al., 2009), *Tbx2* and *Tbx3* therefore have individual as well as redundant functions in early inner ear development depending on their co-expression patterns.

In humans, heterozygous mutations of *TBX2* have been associated with vertebral anomalies, and variable endocrine and T-cell dysfunctions (Liu et al., 2018), and heterozygous mutations of *TBX3* have been linked to ulnar-mammary syndrome (Bamshad et al., 1997). In neither case were deficits in hearing and balance reported. Our findings, together with recent reports that the heterozygous loss of several genes, including *TBX2*, in a microdeletion at 17q23.1q23.2 is associated with sensorineural hearing loss in humans (Ballif et al., 2010; Nimmakayalu et al., 2011) suggest that it might be beneficial to screen individuals with known mutations in *TBX2* or *TBX3* for subtle defects of inner ear functions.

***Tbx2* and *Tbx3* exert crucial patterning functions in early inner ear development**

Our morphological analysis of midgestation stages revealed that inner ear defects in *Tbx2* and *Tbx3* single and double mutant embryos manifested around E10.5, indicating that *Tbx2/Tbx3* are not involved in formation of the otic placode and the otocyst but are required for the subsequent regionalised outgrowth of the otic epithelium. Although *Tbx2* and *Tbx3* have been implicated in the maintenance of cell proliferation by direct repression of cell cycle inhibitors *in vitro* and *in vivo* (Brummelkamp et al., 2002; Jacobs et al., 2000; Lingbeek et al., 2002; Lüdtke et al., 2013), neither our BrdU assay nor our transcriptional profiling provided support for reduced proliferation as a cause of morphogenetic impairment in *Tbx2/3cDKO* otocysts. However, we detected a massive increase in apoptotic cells in the dorso-lateral and ventro-lateral aspects of the *Tbx2/3cDKO* otocyst at E10.5, and in the ventral otocyst at E11.5,

arguing that increased apoptosis depletes the epithelial progenitor pool required for localised outgrowth of the epithelial ducts and chambers similar to other mouse mutants with morphogenetic defects in the inner ear (Merlo et al., 2002; Vitelli et al., 2003; Xu et al., 1999; Zheng et al., 2003).

Involvement of *Tbx2* and *Tbx3* in the negative regulation of apoptosis has been demonstrated in several contexts (Du et al., 2017; Singhvi et al., 2008). However, we think that apoptosis, and hence morphogenetic impairment in the mutant otocyst, is secondary to a disturbed establishment of regional identities. Apoptosis at E10.5 was found in regions that exhibited specific loss or reduction of regional markers, including *Aldh1a2*, *Gata3*, *Hmx3* and *Lmo4* in the dorso-lateral, and *Otx1* and *Otx2* in the ventro-lateral otocyst, that have been implicated in vestibular morphogenesis (Deng et al., 2010; Karis et al., 2001; Morsli et al., 1999; Wang et al., 1998). Apoptosis in the ventral region of *Tbx2cKO* and *Tbx2/3cDKO* otocysts at E11.5 was preceded by gain of a neurogenic programme and by loss or reduction of genes that are essential for cochlear outgrowth (*Gata3*, *Gdf6*, *Fgf10*) (Bademci et al., 2020; Karis et al., 2001; Urness et al., 2015), and possibly for survival of delaminating neuroblasts (*Fgf10*) (Pirvola et al., 2000; Vázquez-Echeverría et al., 2008).

Previous work implicated WNT signals from the dorsal hindbrain and SHH signals from the ventral hindbrain and notochord in the establishment of dorsal or ventral fates, respectively, in the otocyst. These signals induce regionalised expression of transcription factor genes such as *Dlx5/6*, *Hmx2/3* and *Gbx2* (dorsal) and *Pax2* and *Otx2* (ventral) that regulate distinct morphogenetic subprogrammes along the dorso-ventral axis of the otocyst (Hatch et al., 2007; Ohta et al., 2016; Pirvola et al., 2000; Riccomagno et al., 2002, 2005). Our expression analysis characterised weak yet discernible expansion of WNT signalling into ventro-medial regions, a downregulation of ventral SHH signalling, and a loss of *Otx1/Otx2* expression in the ventro-lateral otocyst of *Tbx2/Tbx3cDKO* embryos at E10.5, suggesting a (partial) reduction of ventral and a possible expansion of dorsal fates. However, many ventral genes, including *Six1*, *Eya1*, *Pax2*, *Gata3*, were still expressed and dorsal genes, including *Dlx5*, *Gbx2*, *Aldh1a2*, *Smpx*, were not ventrally expanded, but reduced in their dorsal expression indicating that dorso-ventral polarity was normally established and that changes in the activity of WNT and SHH signalling contribute only in a minor fashion to the morphogenetic defects of *Tbx2/3cDKO* otocysts.

In contrast, we think that altered BMP and FGF signalling may impact on axial patterning and regionalisation in *Tbx2/3cDKO* otocysts. Loss- and gain-of-function experiments in chicken and mouse demonstrated that dorsal BMP signalling is both required and sufficient to mediate a dorsal vestibular fate, possibly via induction of *Dlx5* and *Hmx3*, and by repression of SHH-dependent ventral genes (Chang et al., 2008; Gerlach et al., 2000; Ohta and Schoenwolf, 2018; Ohta et al., 2016). Given the dorsal downregulation of *Id3* expression in *Tbx2/3cDKO* otocysts, and hence of BMP signalling, it is likely that reduced expression of some dorsal genes, including *Hmx3*, can be attributed to changes in this pathway. Loss of *Fgf3* from the hindbrain leads to a failure of endolymphatic duct and common crus formation, accompanied by epithelial dilatation and reduced cochlear coiling (Hatch et al., 2007). FGF10 derived from the developing cristae affects vestibular morphogenesis (Pauley et al., 2003). Conceivably, ectopic expression of *Fgf8* in the ventral and of *Fgf3* in the posterior-dorso-medial region of *Tbx2/3cDKO* otocysts may constitute novel signalling centres that directly interfere with regionalisation along the otocyst axes, and/or affect the activity of other signalling

pathways, particularly BMP signalling, required for otocyst patterning as shown in many other developmental contexts (reviewed by Schliermann and Nickel, 2018; Teven et al., 2014). We conclude that TBX2 and TBX3 are essential regulators of signalling activities that confer regional identities important for localised outgrowth in the otocyst.

TBX2 restricts otic neurogenesis via repression of posterior FGF signalling and maintenance of *Tbx1*

Neurogenesis is initiated in the entire ventral half of the otocyst and becomes restricted to a small anterior-ventral region until E10.5 (Raft et al., 2004). Our analysis showed that neurogenesis was correctly initiated in the entire ventral region of *Tbx2/3cDKO* otocysts at E9.5 but failed to restrict to the anterior subregion at E10.5. Such a phenotype can be conceptualised by maintenance or establishment of a neural inducer in the posterior subregion and/or lack of a posterior repressor of this programme.

Previous studies in the mouse but also in other vertebrates provided ample evidence that FGF signals provide an initial cue for neural specification both in the otic but also in other sensory placodes (reviewed by Lassiter et al., 2014; Maier et al., 2014). Pharmacological inhibition of FGF signalling in cultured mouse otocysts abolished formation of *Neurog1*⁺ neuroblasts (Brown and Epstein, 2011), and loss of *Fgf3*, which is expressed in the neurosensory domain, disturbed otic ganglion formation (Mansour et al., 1993). In chicken, *Fgf10*, which is also expressed in the neurosensory domain, specifies neuronal fate (Alsina et al., 2004), and treatment with FGF2 enhances neuronal differentiation via an unknown mechanism (Adamska et al., 2001). In zebrafish, *fgf3* and *fgf8* are implicated in the specification of otic neuroblasts (Vemaraju et al., 2012).

In *Tbx2*-deficient otocysts, we detected ectopic FGF signalling in the posterior-ventral region at E9.5 and E10.5. At E9.5, ectopic FGF signalling correlated with posteriorly expanded *Fgf3* expression, whereas at E10.5 we detected ectopic *Fgf8* expression, which coincided with the posterior expansion of the neurogenic domain and ectopic induction of the neurosensory competence factor *Sox3*. Additionally, pharmacological inhibition of FGF signalling after E9.5 abrogated ectopic expression of *Neurog1* in the posterior-ventral otocyst, suggesting that *Tbx2* is required to repress FGF-induced neuronal competence in the posterior-ventral otocyst. Lack of reduction of *Neurog1* expression at the anterior otocyst may reflect that neurogenesis on this side depends on a different regulatory programme, or that the neurogenic lineage has already been determined and no longer needs FGF signalling at this stage. The discrepancy compared with an earlier report (Brown and Epstein, 2011) may be due to usage of a different inhibitor under different experimental conditions.

In contrast to chicken, in which FGF8-mediated signalling induces otic neurogenic fate via induction of the proneural gene *Sox3* (Abelló et al., 2010) or zebrafish, in which *sox3* promotes neural competence in the otic epithelium (Gou et al., 2018), neither *Fgf8* nor *Sox3* have been associated with otic neurogenesis in the mouse. *Fgf8* is expressed in maturing neuroblasts after delamination but is absent from the otic epithelium, as is *Sox3* (Vitelli et al., 2003; this study). Hence, ectopic neural competence in *Tbx2/3cDKO* otocysts may be due to de-repression of an *Fgf8-Sox3/Sox2-Neurog1* regulatory module that has been lost in mammalian evolution.

Concomitant with the upregulation of FGF signalling, we detected reduced BMP signalling in the posterior-ventral region of *Tbx2/3cDKO* otocysts, indicating a signalling antagonism similar to other biological settings (reviewed by Schliermann and Nickel,

2018). BMP signalling has been implicated in the inhibition of neurogenesis in many developmental contexts (Bond et al., 2012; Imayoshi and Kageyama, 2014; Shou et al., 1999). However, pharmacological inhibition of BMP signalling and activation of the pathway by overexpression of a constitutively active ALK3 at the otic placode stage in chick embryos caused a downregulation and anterior expansion of the posterior marker *Lmx1b*, respectively, but had no effect on the establishment of the neurogenic fate (Abelló et al., 2010). We, therefore, posit that loss of ventral BMP signalling in *Tbx2/3cDKO* otocysts does not directly account for the expansion of neurogenesis.

Previous work demonstrated that *Tbx1* is both essential and sufficient to restrict neural fate to the anterior-ventral otocyst (Raft et al., 2004; Xu et al., 2007). Loss of *Tbx1* expression in the posterior-ventral region of *Tbx2*-deficient otocysts at E10.5, is therefore likely to contribute in a major fashion to the observed phenotypic changes. Our analyses revealed ventral apoptosis (Fig. S11) and expanded posterior FGF signalling in *Tbx1KO* otocysts, similar to *Tbx2/3cDKO* mutants. However, ectopic posterior expression of *Fgf8* and *Sox3* and strong ventral induction of FGF signalling did not occur in *Tbx1KO* otocysts, indicating a functional diversity between TBX1 and TBX2.

In different contexts, FGF and RA have been shown to act antagonistically (Diez del Corral and Storey, 2004; Marklund et al., 2004), suggesting that FGF inhibits RA-mediated *Tbx1* induction. However, normal expression of *Tbx1* at E9.5 argues against such a scenario. Given the similar expression patterns of *Tbx1* and *Id3* in controls as well as loss of *Tbx1* expression and BMP signalling in the posterior-ventral otocyst of E10.5 *Tbx2/3cDKO* embryos, it is tempting to speculate that induction of *Fgf8* expression leads to reduced BMP signalling which, in turn, causes loss of *Tbx1*. Irrespective of the precise mechanism, our findings add to the overarching theme that TBX1, TBX2, TBX3 and most other T-box transcription factors act in cross-regulatory networks in a variety of developmental settings (Goering et al., 2003; Greulich et al., 2011; Mesbah et al., 2012; Sheeba and Logan, 2017).

In summary, we suggest that in *Tbx2*-deficient otocysts ectopic FGF signalling accounts for posterior expansion of the neurogenic region in a dual manner. First, FGF signalling activates the neurogenic regulatory network via *Sox3* and *Neurog1*. Second, FGF signalling leads to repression of the neural repressor *Tbx1*, possibly via reduced BMP signalling (Fig. 8).

TBX2 may directly repress *Fgf8* and other neuronal genes

Given the upregulation of *Fgf8* and *Fgf3*, and a possible role of FGF signalling in inducing the loss of *Tbx1* and the gain of neurogenesis in *Tbx2/3cDKO* otocysts, it is tempting to speculate that TBX2 directly represses *Fgf8* and/or other FGF ligand genes. In order to identify TBX2 target genes, we performed a ChIP-seq experiment from more than 1000 E10.5 otocysts. Possibly owing to the paucity of tissue or antibody limitations, we failed to enrich for TBX2-bound fragments. However, interrogation of the web-platform ChIP-Atlas (chip-atlas.org; Oki et al., 2018) in which ChIP-Seq data sets for mouse and human tissues are deposited, identified TBX2/TBX3 bound genomic regions associated with *Fgf8* (Tables S8–S10). Moreover, the web-tool oPOSSUM (opossum.cisreg.ca; Kwon et al., 2012) revealed evolutionarily conserved binding sites for TBX proteins in *Fgf8* (Tables S8 and S11). These *in silico* data, together with the finding that TBX1 binds to and transactivates an ultraconserved cis-regulatory element downstream of *Fgf8* (Castellanos et al., 2014), supports the notion that *Fgf8* might present a direct target of TBX2 repressive activity in the otocyst.

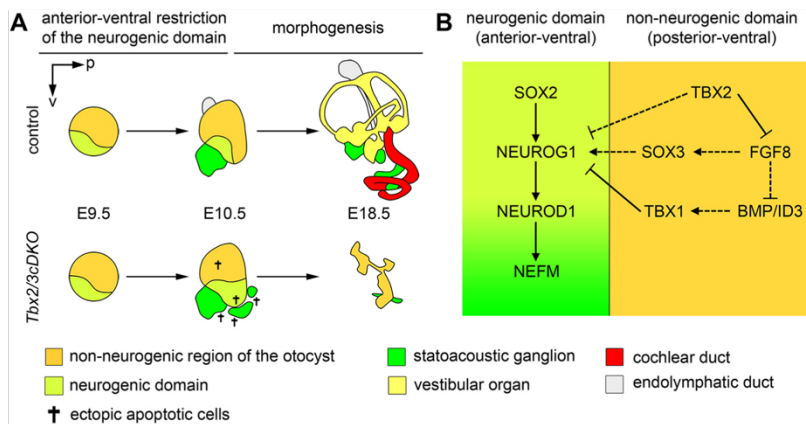


Fig. 8. Model of the role of TBX2 and TBX3 in early inner ear development. (A) Combined loss of *Tbx2* and *Tbx3* leads to a failure in the anterior-ventral restriction of the neurogenic domain between E9.5 and E10.5, increased apoptosis and impairment of inner ear morphogenesis thereafter. (B) Possible interaction of TBX2 and the neurogenic gene regulatory network. Dashed lines indicate as-yet hypothetical relationships. p, posterior; v, ventral.

Interestingly, additional neuronal genes with increased expression in *Tbx2/3cDKO* otocysts are associated with TBX2/TBX3 ChIP peaks in other tissues (*Pou4f1*, *Nefm*, *Nefl*, *Foxn4*, *Dll1*, *Insm1*, *Nhlh2*, *Neurog1*, *Neurod1*), and harbour TBX-binding sites (*Pou4f1*, *Dll1*, *Neurod1*) (Tables S8-S11), suggesting that TBX2 suppresses the neurogenic gene regulatory network at multiple levels beyond the repression of *Fgf8* and the (indirect) maintenance of *Tbx1*. Supporting that notion, recent work showed that TBX3 represses NEUROD1 target genes via DNA binding in the absence of NEUROD1, thereby suppressing the neuronal lineage, but is displaced from cis-regulatory regions once NEUROD1 binds (Pataskar et al., 2016).

We conclude that TBX2 and TBX3 are novel regulators of otocyst patterning and that TBX2 exerts its function in the posterior-ventral region at least partly by repression of a neurogenic gene regulatory network.

MATERIALS AND METHODS

Mice and genotyping

Mice carrying a null allele of *Tbx1* (*Tbx1^{tm1Pa}*) (Jerome and Papaioannou, 2001), mice with a conditional floxed allele of *Tbx2* (*Tbx2^{tm2.1Vmc}*, synonym *Tbx2^{lox}*) (Wakker et al., 2010) or *Tbx3* (*Tbx3^{tm1Pa}*, synonym *Tbx3^{lox}*) (Frank et al., 2013), the double fluorescent Cre reporter line *Gt(ROSA)26Sor^{tm4}(ACTB-IdTomato,-EGFP)^{Luo/J}* (synonym *R26^{mtmG}*) (Muzumdar et al., 2007) and the transgenic cre driver line *Tg(Pax2-cre)1AKis* (synonym *Pax2-cre*) (Trowe et al., 2011) were maintained on an NMRI outbred background. Embryos for *Tbx2* and *Tbx3* gene expression analyses were derived from matings of NMRI wild-type mice. *Pax2-cre/+*; *Tbx2^{lox/lox}*; *Tbx3^{lox/lox}*; *R26^{mtmG}/+* (*Tbx2/3cDKO*) mice were obtained from matings of *Pax2-cre/+*; *Tbx2^{lox/+}*; *Tbx3^{lox/+}* males and *Tbx2^{lox/lox}*; *Tbx3^{lox/lox}*; *R26^{mtmG}/mtmG* females. For generation of *Pax2-cre/+*; *Tbx2^{lox/lox}* (*Tbx2cKO*) embryos, *Pax2-cre/+*; *Tbx2^{lox/+}* males were mated to *Tbx2^{lox/lox}* females. *Pax2-cre/+*; *Tbx3^{lox/lox}* (*Tbx3cKO*) mice were obtained from matings of *Pax2-cre/+*; *Tbx3^{lox/+}* males and *Tbx3^{lox/lox}* females. For conditional mutant mice, *cre*-negative littermates served as controls. *Tbx1*-deficient embryos were generated from matings of *Tbx1/+* animals. The presence of a vaginal plug on the morning after mating defined midday as time of fertilisation; noon was correspondingly defined as E0.5. Pregnant females were sacrificed by cervical dislocation. Embryos were dissected in PBS, fixed in 4% paraformaldehyde (PFA)/PBS overnight and stored in 100% methanol at -20°C until use. Somite numbers were used for embryo staging. Genotyping was carried out by PCR on genomic DNA prepared from embryonic tissues or ear clips.

All animal work conducted for this study was performed according to European and German legislation. The breeding and handling of mice lines was approved by the Niedersächsisches Landesamt für Verbraucherschutz und Lebensmittelsicherheit (permit number AZ33.12-42502-04-13/1356).

Histological and immunofluorescence analyses

For histological analysis, 5- μm -thick paraffin sections were stained with Haematoxylin and Eosin or with Alcian Blue and Eosin. 3D reconstruction of stained serial sections was performed with the Amira software (version 5.3.3, ThermoFisher Scientific).

For detection of antigens on 5- μm -thick paraffin sections, labelling with primary antibodies was performed at 4°C overnight after antigen retrieval (15 min at 100°C ; H-3300, Vector Laboratories), blocking of endogenous peroxidases with 3% H_2O_2 /PBS for 15 min and incubation in blocking buffer (TNB) provided by the Tyramide Signal Amplification (TSA) kit (NEL702001KT, Perkin Elmer) for 45 min. The following primary antibodies were used: rabbit-anti-TBX2 (1:4000, 07-318, Merck Millipore), polyclonal goat-anti-TBX3 (1:500, sc-31656, Santa Cruz Biotechnology), polyclonal rabbit-anti-cleaved CASPASE-3 (1:400, 9661, Cell Signaling Technology), monoclonal mouse-anti-GFP (1:250, 11814460001, Roche). Primary antibodies were visualised with either biotinylated Fab fragment goat-anti-rabbit IgG (1:200, 111-067-003, Dianova), biotinylated donkey-anti-goat IgG (1:200, 705-065-147, Dianova) and the TSA system (NEL702001KT, Perkin Elmer) or Alexa 488-conjugated donkey-anti-mouse IgG (1:200, A21202, Invitrogen). Nuclei were counterstained with 4',6-diamidino-2-phenylindole (DAPI, 6335.1, Carl Roth) according to the manufacturer's instruction. At least three specimens of each genotype were used for each experiment.

Proliferation and apoptosis assays

Cell proliferation rates were investigated by the detection of incorporated BrdU on 5- μm -thick transverse paraffin sections according to published protocols (Bussen et al., 2004). For each specimen ($n=6$ per genotype), eight adjacent sections were assessed. The BrdU labelling index was defined as the number of BrdU-positive nuclei relative to the total number of nuclei as detected by DAPI counterstaining in arbitrarily defined regions. Statistical analysis was performed using the two-tailed Student's *t*-test. Data were expressed as mean \pm s.d. Differences were considered significant when the *P*-value was below 0.05. Apoptosis was assessed by TUNEL assay using the ApopTag Plus In Situ Apoptosis Fluorescein Detection Kit (S7111, Merck Millipore) and by anti-cleaved CASPASE-3 staining on at least three specimens per genotype.

RNA in situ hybridisation analysis

Whole-mount RNA *in situ* hybridisation was performed following a standard procedure with digoxigenin-labelled antisense riboprobes (Wilkinson and Nieto, 1993). Stained specimens were transferred to 80% glycerol prior to documentation. RNA *in situ* hybridisation on 10- μm -thick paraffin sections (5- μm -thick paraffin sections for reconstructions) was performed as previously described (Moorman et al., 2001). For each marker at least three independent specimens were analysed. Primers for PCR amplification of new DNA templates for *in vitro* transcription of RNA probes are listed in Table S12.

Organ culture

For explant cultures of otocysts, the part anterior of the 4th branchial arch of E9.0-E9.5 (23-28 somites) embryos was dissected and cut in half along the neural tube in L-15 Leibovitz medium (F1315, Biochrom). The tissue pieces were placed on 0.4 µm polyester membrane Transwell supports (3450, Corning) with the medial side down, and incubated at 37°C and 5% CO₂ in organ culture medium (DMEM/F12) (21331-020, ThermoFisher Scientific) supplemented with 10% fetal calf serum (S0115, Biochrom), 100 units/ml penicillin/100 µg/ml streptomycin (15140-122, ThermoFisher Scientific), 1 mM sodium pyruvate (11360-039, ThermoFisher Scientific), 1× MEM NEAA (11140-035, ThermoFisher Scientific) and 1× GlutaMAX (35050-038, ThermoFisher Scientific) at the air-liquid interface for 24 h. For inhibition of FGF signalling, AZD4547 (HY-13330, MedChemExpress) was added to the medium at a final concentration of 1 µM. At the end of the culture period, the tissue was fixed in 4% PFA overnight at 4°C, and then processed for whole-mount RNA *in situ* hybridisation. Otocysts were punctured to avoid probe trapping.

Microarray experiments and data analysis

Total RNA was extracted from pools of otocysts ($n=14-18$) mechanically dissected from E10.5 control and *Tbx2/3cDKO* embryos using the peqGOLD RNAPure reagent (732-3312, Peqlab) and sent to the Research Core Unit Transcriptomics of Hannover Medical School where it was hybridised to Agilent Whole Mouse Genome Oligo v2 (4×44 K) Microarrays (G4846A, Agilent Technologies) in a dual-colour mode. Data were averaged from four independent biological samples per genotype.

Log2-converted expression data were imported into Qlucore Omics Explorer (version 3.6, Lund, Sweden) and normalised (mean=0, Var=1). For the identification of deregulated genes, probe sets with the highest values for a gene were used in a two-group comparison (*t*-test). Genes with a FDR-adjusted *P*-value (*q*-value) < 0.05 were considered deregulated, and further subjected to filtering using a signal intensity threshold (≥ 100 either for control or mutant pool) and a fold change threshold ($FC \geq 2$, $FC \leq -2$). Functional enrichment analysis was performed using DAVID 6.8 software (Huang et al., 2009a,b), and terms were selected based on Gene Functional Annotation Clustering on GO-BP-FAT annotations, 'medium' stringency and final group membership of ≥ 5 .

For the prediction of direct target genes of TBX2/TBX3, we used the 'Target Genes' tool of the public ChIP-seq database ChIP-Atlas (<http://chip-atlas.org>) (Oki et al., 2018). MACS2 scores for all genes were retrieved for TBX2 (in human, hg38) and TBX3 (in mouse, mm10) (setting 'Distance from TSS': ± 10 kb), and joined to genes upregulated in our microarray based on the gene symbol. Evolutionarily conserved T-box transcription factor-binding sites were identified using the oPOSSUM3 software (<http://opossum.cisreg.ca>) (Kwon et al., 2012) using the JASPAR Core profile for Brachyury (T) and 10 kb up/downstream sequence.

Documentation

Sections were photographed using a Leica DM5000 microscope with a Leica DFC300FX digital camera. Whole-mount specimens were photographed on a Leica M420 with Fujix digital camera HC-300Z. All images were processed in Adobe Photoshop CS4.

Statistical analysis

Results are expressed as mean \pm s.d. Normal distribution of data was tested by Shapiro-Wilk test ($P > 0.05$) and Q-Q-plots. For comparison of two groups, an unpaired two-tailed Student's *t*-test was performed. $P < 0.05$ was considered statistically significant. Statistical analyses were performed using Microsoft Excel (version 16.16.24) and JASP (version 0.13.1).

Acknowledgements

We thank Robert Kelly (Marseille) for the *Tbx1* mice and the Research Core Unit Transcriptomics of Hannover Medical School for microarray analysis.

Competing interests

The authors declare no competing or financial interests.

Author contributions

Conceptualization: A.K., M.-O.T.; Formal analysis: M.K., A.K., M.-O.T.; Investigation: M.K., I.W., C.R., T.H.L., M.-O.T.; Resources: V.M.C., A.M.; Data curation: M.K., M.-O.T.; Writing - original draft: M.K., A.K., M.-O.T.; Writing - review & editing: M.K., I.W., C.R., T.H.L., V.M.C., A.M., A.K., M.-O.T.; Visualization: M.K.; Supervision: A.K., M.-O.T.; Project administration: M.-O.T.; Funding acquisition: M.-O.T.

Funding

This work was supported by the German Research Council (Deutsche Forschungsgemeinschaft) [DFG TR1325/1-1 to M.-O.T.]

Data availability

Microarray data have been deposited in Gene Expression Omnibus under accession number GSE154305.

Peer review history

The peer review history is available online at <https://journals.biologists.com/dev/article-lookup/doi/10.1242/dev.195651>

References

- Abelló, G., Khatri, S., Radosevic, M., Scotting, P. J., Giraldez, F. and Alsina, B. (2010). Independent regulation of Sox3 and Lmx1b by FGF and BMP signaling influences the neurogenic and non-neurogenic domains in the chick otic placode. *Dev. Biol.* **339**, 166-178. doi:10.1016/j.ydbio.2009.12.027
- Adamska, M., Herbrand, H., Adamski, M., Krüger, M., Braun, T. and Bober, E. (2001). FGFs control the patterning of the inner ear but are not able to induce the full ear program. *Mech. Dev.* **109**, 303-313. doi:10.1016/S0925-4773(01)00550-0
- Agulnik, S. I., Garvey, N., Hancock, S., Ruvinsky, I., Chapman, D. L., Agulnik, I., Bollag, R., Papaioannou, V. and Silver, L. M. (1996). Evolution of mouse T-box genes by tandem duplication and cluster dispersion. *Genetics* **144**, 249-254. doi:10.1093/genetics/144.1.249
- Alsina, B. and Whitfield, T. T. (2017). Sculpting the labyrinth: morphogenesis of the developing inner ear. *Semin. Cell Dev. Biol.* **65**, 47-59. doi:10.1016/j.semdcb.2016.09.015
- Alsina, B., Abelló, G., Ulloa, E., Henrique, D., Pujades, C. and Giraldez, F. (2004). FGF signaling is required for determination of otic neuroblasts in the chick embryo. *Dev. Biol.* **267**, 119-134. doi:10.1016/j.ydbio.2003.11.012
- Aydoğdu, N., Rudat, C., Trowe, M.-O., Kaiser, M., Lüdtkke, T. H., Taketo, M. M., Christoffels, V. M., Moon, A. and Kispert, A. (2018). TBX2 and TBX3 act downstream of canonical WNT signaling in patterning and differentiation of the mouse ureteric mesenchyme. *Development* **145**, dev171827. doi:10.1242/dev.171827
- Bademci, G., Abad, C., Cengiz, F. B., Seyhan, S., Incesulu, A., Guo, S., Fitöz, S., Atli, E. I., Gosstola, N. C., Demir, S. et al. (2020). Long-range cis-regulatory elements controlling GDF6 expression are essential for ear development. *J. Clin. Invest.* **130**, 4213-4217. doi:10.1172/JCI136951
- Ballif, B. C., Theisen, A., Rosenfeld, J. A., Traylor, R. N., Gastier-Foster, J., Thrush, D. L., Astbury, C., Bartholomew, D., McBride, K. L., Pyatt, R. E. et al. (2010). Identification of a recurrent microdeletion at 17q23.1q23.2 flanked by segmental duplications associated with heart defects and limb abnormalities. *Am. J. Hum. Genet.* **86**, 454-461. doi:10.1016/j.ajhg.2010.01.038
- Bamshad, M., Lin, R. C., Law, D. J., Watkins, W. S., Krakowiak, P. A., Moore, M. E., Franceschini, P., Lala, R., Holmes, L. B., Gebuhr, T. C. et al. (1997). Mutations in human TBX3 alter limb, apocrine and genital development in ulnar-mammary syndrome. *Nat. Genet.* **16**, 311-315. doi:10.1038/ng0797-311
- Barrionuevo, F., Naumann, A., Bagheri-Fam, S., Speth, V., Taketo, M. M., Scherer, G. and Neubüser, A. (2008). Sox9 is required for invagination of the otic placode in mice. *Dev. Biol.* **317**, 213-224. doi:10.1016/j.ydbio.2008.02.011
- Bok, J., Raft, S., Kong, K.-A., Koo, S. K., Dräger, U. C. and Wu, D. K. (2011). Transient retinoic acid signaling confers anterior-posterior polarity to the inner ear. *Proc. Natl. Acad. Sci. USA* **108**, 161-166. doi:10.1073/pnas.1010547108
- Bollag, R. J., Siegfried, Z., Cebra-Thomas, J. A., Garvey, N., Davison, E. M. and Silver, L. M. (1994). An ancient family of embryonically expressed mouse genes sharing a conserved protein motif with the T locus. *Nat. Genet.* **7**, 383-389. doi:10.1038/ng0794-383
- Bond, A. M., Bhalala, O. G. and Kessler, J. A. (2012). The dynamic role of bone morphogenetic proteins in neural stem cell fate and maturation. *Dev. Neurobiol.* **72**, 1068-1084. doi:10.1002/dneu.22022
- Brooker, R., Hozumi, K. and Lewis, J. (2006). Notch ligands with contrasting functions: Jagged1 and Delta1 in the mouse inner ear. *Development* **133**, 1277-1286. doi:10.1242/dev.02284
- Brown, A. S. and Epstein, D. J. (2011). Otic ablation of smoothened reveals direct and indirect requirements for Hedgehog signaling in inner ear development. *Development* **138**, 3967-3976. doi:10.1242/dev.066126
- Brummelkamp, T. R., Kortlever, R. M., Lingbeek, M., Trettel, F., MacDonald, M. E., van Lohuizen, M. and Bernards, R. (2002). TBX-3, the gene mutated in Ulnar-Mammary Syndrome, is a negative regulator of p19ARF and inhibits senescence. *J. Biol. Chem.* **277**, 6567-6572. doi:10.1074/jbc.M110492200

- Bussen, M., Petry, M., Schuster-Gossler, K., Leitges, M., Gossler, A. and Kispert, A. (2004). The T-box transcription factor Tbx18 maintains the separation of anterior and posterior somite compartments. *Genes Dev.* **18**, 1209-1221. doi:10.1101/gad.300104
- Carney, P. R. and Silver, J. (1983). Studies on cell migration and axon guidance in the developing distal auditory system of the mouse. *J. Comp. Neurol.* **215**, 359-369. doi:10.1002/cne.902150402
- Carreira, S., Dexter, T. J., Yavuzer, U., Easty, D. J. and Goding, C. R. (1998). Brachyury-related transcription factor Tbx2 and repression of the melanocyte-specific TRP-1 promoter. *Mol. Cell. Biol.* **18**, 5099-5108. doi:10.1128/MCB.18.9.5099
- Castellanos, R., Xie, Q., Zheng, D., Cvekl, A. and Morrow, B. E. (2014). Mammalian TBX1 preferentially binds and regulates downstream targets via a tandem T-site repeat. *PLoS ONE* **9**, e95151. doi:10.1371/journal.pone.0095151
- Chang, W., Lin, Z., Kulesha, H., Hebert, J., Hogan, B. L. M. and Wu, D. K. (2008). Bmp4 is essential for the formation of the vestibular apparatus that detects angular head movements. *PLoS ONE* **4**, e1000050. doi:10.1371/journal.pone.1000050
- Daudet, N., Ariza-McNaughton, L. and Lewis, J. (2007). Notch signalling is needed to maintain, but not to initiate, the formation of prosensory patches in the chick inner ear. *Development* **134**, 2369-2378. doi:10.1242/dev.001842
- Deng, M., Pan, L., Xie, X. and Gan, L. (2010). Requirement for Lmo4 in the vestibular morphogenesis of mouse inner ear. *Dev. Biol.* **338**, 38-49. doi:10.1016/j.ydbio.2009.11.003
- Diez del Corral, R. and Storey, K. G. (2004). Opposing FGF and retinoid pathways: a signalling switch that controls differentiation and patterning onset in the extending vertebrate body axis. *BioEssays* **26**, 857-869. doi:10.1002/bies.20080
- Du, W.-L., Fang, Q., Chen, Y., Teng, J.-W., Xiao, Y.-S., Xie, P., Jin, B. and Wang, J.-Q. (2017). Effect of silencing the T-Box transcription factor TBX2 in prostate cancer PC3 and LNCaP cells. *Mol. Med Rep* **16**, 6050-6058. doi:10.3892/mmr.2017.7361
- Frank, D. U., Emechebe, U., Thomas, K. R. and Moon, A. M. (2013). Mouse TBX3 mutants suggest novel molecular mechanisms for Ulnar-mammary syndrome. *PLoS ONE* **8**, e67841. doi:10.1371/journal.pone.0067841
- Gavine, P. R., Mooney, L., Kilgour, E., Thomas, A. P., Al-Kadhimi, K., Beck, S., Rooney, C., Coleman, T., Baker, D., Mellor, M. J. et al. (2012). AZD4547: an orally bioavailable, potent, and selective inhibitor of the fibroblast growth factor receptor tyrosine kinase family. *Cancer Res.* **72**, 2045-2056. doi:10.1158/0008-5472.CAN-11-3034
- Gerlach, L. M., Hutson, M. R., Germiller, J. A., Nguyen-Luu, D., Victor, J. C. and Barald, K. F. (2000). Addition of the BMP4 antagonist, noggin, disrupts avian inner ear development. *Development* **127**, 45-54.
- Goering, L. M., Hoshijima, K., Hug, B., Bisgrove, B., Kispert, A. and Grunwald, D. J. (2003). An interacting network of T-box genes directs gene expression and fate in the zebrafish mesoderm. *Proc. Natl. Acad. Sci. USA* **100**, 9410-9415. doi:10.1073/pnas.1633548100
- Gou, Y., Vemaraju, S., Sweet, E. M., Kwon, H.-J. and Riley, B. B. (2018). sox2 and sox3 play unique roles in development of hair cells and neurons in the zebrafish inner ear. *Dev. Biol.* **435**, 73-83. doi:10.1016/j.ydbio.2018.01.010
- Greulich, F., Rudat, C. and Kispert, A. (2011). Mechanisms of T-box gene function in the developing heart. *Cardiovasc. Res.* **91**, 212-222. doi:10.1093/cvr/cvr112
- Gudernova, I., Vesela, I., Balek, L., Buchtova, M., Dosedelova, H., Kunova, M., Pivnicka, J., Jelinkova, I., Roubalova, L., Kozubik, A. et al. (2016). Multikinase activity of fibroblast growth factor receptor (FGFR) inhibitors SU5402, PD173074, AZD1480, AZD4547 and BGJ398 compromises the use of small chemicals targeting FGFR catalytic activity for therapy of short-stature syndromes. *Hum. Mol. Genet.* **25**, 9-23. doi:10.1093/hmg/ddv441
- Hatch, E. P., Noyes, C. A., Wang, X., Wright, T. J. and Mansour, S. L. (2007). Fgf3 is required for dorsal patterning and morphogenesis of the inner ear epithelium. *Development* **134**, 3615-3625. doi:10.1242/dev.006627
- Haugas, M., Lilleväli, K., Hakonen, J. and Salminen, M. (2010). Gata2 is required for the development of inner ear semicircular ducts and the surrounding perilymphatic space. *Dev. Dyn.* **239**, 2452-2469. doi:10.1002/dvdy.22373
- Hollnagel, A., Oehlmann, V., Heymer, J., Rütger, U. and Nordheim, A. (1999). Id genes are direct targets of bone morphogenetic protein induction in embryonic stem cells. *J. Biol. Chem.* **274**, 19838-19845. doi:10.1074/jbc.274.28.19838
- Huang, D. W., Sherman, B. T. and Lempicki, R. A. (2009a). Systematic and integrative analysis of large gene lists using DAVID bioinformatics resources. *Nat. Protoc.* **4**, 44-57. doi:10.1038/nprot.2008.211
- Huang, D. W., Sherman, B. T., Zheng, X., Yang, J., Imamichi, T., Stephens, R. and Lempicki, R. A. (2009b). Extracting biological meaning from large gene lists with DAVID. *Curr. Protoc. Bioinformatics* **27**, 13.11.1-13.11.13. doi:10.1002/0471250953.bi1311s27
- Huebner, A. K., Gandia, M., Frommolt, P., Maak, A., Wicklein, E. M., Thiele, H., Altmüller, J., Wagner, F., Viñuela, A., Aguirre, L. A. et al. (2011). Nonsense mutations in SMPX, encoding a protein responsive to physical force, result in X-chromosomal hearing loss. *Am. J. Hum. Genet.* **88**, 621-627. doi:10.1016/j.ajhg.2011.04.007
- Imayoshi, I. and Kageyama, R. (2014). bHLH factors in self-renewal, multipotency, and fate choice of neural progenitor cells. *Neuron* **82**, 9-23. doi:10.1016/j.neuron.2014.03.018
- Ingham, P. W. and McMahon, A. P. (2001). Hedgehog signaling in animal development: paradigms and principles. *Genes Dev.* **15**, 3059-3087. doi:10.1101/gad.938601
- Jacobs, J. J. L., Keblusek, P., Robanus-Maandag, E., Kristel, P., Lingbeek, M., Nederlof, P. M., van Welsem, T., van de Vijver, M. J., Koh, E. Y., Daley, G. Q. et al. (2000). Senescence bypass screen identifies TBX2, which represses Cdkn2a (p19(ARF)) and is amplified in a subset of human breast cancers. *Nat. Genet.* **26**, 291-299. doi:10.1038/81583
- Jalali, A., Bassuk, A. G., Kan, L., Israsena, N., Mukhopadhyay, A., McGuire, T. and Kessler, J. A. (2011). HeyL promotes neuronal differentiation of neural progenitor cells. *J. Neurosci. Res.* **89**, 299-309. doi:10.1002/jnr.22562
- Jerome, L. A. and Papaioannou, V. E. (2001). DiGeorge syndrome phenotype in mice mutant for the T-box gene, Tbx1. *Nat. Genet.* **27**, 286-291. doi:10.1038/85845
- Jho, E.-H., Zhang, T., Domon, C., Joo, C.-K., Freund, J.-N. and Costantini, F. (2002). Wnt/beta-catenin/Tcf signaling induces the transcription of Axin2, a negative regulator of the signaling pathway. *Mol. Cell. Biol.* **22**, 1172-1183. doi:10.1128/MCB.22.4.1172-1183.2002
- Karis, A., Pata, I., van Doorninck, J. H., Grosveld, F., de Zeeuw, C. I., de Caprona, D. and Fritsch, B. (2001). Transcription factor GATA-3 alters pathway selection of olivocochlear neurons and affects morphogenesis of the ear. *J. Comp. Neurol.* **429**, 615-630. doi:10.1002/1096-9861(200110122)429:4<615::AID-CNE8>3.0.CO;2-F
- Kim, W.-Y. (2013). NeuroD regulates neuronal migration. *Mol. Cells* **35**, 444-449. doi:10.1007/s10059-013-0065-2
- Kim, W. Y., Fritsch, B., Serls, A., Bakel, L. A., Huang, E. J., Reichardt, L. F., Barth, D. S. and Lee, J. E. (2001). NeuroD-null mice are deaf due to a severe loss of the inner ear sensory neurons during development. *Development* **128**, 417-426.
- Kwon, A. T., Arenillas, D. J., Hunt, R. W. and Wasserman, W. W. (2012). oPOSSUM-3: advanced analysis of regulatory motif over-representation across genes or ChIP-Seq datasets. *G3 (Bethesda)* **2**, 987-1002. doi:10.1534/g3.112.003202
- Lassiter, R. N. T., Stark, M. R., Zhao, T. and Zhou, C. J. (2014). Signaling mechanisms controlling cranial placode neurogenesis and delamination. *Dev. Biol.* **389**, 39-49. doi:10.1016/j.ydbio.2013.11.025
- Lilleväli, K., Haugas, M., Matilainen, T., Pussinen, C., Karis, A. and Salminen, M. (2006). Gata3 is required for early morphogenesis and Fgf10 expression during otic development. *Mech. Dev.* **123**, 415-429. doi:10.1016/j.mod.2006.04.007
- Lin, Z., Cantos, R., Patente, M. and Wu, D. K. (2005). Gbx2 is required for the morphogenesis of the mouse inner ear: a downstream candidate of hindbrain signaling. *Development* **132**, 2309-2318. doi:10.1242/dev.01804
- Lingbeek, M. E., Jacobs, J. J. L. and van Lohuizen, M. (2002). The T-box repressors TBX2 and TBX3 specifically regulate the tumor suppressor gene p14ARF via a variant T-site in the initiator. *J. Biol. Chem.* **277**, 26120-26127. doi:10.1074/jbc.M200403200
- Liu, M., Pereira, F. A., Price, S. D., Chu, M. J., Shope, C., Himes, D., Eatock, R. A., Brownell, W. E., Lysakowski, A. and Tsai, M. J. (2000). Essential role of BETA2/NeuroD1 in development of the vestibular and auditory systems. *Genes Dev.* **14**, 2839-2854. doi:10.1101/gad.840500
- Liu, N., Schoch, K., Luo, X., Pena, L. D. M., Bhavana, V. H., Kukulich, M. K., Stringer, S., Powis, Z., Radtke, K., Mroske, C. et al. (2018). Functional variants in TBX2 are associated with a syndromic cardiovascular and skeletal developmental disorder. *Hum. Mol. Genet.* **27**, 2454-2465. doi:10.1093/hmg/ddy146
- Lüdtke, T. H.-W., Farin, H. F., Rudat, C., Schuster-Gossler, K., Petry, M., Barnett, P., Christoffels, V. M. and Kispert, A. (2013). Tbx2 controls lung growth by direct repression of the cell cycle inhibitor genes Cdkn1a and Cdkn1b. *PLoS Genet.* **9**, e1003189. doi:10.1371/journal.pgen.1003189
- Lüdtke, T. H., Rudat, C., Wojahn, I., Weiss, A.-C., Kleppa, M.-J., Kurz, J., Farin, H. F., Moon, A., Christoffels, V. M. and Kispert, A. (2016). Tbx2 and Tbx3 act downstream of Shh to maintain canonical wnt signaling during branching morphogenesis of the murine lung. *Dev. Cell* **39**, 239-253. doi:10.1016/j.devcel.2016.08.007
- Ma, Q., Chen, Z., del Barco Barrantes, I., de la Pompa, J. L. and Anderson, D. J. (1998). neurogenin1 is essential for the determination of neuronal precursors for proximal cranial sensory ganglia. *Neuron* **20**, 469-482. doi:10.1016/S0896-6273(00)80988-5
- Ma, Q., Anderson, D. J. and Fritsch, B. (2000). Neurogenin 1 null mutant ears develop fewer, morphologically normal hair cells in smaller sensory epithelia devoid of innervation. *J. Assoc. Res. Otolaryngol.* **1**, 129-143. doi:10.1007/s101620010017
- Maier, E. C., Saxena, A., Alsina, B., Bronner, M. E. and Whitfield, T. T. (2014). Sensational placodes: neurogenesis in the otic and olfactory systems. *Dev. Biol.* **389**, 50-67. doi:10.1016/j.ydbio.2014.01.023
- Mansour, S. L., Goddard, J. M. and Capecchi, M. R. (1993). Mice homozygous for a targeted disruption of the proto-oncogene int-2 have developmental defects in the tail and inner ear. *Development* **117**, 13-28.
- Marklund, M., Sjodal, M., Beehler, B. C., Jessell, T. M., Edlund, T. and Gunhaga, L. (2004). Retinoic acid signalling specifies intermediate character in the developing telencephalon. *Development* **131**, 4323-4332. doi:10.1242/dev.01308
- Martin, P. and Swanson, G. J. (1993). Descriptive and experimental analysis of the epithelial remodellings that control semicircular canal formation in the developing mouse inner ear. *Dev. Biol.* **159**, 549-558. doi:10.1006/dbio.1993.1263

RESEARCH ARTICLE

Development (2021) 148, dev195651. doi:10.1242/dev.195651

- McKay, I. J., Lewis, J. and Lumsden, A. (1996). The role of FGF-3 in early inner ear development: an analysis in normal and kreisler mutant mice. *Dev. Biol.* **174**, 370-378. doi:10.1006/dbio.1996.0081
- Mendelsohn, C., Ruberte, E., LeMeur, M., Morriss-Kay, G. and Chambon, P. (1991). Developmental analysis of the retinoic acid-inducible RAR-beta 2 promoter in transgenic animals. *Development* **113**, 723-734.
- Merlo, G. R., Paleari, L., Mantero, S., Zerega, B., Adamska, M., Rinkwitz, S., Bober, E. and Levi, G. (2002). The Dlx5 homeobox gene is essential for vestibular morphogenesis in the mouse embryo through a BMP4-mediated pathway. *Dev. Biol.* **248**, 157-169. doi:10.1006/dbio.2002.0713
- Mesbah, K., Rana, M. S., Francou, A., van Duijvenboden, K., Papaioannou, V. E., Moorman, A. F., Kelly, R. G. and Christoffels, V. M. (2012). Identification of a Tbx1/Tbx2/Tbx3 genetic pathway governing pharyngeal and arterial pole morphogenesis. *Hum. Mol. Genet.* **21**, 1217-1229. doi:10.1093/hmg/ddr553
- Miyazaki, H., Kobayashi, T., Nakamura, H. and Funahashi, J.-I. (2006). Role of Gbx2 and Otx2 in the formation of cochlear ganglion and endolymphatic duct. *Dev. Growth Differ.* **48**, 429-438. doi:10.1111/j.1440-169X.2006.00879.x
- Moorman, A. F. M., Houweling, A. C., de Boer, P. A. J. and Christoffels, V. M. (2001). Sensitive nonradioactive detection of mRNA in tissue sections: novel application of the whole-mount in situ hybridization protocol. *J. Histochem. Cytochem.* **49**, 1-8. doi:10.1177/002215540104900101
- Morsli, H., Choo, D., Ryan, A., Johnson, R. and Wu, D. K. (1998). Development of the mouse inner ear and origin of its sensory organs. *J. Neurosci.* **18**, 3327-3335. doi:10.1523/JNEUROSCI.18-09-03327.1998
- Morsli, H., Tuorto, F., Choo, D., Postiglione, M. P., Simeone, A. and Wu, D. K. (1999). Otx1 and Otx2 activities are required for the normal development of the mouse inner ear. *Development* **126**, 2335-2343.
- Muzumdar, M. D., Tasic, B., Miyamichi, K., Li, L. and Luo, L. (2007). A global double-fluorescent Cre reporter mouse. *Genesis* **45**, 593-605. doi:10.1002/dvg.20335
- Nimmakayalu, M., Major, H., Sheffield, V., Solomon, D. H., Smith, R. J., Patil, S. R. and Shchelochkov, O. A. (2011). Microdeletion of 17q22q23.2 encompassing TBX2 and TBX4 in a patient with congenital microcephaly, thyroid duct cyst, sensorineural hearing loss, and pulmonary hypertension. *Am. J. Med. Genet. A* **155A**, 418-423. doi:10.1002/ajmg.a.33827
- Nishikori, T., Hatta, T., Kawachi, H. and Otani, H. (1999). Apoptosis during inner ear development in human and mouse embryos: an analysis by computer-assisted three-dimensional reconstruction. *Anat. Embryol.* **200**, 19-26. doi:10.1007/s004290050255
- Ohta, S. and Schoenwolf, G. C. (2018). Hearing crosstalk: the molecular conversation orchestrating inner ear dorsoventral patterning. *Wiley Interdiscip. Rev. Dev. Biol.* **7**, e302. doi:10.1002/wdev.302
- Ohta, S., Wang, B., Mansour, S. L. and Schoenwolf, G. C. (2016). BMP regulates regional gene expression in the dorsal otocyst through canonical and non-canonical intracellular pathways. *Development* **143**, 2228-2237. doi:10.1242/dev.137133
- Oki, S., Ohta, T., Shioi, G., Hatanaka, H., Ogasawara, O., Okuda, Y., Kawaji, H., Nakaki, R., Sese, J. and Meno, C. (2018). ChIP-Atlas: a data-mining suite powered by full integration of public ChIP-seq data. *EMBO Rep.* **19**, e46255. doi:10.15252/embr.201846255
- Ozaki, H., Nakamura, K., Funahashi, J., Ikeda, K., Yamada, G., Tokano, H., Okamura, H. O., Kitamura, K., Muto, S., Kotaki, H. et al. (2004). Six1 controls patterning of the mouse otic vesicle. *Development* **131**, 551-562. doi:10.1242/dev.00943
- Papaioannou, V. E. (2014). The T-box gene family: emerging roles in development, stem cells and cancer. *Development* **141**, 3819-3833. doi:10.1242/dev.104471
- Pataskar, A., Jung, J., Smialowski, P., Noack, F., Calegari, F., Straub, T. and Tiwari, V. K. (2016). NeuroD1 reprograms chromatin and transcription factor landscapes to induce the neuronal program. *EMBO J.* **35**, 24-45. doi:10.15252/emboj.201591206
- Pauley, S., Wright, T. J., Pirvola, U., Ornitz, D., Beisel, K. and Fritzsche, B. (2003). Expression and function of FGF10 in mammalian inner ear development. *Dev. Dyn.* **227**, 203-215. doi:10.1002/dvdy.10297
- Pirvola, U., Spencer-Dene, B., Xing-Qun, L., Kettunen, P., Thesleff, I., Fritzsche, B., Dickson, C. and Ylikoski, J. (2000). FGF/FGFR-2(IIIb) signaling is essential for inner ear morphogenesis. *J. Neurosci.* **20**, 6125-6134. doi:10.1523/JNEUROSCI.20-16-06125.2000
- Raft, S. and Groves, A. K. (2015). Segregating neural and mechanosensory fates in the developing ear: patterning, signaling, and transcriptional control. *Cell Tissue Res.* **359**, 315-332. doi:10.1007/s00441-014-1917-6
- Raft, S., Nowotschin, S., Liao, J. and Morrow, B. E. (2004). Suppression of neural fate and control of inner ear morphogenesis by Tbx1. *Development* **131**, 1801-1812. doi:10.1242/dev.01067
- Raible, F. and Brand, M. (2001). Tight transcriptional control of the ETS domain factors *Erm* and *Pea3* by Fgf signaling during early zebrafish development. *Mech. Dev.* **107**, 105-117. doi:10.1016/S0925-4773(01)00456-7
- Riccomagno, M. M., Martinu, L., Mulheisen, M., Wu, D. K. and Epstein, D. J. (2002). Specification of the mammalian cochlea is dependent on Sonic hedgehog. *Genes Dev.* **16**, 2365-2378. doi:10.1101/gad.1013302
- Riccomagno, M. M., Takada, S. and Epstein, D. J. (2005). Wnt-dependent regulation of inner ear morphogenesis is balanced by the opposing and supporting roles of Shh. *Genes Dev.* **19**, 1612-1623. doi:10.1101/gad.1303905
- Robledo, R. F. and Lufkin, T. (2006). Dlx5 and Dlx6 homeobox genes are required for specification of the mammalian vestibular apparatus. *Genesis* **44**, 425-437. doi:10.1002/dvg.20233
- Romand, R., Sobkowicz, H., Emmerling, M., Whitton, D. and Dahl, D. (1990). Patterns of neurofilament stain in the spiral ganglion of the developing and adult mouse. *Hear. Res.* **49**, 119-125. doi:10.1016/0378-5955(90)90099-B
- Schliermann, A. and Nickel, J. (2018). Unraveling the connection between fibroblast growth factor and bone morphogenetic protein signaling. *Int. J. Mol. Sci.* **19**, 3220. doi:10.3390/ijms19103220
- Sheeba, C. J. and Logan, M. P. O. (2017). The roles of T-box genes in vertebrate limb development. *Curr. Top. Dev. Biol.* **122**, 355-381. doi:10.1016/bs.ctdb.2016.08.009
- Shou, J., Rim, P. C. and Calof, A. L. (1999). BMPs inhibit neurogenesis by a mechanism involving degradation of a transcription factor. *Nat. Neurosci.* **2**, 339-345. doi:10.1038/7251
- Singh, R., Hoogaars, W. M., Barnett, P., Grieskamp, T., Rana, M. S., Buermans, H., Farin, H. F., Petry, M., Heallen, T., Martin, J. F. et al. (2012). Tbx2 and Tbx3 induce atrioventricular myocardial development and endocardial cushion formation. *Cell. Mol. Life Sci.* **69**, 1377-1389. doi:10.1007/s00018-011-0884-2
- Singhvi, A., Frank, C. A. and Garriga, G. (2008). The T-box gene *tbx-2*, the homeobox gene *egl-5* and the asymmetric cell division gene *ham-1* specify neural fate in the HSN/PHB lineage. *Genetics* **179**, 887-898. doi:10.1534/genetics.108.088948
- Teven, C. M., Farina, E. M., Rivas, J. and Reid, R. R. (2014). Fibroblast growth factor (FGF) signaling in development and skeletal diseases. *Genes Dis.* **1**, 199-213. doi:10.1016/j.gendis.2014.09.005
- Torres, M., Gomez-Pardo, E. and Gruss, P. (1996). Pax2 contributes to inner ear patterning and optic nerve trajectory. *Development* **122**, 3381-3391.
- Trowe, M.-O., Maier, H., Petry, M., Schweizer, M., Schuster-Gossler, K. and Kispert, A. (2011). Impaired stria vascularis integrity upon loss of E-cadherin in basal cells. *Dev. Biol.* **359**, 95-107. doi:10.1016/j.ydbio.2011.08.030
- Urness, L. D., Wang, X., Shibata, S., Ohyama, T. and Mansour, S. L. (2015). Fgf10 is required for specification of non-sensory regions of the cochlear epithelium. *Dev. Biol.* **400**, 59-71. doi:10.1016/j.ydbio.2015.01.015
- Vázquez-Echeverría, C., Domínguez-Frutos, E., Charnay, P., Schimmang, T. and Pujades, C. (2008). Analysis of mouse kreisler mutants reveals new roles of hindbrain-derived signals in the establishment of the otic neurogenic domain. *Dev. Biol.* **322**, 167-178. doi:10.1016/j.ydbio.2008.07.025
- Vemarraju, S., Kantarci, H., Padanad, M. S. and Riley, B. B. (2012). A spatial and temporal gradient of Fgf differentially regulates distinct stages of neural development in the zebrafish inner ear. *PLoS Genet.* **8**, e1003068. doi:10.1371/journal.pgen.1003068
- Vitelli, F., Viola, A., Morishima, M., Pramparo, T., Baldini, A. and Lindsay, E. (2003). TBX1 is required for inner ear morphogenesis. *Hum. Mol. Genet.* **12**, 2041-2048. doi:10.1093/hmg/ddg216
- Wakker, V., Brons, J. F., Aanhaenen, W. T. J., van Roon, M. A., Moorman, A. F. M. and Christoffels, V. M. (2010). Generation of mice with a conditional null allele for Tbx2. *Genesis* **48**, 195-199. doi:10.1002/dvg.20596
- Wang, W., Van De Water, T. and Lufkin, T. (1998). Inner ear and maternal reproductive defects in mice lacking the Hmx3 homeobox gene. *Development* **125**, 621-634.
- Wang, W., Chan, E. K., Baron, S., Van de Water, T. and Lufkin, T. (2001). Hmx2 homeobox gene control of murine vestibular morphogenesis. *Development* **128**, 5017-5029.
- Wang, W., Grimmer, J. F., Van De Water, T. R. and Lufkin, T. (2004). Hmx2 and Hmx3 homeobox genes direct development of the murine inner ear and hypothalamus and can be functionally replaced by Drosophila Hmx. *Dev. Cell* **7**, 439-453. doi:10.1016/j.devcel.2004.06.016
- Wilkinson, D. G. and Nieto, M. A. (1993). Detection of messenger RNA by in situ hybridization to tissue sections and whole mounts. *Methods Enzymol.* **225**, 361-373. doi:10.1016/0076-6879(93)25025-W
- Wu, D. K. and Sandell, L. (2016). 21 - Development and lineage relationships of the mouse inner ear. In *Kaufman's Atlas of Mouse Development Supplement* (ed. R. Baldock, J. Bard, D. R. Davidson and G. Morriss-Kay), pp. 267-274. Academic Press.
- Xu, P.-X., Adams, J., Peters, H., Brown, M. C., Heaney, S. and Maas, R. (1999). Eya1-deficient mice lack ears and kidneys and show abnormal apoptosis of organ primordia. *Nat. Genet.* **23**, 113-137. doi:10.1038/12722
- Xu, H., Viola, A., Zhang, Z., Gerken, C. P., Lindsay-Iltingworth, E. A. and Baldini, A. (2007). Tbx1 regulates population, proliferation and cell fate determination of otic epithelial cells. *Dev. Biol.* **302**, 670-682. doi:10.1016/j.ydbio.2006.10.002
- Zheng, W., Huang, L., Wei, Z. B., Silvius, D., Tang, B. and Xu, P. X. (2003). The role of Six1 in mammalian auditory system development. *Development* **130**, 3989-4000. doi:10.1242/dev.00628
- Zirzow, S., Lütke, T. H.-W., Brons, J. F., Petry, M., Christoffels, V. M. and Kispert, A. (2009). Expression and requirement of T-box transcription factors Tbx2 and Tbx3 during secondary palate development in the mouse. *Dev. Biol.* **336**, 145-155. doi:10.1016/j.ydbio.2009.09.020

Supplementary Figures

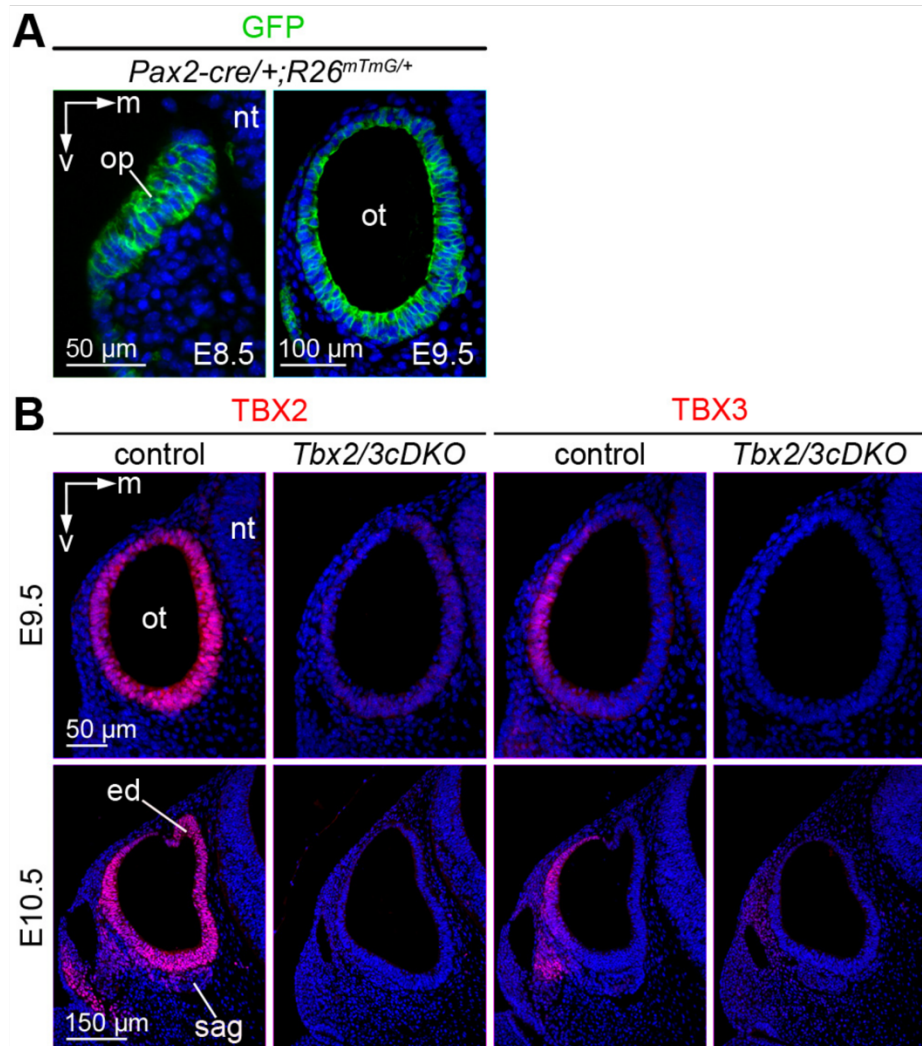


Fig. S1. The *Pax2-cre* line mediates recombination in the otic epithelium from E8.5 onwards. (A) Immunofluorescence analysis of GFP expression (green) on mid-transverse sections of the hindbrain region of *Pax2-cre/+;Rosa26^{mTmG}/+* embryos shows that the *Pax2-cre* line mediates robust recombination of the *R26^{mTmG}* reporter allele in the epithelium of the otic placode at E8.5 and of the otic vesicle at E9.5. (B) Mid-transverse sections of control and *Tbx2/3cDKO* otocysts immunolabelled for TBX2 and TBX3 expression. Expression of TBX2 and TBX3 (red) is completely lost in the otic epithelium at E9.5 and E10.5 showing that the *Pax2-cre* line efficiently recombined floxed alleles of *Tbx2* and *Tbx3* to null alleles. TBX2 and TBX3 are also lost in a subset of cells within the SAG indicating the origin of these cells from the otic epithelium. Stages are as indicated. $n \geq 3$ per genotype and stage. ed, endolymphatic duct; m, medial; nt, neural tube; ot, otocyst; op, otic placode; sag, statoacoustic ganglion; v, ventral.

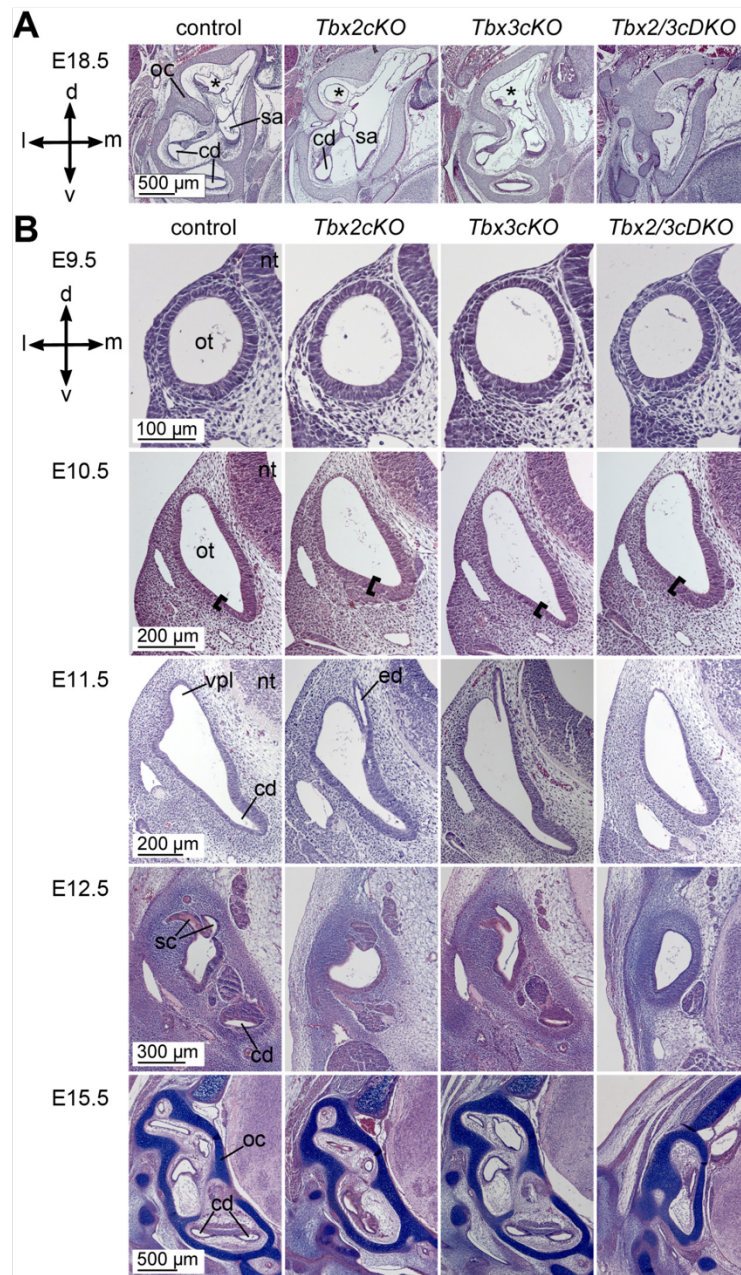


Fig. S2. Loss of *Tbx2* and/or *Tbx3* severely affects inner ear histology in embryonic development. (A,B) Histological analysis of the inner ear by hematoxylin and eosin (E9.5-E12.5, E18.5) or alcian blue staining (E15.5) on transverse head sections of control and mutant embryos at E18.5 (A) and E9.5 to E15.5 (B). Otocysts of all mutants appear normal at E9.5. At E10.5, the ventrolateral epithelium (black brackets) is thickened in *Tbx2cKO* and *Tbx2/3cDKO* embryos. From E12.5 to E18.5, *Tbx2cKO* inner ears exhibit a severely shortened cochlear duct and the saccular cavity is not separated from the utricle. No obvious histological alterations are observed in *Tbx3cKO* mutants. In *Tbx2/3cDKO* embryos, the membranous inner ear labyrinth and the otic capsule are severely hypoplastic. Asterisks in (A) mark the ampulla at the base of the posterior semicircular canal. n=3 per genotype and stage. cd, cochlear duct; d, dorsal; ed, endolymphatic duct; l, lateral; m, medial; nt, neural tube; oc, otic capsule; ot, otocyst; sa, saccule; sc, semicircular canal; v, ventral; vpl, vertical canal plate.

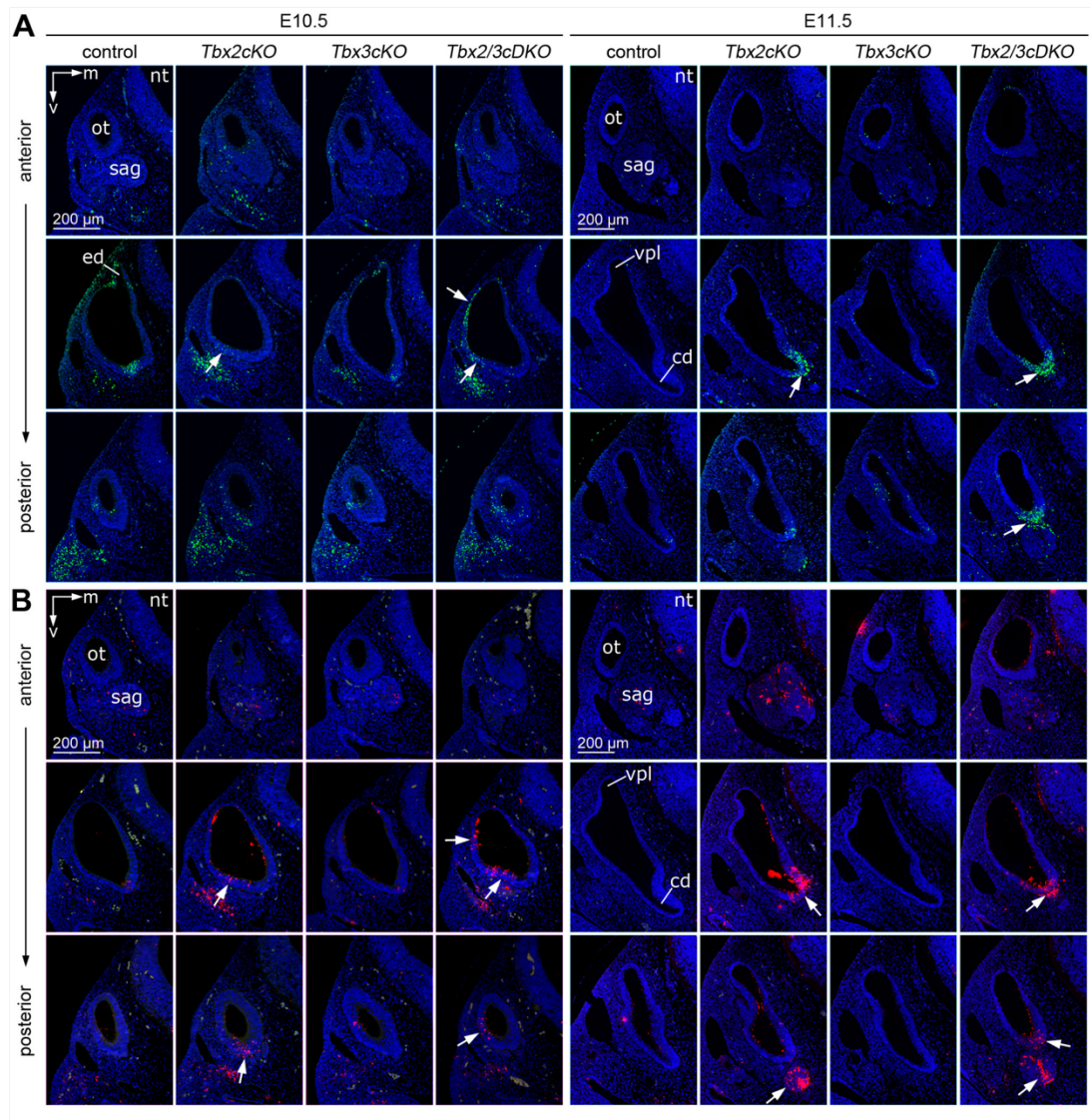


Fig. S3. Individual and combined loss of *Tbx2* and/or *Tbx3* severely affects cell survival in the otic epithelium. (A,B) Analysis of cell death by the TUNEL assay (A) and by immunofluorescence staining against cleaved CASPASE-3 (B) on transverse otocyst sections at anterior, medial and posterior regions of E10.5 and E11.5 control, *Tbx2cKO*, *Tbx3cKO* and *Tbx2/3cDKO* embryos. White arrows point to regions of ectopic apoptosis in the dorso-lateral and ventro-lateral otocyst of E10.5 *Tbx2/3cDKO* embryos, and in the posterior-ventral region, the adjacent otic mesenchyme and ganglion-like structures in *Tbx2cKO* and *Tbx2/3cDKO* embryos. Nuclei are counterstained with DAPI. n=3 per genotype and stage. cd, cochlear duct; ed, endolymphatic duct; m, medial; nt, neural tube; ot, otocyst; sag, statoacoustic ganglion; v, ventral; vpl, vertical canal plate.

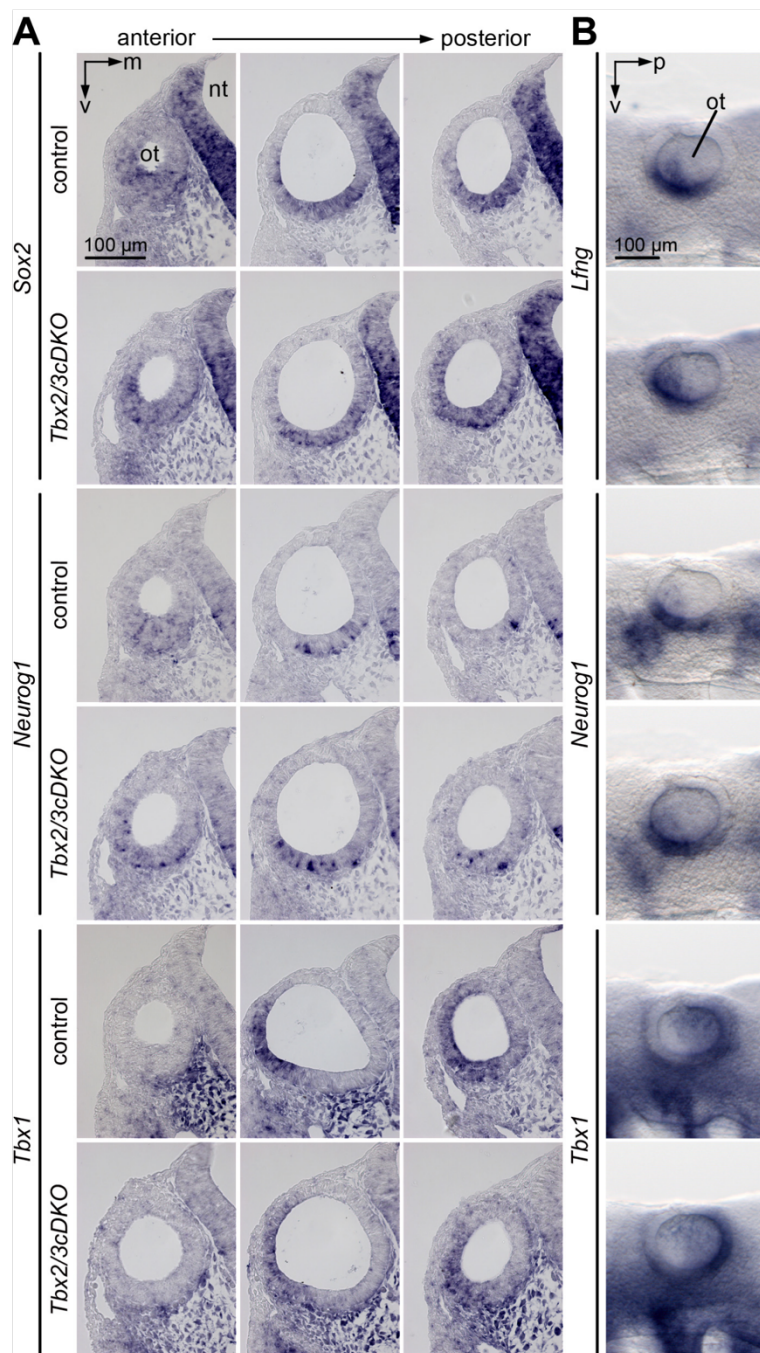


Fig. S4. Anterior-posterior patterning and neurogenesis are unaffected in *Tbx2/3cDKO* otocysts at E9.5. RNA *in situ* hybridisation analysis of genes relevant for neurogenesis on transverse otocyst sections (A) and on embryo halves (B) at E9.5. Probes and genotypes are as indicated. n=3 per genotype and probe. m, medial; nt, neural tube; ot, otocyst; p, posterior; v, ventral.

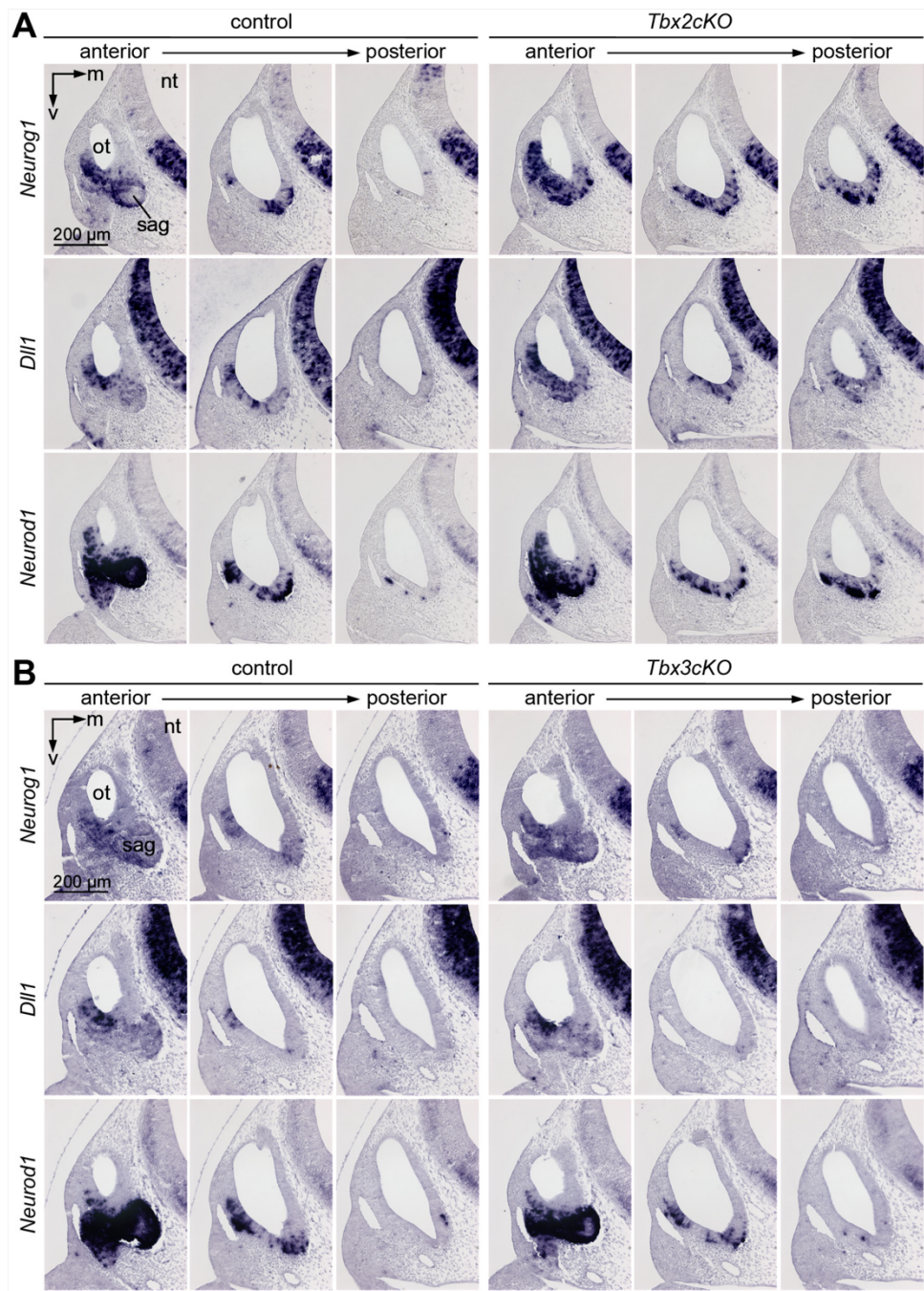


Fig. S5. The neurogenic domain is posteriorly expanded in *Tbx2cKO* but not in *Tbx3cKO* otocysts at E10.5. (A,B) RNA *in situ* hybridisation analysis of pro-neuronal genes of E10.5 control, *Tbx2cKO* (A) and *Tbx3cKO* (B) otocysts using three different section planes: anterior, mid-transverse, posterior. Expression of *Neurog1*, *Dll1* and *Neurod1* is expanded posterior-ventrally in *Tbx2cKO* but not in *Tbx3cKO* otocysts. $n \geq 4$ per genotype and probe. m, medial; nt, neural tube; ot, otocyst; sag, statoacoustic ganglion; v, ventral.

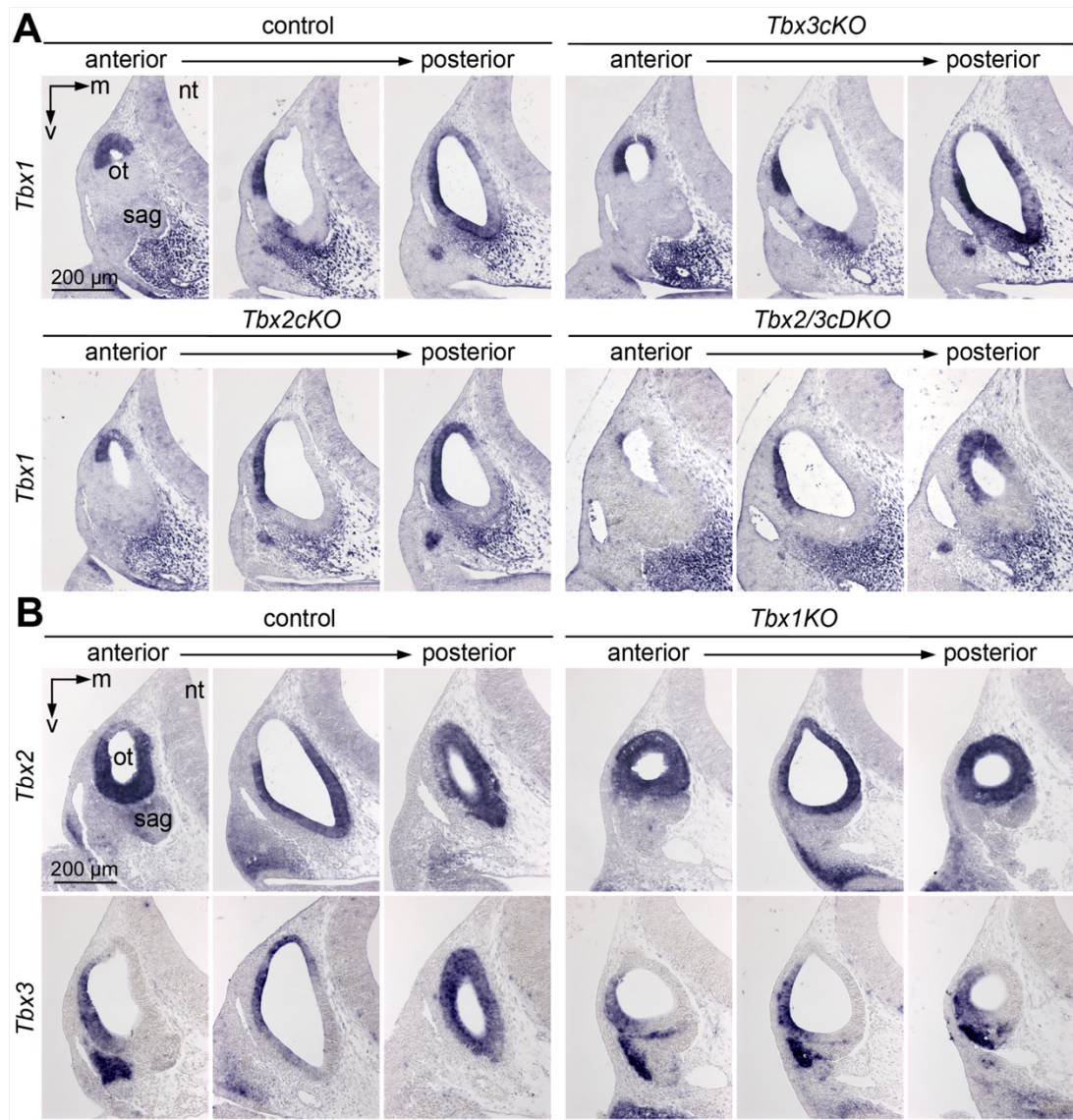


Fig. S6. Posterior-ventral expression of *Tbx1* in E10.5 otocysts depends on *Tbx2*. RNA *in situ* hybridisation analysis on anterior, mid-transverse and posterior sections of E10.5 otocysts for (A) *Tbx1* expression in *Tbx3cKO*, *Tbx2cKO* and *Tbx2/3cDKO* embryos, and (B) for *Tbx2* and *Tbx3* expression in *Tbx1KO* embryos. Posterior-ventral expression of *Tbx1* is abolished in *Tbx2cKO* and *Tbx2/3cDKO* but not in *Tbx3cKO* otocysts. $n \geq 3$ per genotype and probe. m, medial; nt, neural tube; ot, otocyst; sag, statoacoustic ganglion; v, ventral.

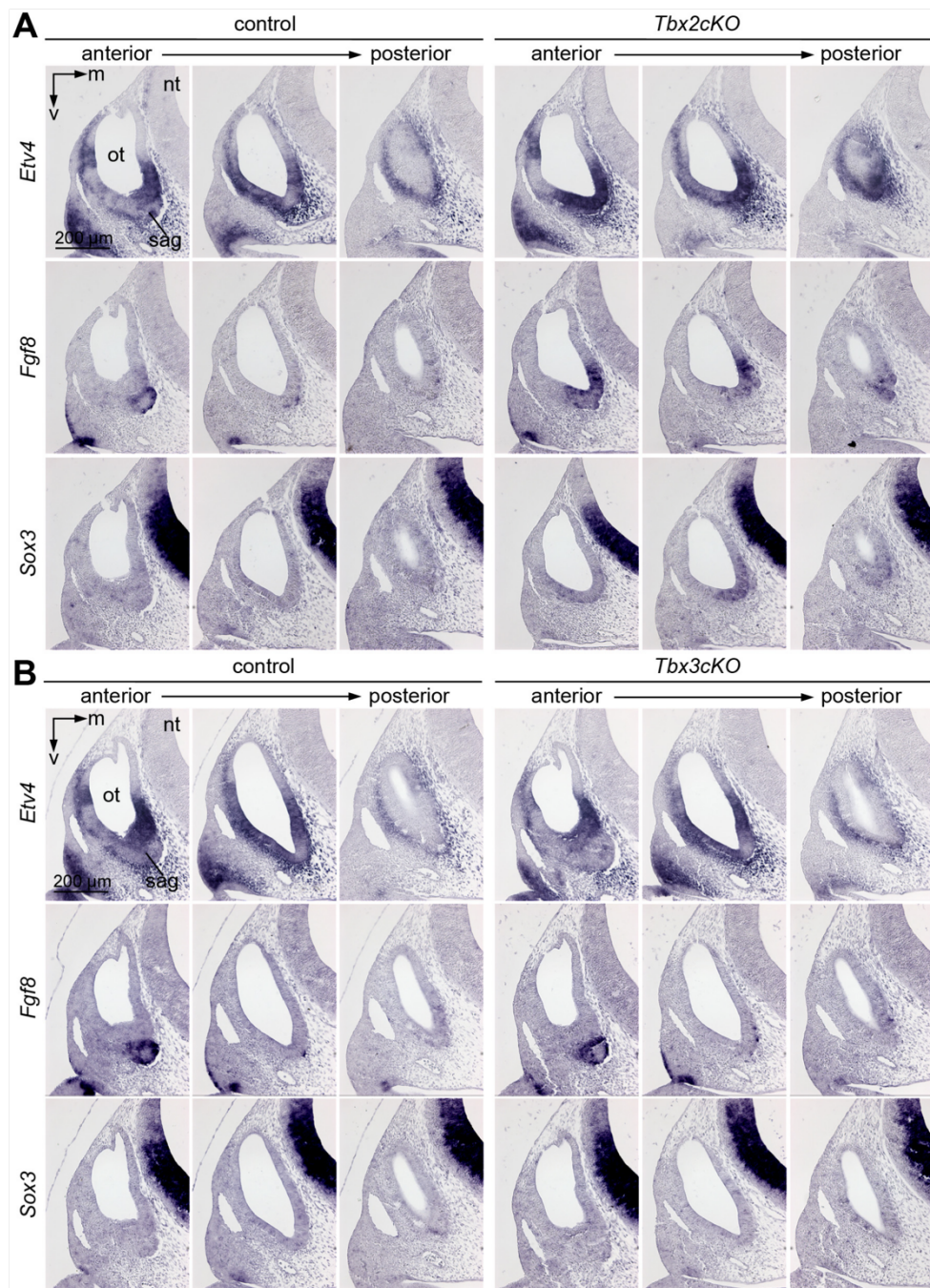


Fig. S7. FGF signalling is changed in *Tbx2cKO* but not in *Tbx3cKO* otocysts at E10.5. (A,B) RNA *in situ* hybridisation analysis of expression of the FGF ligand gene *Fgf8*, of the target gene of FGF signalling *Etv4*, and of the proneural gene *Sox3* on sections at the anterior, mid-transverse and posterior otocyst level in *Tbx2cKO* (A) and *Tbx3cKO* (B) embryos at E10.5. *Etv4*, *Fgf8* and *Sox3* are ectopically expressed in posterior-ventral otocysts of *Tbx2cKO* mutants, but not in *Tbx3cKO* embryos. $n \geq 4$ per genotype and probe. m, medial; nt, neural tube; ot, otocyst; sag, statoacoustic ganglion; v, ventral.

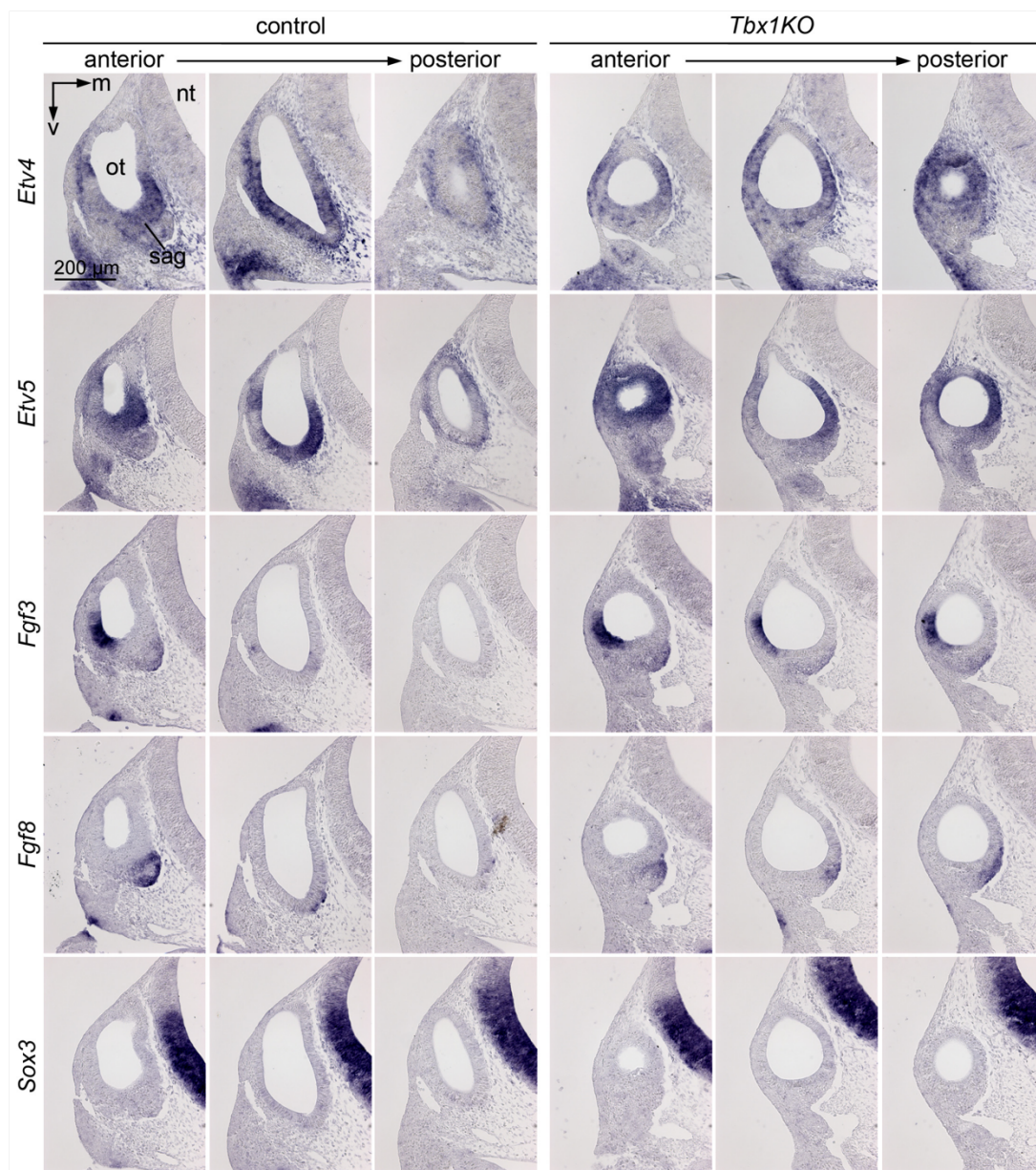


Fig. S8. Expression of *Fgf8* and *Sox3* is not ectopically activated in *Tbx1KO* otocysts at E10.5. RNA *in situ* hybridisation analysis of expression of FGF ligand genes (*Fgf8*, *Fgf3*), target genes of FGF signalling (*Etv4*, *Etv5*) and of the proneural gene *Sox3* on transverse sections of E10.5 control and *Tbx1KO* otocysts at the anterior, mid-transverse, and posterior region. n=4 per genotype and probe. m, medial; nt, neural tube; ot, otocyst; sag, statoacoustic ganglion; v, ventral.

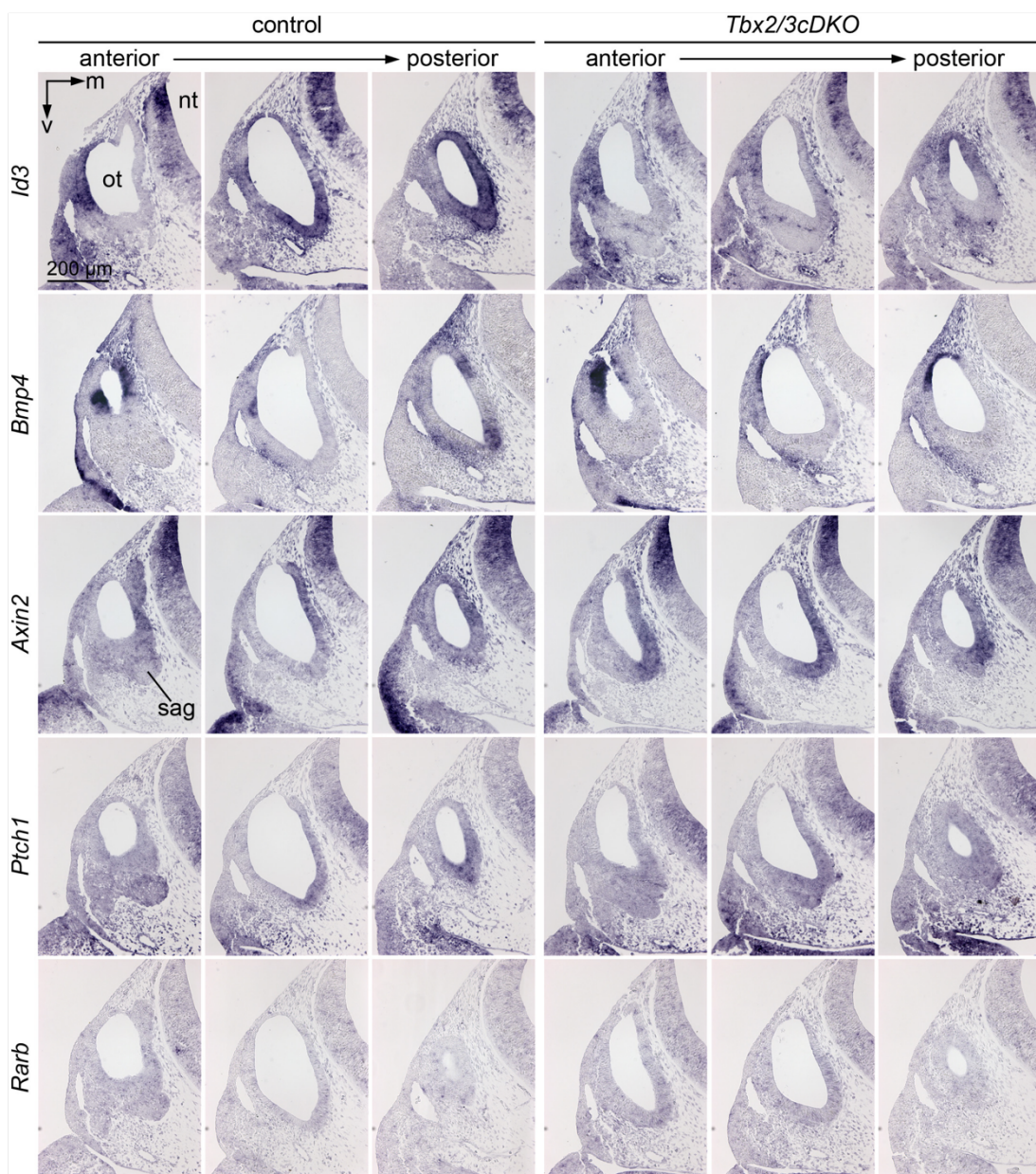


Fig. S9. Spatial distribution of signalling activities important for axial patterning of the otocyst is partly affected in *Tbx2/3cDKO* embryos at E10.5. RNA *in situ* hybridisation analysis of expression of *Bmp4*, and of targets of different signalling pathways (*Id3*: BMP; *Axin2*: WNT; *Ptch1*: SHH; *Rarb*: RA) on transverse sections of control and *Tbx2/3cDKO* otocysts at the anterior, mid-transverse, and posterior level. *Id3* and *Bmp4* expression is lost in the posterior-ventral region of *Tbx2/3cDKO* otocysts. *Axin2* expression is expanded ventrally; *Ptch1* is slightly downregulated. $n \geq 4$ per genotype and probe. m, medial; nt, neural tube; ot, otocyst; sag, statoacoustic ganglion; v, ventral.

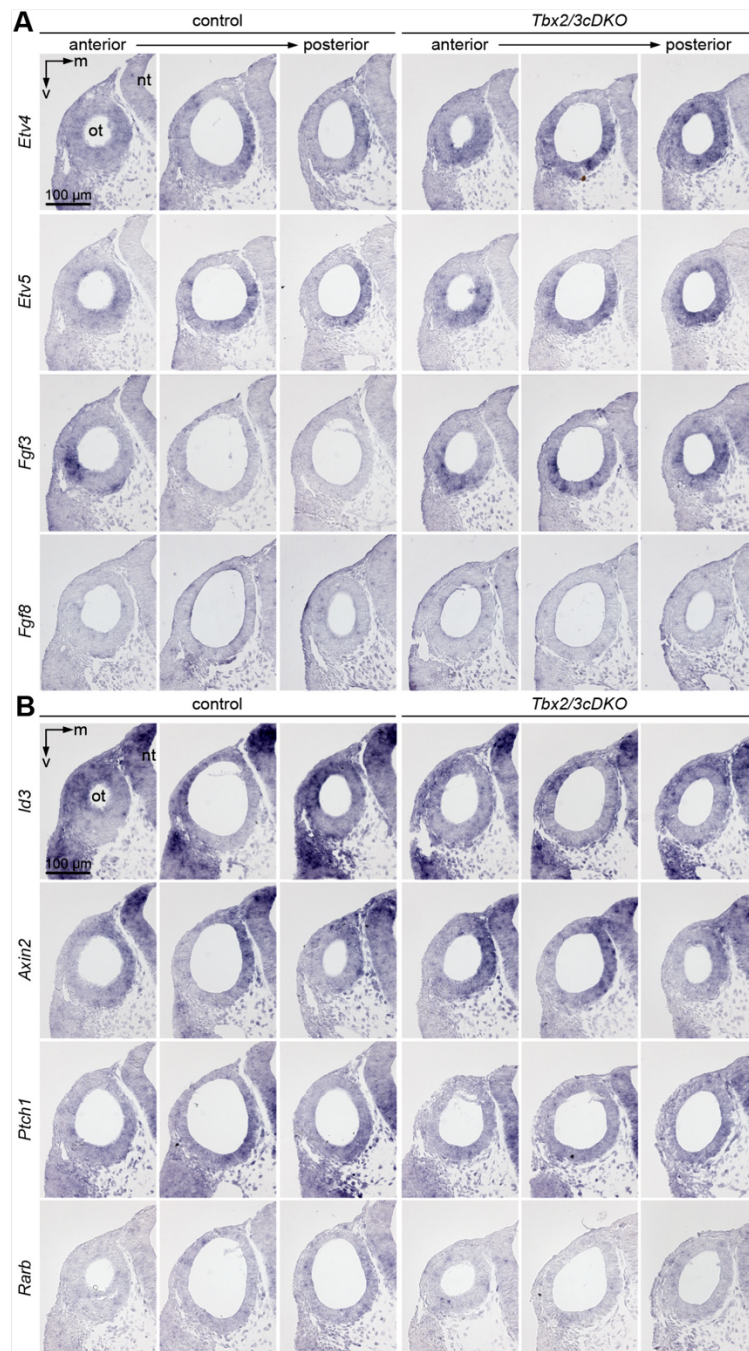


Fig. S10. Spatial distribution of signalling activities important for patterning of the otocyst is weakly affected in *Tbx2/3cDKO* embryos at E9.5. (A,B) RNA *in situ* hybridisation analysis of expression of targets of FGF signalling (*Etv4*, *Etv5*) and of FGF ligand genes (*Fgf3*, *Fgf8*) (A), and of targets of additional signalling pathways (*Id3*: BMP; *Axin2*: WNT; *Ptch1*: SHH; *Rarb*: RA) (B) on transverse sections of control and *Tbx2/3cDKO* otocysts at the anterior, mid-transverse, and posterior level. $n \geq 3$ per genotype and probe. m, medial; nt, neural tube; ot, otocyst; v, ventral.

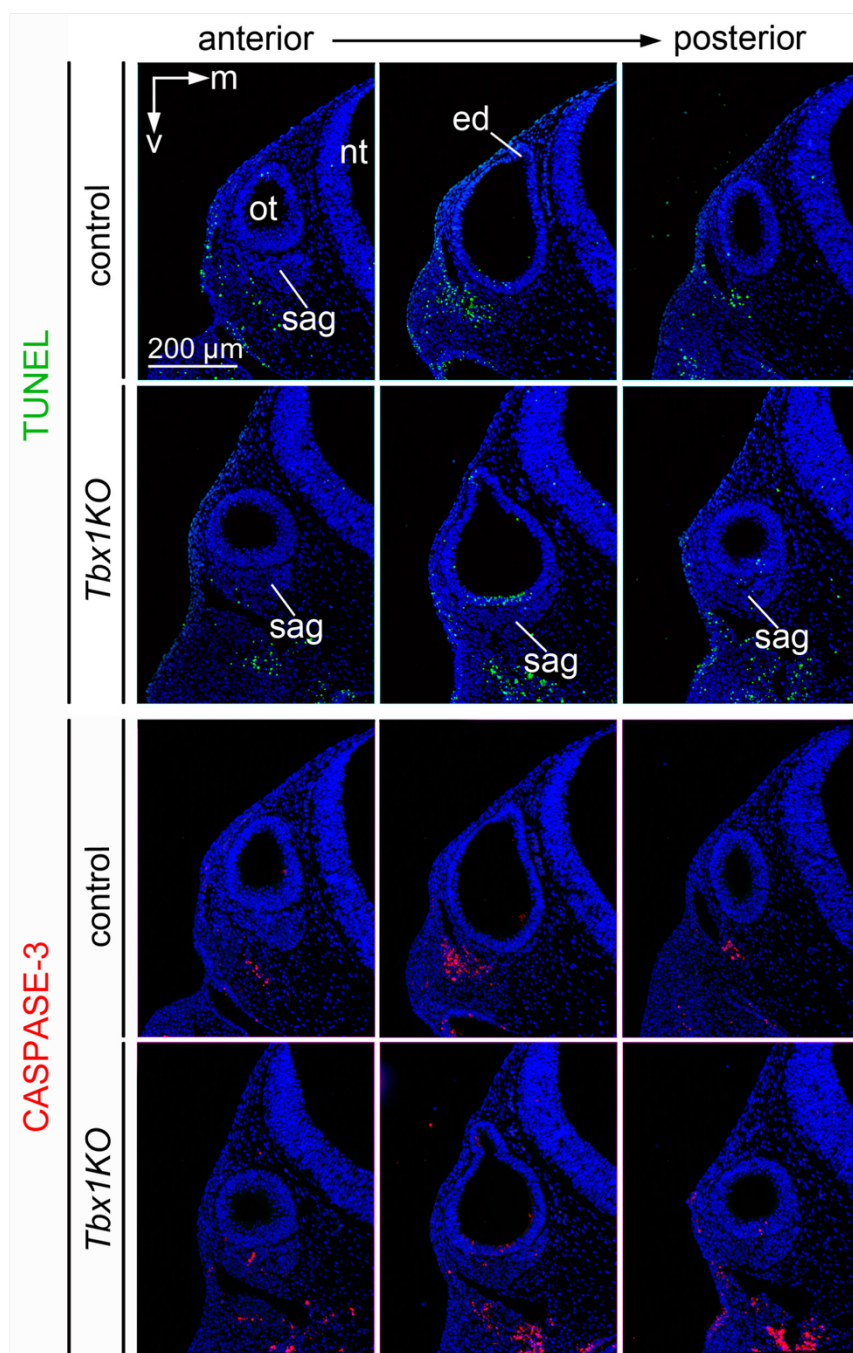


Fig. S11. Loss of *Tbx1* affects cell survival in the ventral region of the otic epithelium at E10.5. (A,B) Analysis of cell death by the TUNEL assay (A) and by immunofluorescence staining against cleaved CASPASE-3 (B) on transverse sections at the anterior, medial and posterior region of E10.5 control and *Tbx1*KO otocysts. Apoptosis is increased in the ventral aspect of *Tbx1*KO otocysts. Nuclei are counterstained with DAPI. n=4 per genotype and assay. ed, endolymphatic duct; m, medial; nt, neural tube; ot, otocyst; sag, statoacoustic ganglion; v, ventral.

Table S1. Genotype frequencies of E18.5 embryos derived from the breeding of *Pax2-cre/+;Tbx2^{flox/+};Tbx3^{flox/+}* males and *Tbx2^{flox/flox};Tbx3^{flox/flox};R26^{mTmG/mTmG}* females followed a Mendelian ratio. A Chi-square test performed by the statistical analysis software JASP (<https://jasp-stats.org>) did not detect significant differences between observed and expected genotype frequencies ($p=0.301$). The observed distribution of genotypes follows the expected Mendelian ratio. The *R26^{mTmG}* allele was neglected for the test.

[Click here to download Table S1](#)

Table S2. Analysis of cell proliferation by the BrdU incorporation assay in *Tbx2/3cDKO* otocysts at E10.5. Transverse sections of control and *Tbx2/3cDKO* otocysts were divided into four quadrants to enable detection of even minor changes in the proliferation rate. zone 1: dorso-medial, zone 2: ventro-medial, zone 3: ventro-lateral, zone 4: dorso-lateral.

[Click here to download Table S2](#)

Table S3. List of transcripts which were significantly deregulated in E10.5 *Tbx2/3cDKO* otocysts. Data were averaged from four independent pools per genotype. Log2-converted expression data were imported into Qlucore Omics Explorer (version 3.6) and normalised. For identification of deregulated genes, probe sets with highest values were used in a two-group comparison (t-test). Genes with FDR-adjusted p-value (q-value) < 0.05 were considered as deregulated.

[Click here to download Table S3](#)

Table S4. List of transcripts which were significantly downregulated in E10.5 *Tbx2/3cDKO* otocysts. Significantly deregulated transcripts (Table S3) were further subjected to filtering using a signal intensity threshold (≥ 100 for control pools) and a Fold change threshold ($FC \leq -2$).

[Click here to download Table S4](#)

Table S5. List of transcripts which were significantly upregulated in E10.5 *Tbx2/3cDKO* otocysts. Significantly deregulated transcripts (Table S3) were further subjected to filtering using a signal intensity threshold (≥ 100 for mutant pools) and a Fold change threshold ($FC \geq 2$).

[Click here to download Table S5](#)

Table S6. Functional annotation clustering analysis for transcripts downregulated in E10.5 *Tbx2/3cDKO* otocysts. Functional enrichment analysis for 169 (Table S4) downregulated genes was performed with DAVID 6.8 web software (<https://david.ncifcrf.gov>). Clusters were defined using Gene Functional Annotation Clustering on GO-BP annotations, 'medium' stringency and Final Group Membership of 5. Shown are the TOP5 annotation clusters.

[Click here to download Table S6](#)

Table S7. Functional annotation clustering analysis for transcripts upregulated in E10.5 *Tbx2/3cDKO* otocysts. Functional enrichment analysis for 234 (Table S5) upregulated genes was performed with DAVID 6.8 web software (<https://david.ncifcrf.gov>). Clusters were defined using Gene Functional Annotation Clustering on GO-BP annotations, 'medium' stringency and Final Group Membership of 5. Shown are the TOP5 annotation clusters.

[Click here to download Table S7](#)

Table S8. Potential direct target genes of TBX2/TBX3 in E10.5 otocysts. The list shows which genes, that are upregulated upon loss of *Tbx2* and *Tbx3* in E10.5 otocysts, are direct targets of TBX2 or TBX3 in other organs as determined by ChIP-Atlas (Tables S9 and S10) or possess evolutionarily conserved TBX-binding sites as determined with the oPOSSUM software tool (Table S11).

[Click here to download Table S8](#)

Table S9. List of predicted direct TBX2 target genes in human based on public ChIP-seq data. Potential direct TBX2 target genes in human (hg38) were determined using the 'Target-Gene' function of the data-mining platform ChIP-Atlas (<https://chip-atlas.org>), that predicts genes directly regulated by given transcription factors based on binding profiles of all public ChIP-seq data. For the analysis we included all binding sites within a range of 10.000 bp up/downstream of the transcriptional start sites.

[Click here to download Table S9](#)

Table S10. List of predicted direct TBX3 target genes in mouse based on public ChIP-seq data. Potential direct TBX3 target genes in mouse (mm10) were determined using the 'Target-Gene' function of the data-mining platform ChIP-Atlas (<https://chip-atlas.org>), that predicts genes directly regulated by given transcription factors based on binding profiles of all public ChIP-seq data. For the analysis we included all binding sites within a range of 10.000 bp up/downstream of the transcriptional start sites.

[Click here to download Table S10](#)

Table S11. List of upregulated transcripts with evolutionary conserved Brachyury (T)-binding sites in mouse. 935 transcripts that were upregulated in E10.5 *Tbx2/3cDKO* otocysts (Table S3) with a FC of ≥ 1.5 and the additional candidate genes *Dll1* and *Neurog1* were analysed for evolutionary conserved transcription factor binding sites using the webtool oPOSSUM (<http://opossum.cisreg.ca/oPOSSUM3/>, Kwon et al., 2012). For the analysis we used the 'Mouse Single Site Analysis' with the JASPAR core profile for Brachyury (T) and default settings, except the amount of upstream and downstream sequence was increased to 10000 bp.

[Click here to download Table S11](#)

Table S12. Sequences of primers used for the generation of probe templates by PCR amplification. A T7 RNA polymerase binding site (CGCGCG-TAATACGACTCACTATAGGG) was added to the 5'-end of the reverse primer to allow subsequent transcription.

[Click here to download Table S12](#)

Part 2 – *Tbx2* in hair and supporting cell differentiation

TBX2 specifies and maintains inner hair and supporting cell fate in the Organ of Corti

Marina Kaiser¹, Timo Lüdtke¹, Vincent M. Christoffels², Andreas Kispert^{1,*} & Mark-Oliver Trowe^{1,*}

¹Institut für Molekularbiologie, Medizinische Hochschule Hannover, Hannover, Germany. ²Department of Anatomy, Embryology and Physiology, Academic Medical Center, University of Amsterdam, Amsterdam, The Netherlands.

*e-mail: kispert.andreas@mh-hannover.de; trowe.mark-oliver@mh-hannover.de.

Type of authorship:	First author
Type of article:	Research article
Share of the work:	80%
Contribution:	(co)-planed, and performed experiments, analysed data, prepared figures, assisted in writing the manuscript
Journal:	<i>Nature</i>
Impact factor:	42.778 (2019)
Number of citations:	0
Date of publication:	under revision
DOI:	—

Note that the supplementary tables of this paper are not included in the printed version of this thesis! They are included on the accompanied compact disc.

TBX2 specifies and maintains inner hair and supporting cell fate in the Organ of Corti

Marina Kaiser¹, Timo Lütke¹, Vincent M. Christoffels², Andreas Kispert^{1,*} & Mark-Oliver Trowe^{1,*}

Hearing relies on two types of highly specialized mechanosensory cells in the Organ of Corti, the sensory epithelium of the mammalian cochlea. Inner hair cells (IHCs) are the main sensory cells since they convert sound into auditory information; outer hair cells (OHCs) act as mechanical amplifiers that enhance sensitivity to sound and adjust frequency selectivity. IHCs and OHCs, as well as a complex array of nonsensory cells that support them, differentiate from common prosensory progenitors during embryonic development. Recent studies identified the transcription factors INSM1 and IKZF2 as regulators of OHC fate^{1,2}, but transcriptional regulators of IHC differentiation have remained enigmatic. Here, we show that the transcriptional repressor TBX2 specifies and maintains the fate of IHCs and inner supporting cells (ISCs) by preventing differentiation into OHCs and outer supporting cells (OSCs), respectively. TBX2

expression was restricted to IHCs and ISCs from the onset of differentiation until adulthood. *Tbx2* inactivation in prosensory cells caused differentiation of OHC- and OSC-like cells at the position of IHCs and ISCs. Conversely, *Tbx2* misexpression led to an increase of IHC- and ISC-like cells at the position of OHCs and OSCs. Inactivation of *Tbx2* in differentiating IHCs and ISCs led to a conversion to OHC- and OSC-like cells, respectively. Finally, hair cell-specific *Tbx2* inactivation or misexpression caused cell-autonomous transdifferentiation of hair cells. Transcriptional profiling identified *Fgfr3* as a target of TBX2 in patterning of prosensory progenitors into an inner and outer compartment in the early development of the organ of Corti. At later stages, TBX2 represses OHC-fate regulators, such as IKZF2, to prevent transdifferentiation of IHCs.

IHCs and OHCs are structurally and functionally diverse, differ in number, and associate with distinct nonsensory supporting cells in separate compartments in the organ of Corti. A single row of large IHCs associates with two types of ISCs (inner phalangeal and inner border cells) in the inner compartment; smaller OHCs form three rows which are each supported by OSCs (Deiters' cells) in the outer compartment. OHCs and IHCs are separated by two pillar cells that flank the fluid-filled tunnel of Corti (Fig. 1a).

Hair and supporting cells arise from common SOX2⁺ prosensory progenitors in embryonic development³. Activation of the transcription factor ATOH1 triggers hair cell differentiation, while the remaining prosensory cells differentiate into supporting cells⁴. Only at postnatal stages, hair cell differentiation is completed and IHCs and OHCs become functional⁵. Since mature cochlear hair cells cannot be regenerated⁶, their progressive loss due to age, excessive sound or ototoxic drugs contributes to (age-related) deafness. Cell-based strategies may enable targeted regenerative therapies in the future but require the knowledge of factors driving hair cell diversification.

Recent work identified IKZF2 (Helios) and INSM1 as transcriptional regulators of OHC differentiation in

the mouse. IKZF2 is expressed in OHCs starting from P4. It is required for OHC maturation and is sufficient to induce an OHC-like fate in IHCs¹. INSM1 is transiently expressed in OHCs at fetal and early postnatal stages (E15.5-P2)⁷. Loss of this factor leads to transdifferentiation of a subset of OHCs into IHC-like cells with concomitant derepression of a set of IHC-specific genes including the T-box transcription factor gene *Tbx2*². Since TBX2 acts as a patterning and differentiation factor in many developmental contexts⁸, including the anterior-ventral restriction of the neurogenic domain in the early otocyst⁹, it presents a strong candidate for an as yet unknown regulator of IHC differentiation.

***Tbx2* expression progressively restricts to IHCs and ISCs during cochlear development**

Tbx2 mRNA and TBX2 protein expression during cochlear development was analysed by mRNA *in situ* hybridization and (co-)immunofluorescence analyses from cochlear outgrowth (E12.5) to a stage when hair cells have reached full maturity (P21) (Fig. 1b-e). At E12.5 and E13.5, *Tbx2* was widely expressed in the floor of the cochlear duct. Starting at E14.5, expression was excluded from the outer (lateral) region of the developing organ of Corti and was strongly upregulated in the inner (medial) region until

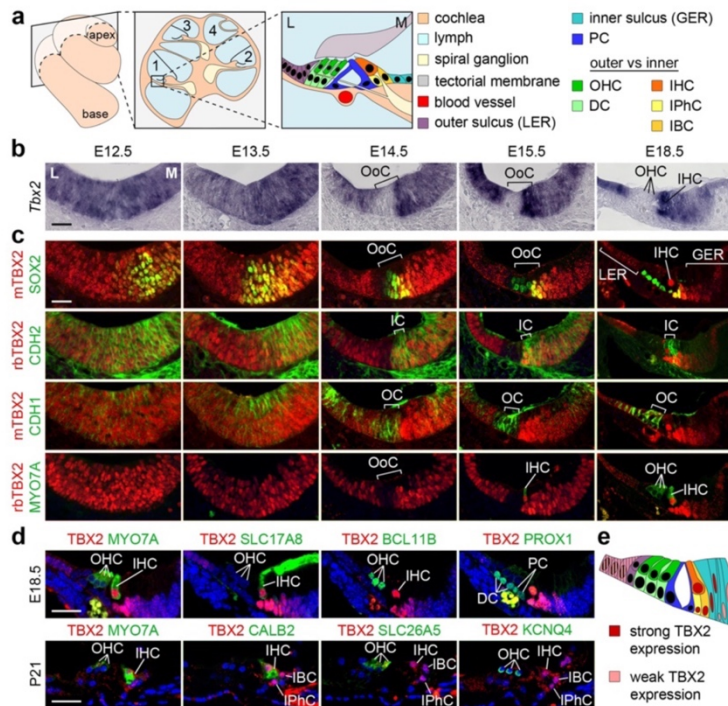


Fig. 1: *Tbx2*/TBX2 expression is progressively confined to IHCs and ISCs during cochlear development. **a**, Scheme showing the basal (1) and the apical (4) turn of the mature cochlea, a cross section through the cochlea, and a magnification of the basal turn with the cellular organization in and around the organ of Corti (OoC): with Deiters' cells (DCs) and OHCs in the outer compartment (OC, shades of green), inner phalangeal cells (IPhCs), inner border cells (IBCs) and IHCs in the inner compartment (IC, shades of yellow) separated by pillar cells (PCs) that form the tunnel of Corti. Laterally, the OoC is flanked by cells of the outer and medially, by cells of the inner sulcus. GER, greater epithelial ridge (primordium of the inner sulcus); L, lateral; LER, lesser epithelial ridge (primordium of the outer sulcus); M, medial. **b**, RNA *in situ* hybridization analysis of *Tbx2* expression in the prosensory epithelium of the cochlea at E12.5 and E13.5 as well as in the developing OoC between E14.5 and E18.5. **c**, Co-immunofluorescence analysis of expression of TBX2 with markers for differentiation (SOX2: pro-sensory cells/supporting cells; MYO7A: hair cells) and compartmentalization (CDH2: inner; CDH1: outer). Two different antibodies were used for detection of TBX2 (m, mouse; rb, rabbit). **d**, Co-immunofluorescence analysis of expression of TBX2 with markers for specific cell types at E18.5 and P21: all hair cells (MYO7A), IHCs (SLC17A8, CALB2), OHCs (BCL11B, SLC26A5, KCNQ4), DCs and PCs (PROX1). **e**, Scheme of TBX2 expression (red nuclei) in the OoC at E18.5. The color code is the same as in (a). n=3 embryos/mice per stage and analysis. Scale bars: 30 μ m.

E18.5. Weaker *Tbx2* expression was detected in cells of the adjacent greater and lesser epithelial ridges (Fig. 1b). TBX2 protein followed the pattern of the mRNA. Regionalisation of TBX2 expression in the developing organ of Corti succeeded the specification of prosensory cells (marked by SOX2) at E12.5 and E13.5, coincided spatially and temporarily with the formation of CDH1⁺ outer and CDH2⁺ inner compartments at E14.5, and preceded the differentiation of hair cells (marked by MYO7A) at E15.5 (Fig. 1c). Co-immunofluorescence analysis using specific markers for all hair cells (MYO7A), IHCs (SLC17A8, CALB2), OHCs (BCL11B, SLC26A5, KCNQ4), Deiters' and pillar cells (PROX1) revealed that TBX2 is confined to IHCs and ISCs at E18.5 and P21 (Fig. 1d,e). This expression profile suggests a role for TBX2 in establishing and/or maintaining hair and supporting cells in the inner compartment of the organ of Corti.

TBX2 specifies the inner compartment of the organ of Corti

To explore the functional significance of compartmentalisation of TBX2 expression in the early development of the organ of Corti, we inactivated and misexpressed *Tbx2* in the entire prosensory domain at E12.5, using a tamoxifen-inducible *Sox2^{creERT2}* mouse line¹⁰ in combination with a *Tbx2^{fllox}* loss-of-function¹¹ or an *Hprt^{TBX2}* gain-of-function allele¹², (Extended Data Fig. 1), and analysed hair and supporting cells in mutant cochleae at E18.5 (Fig. 2a-c).

In both *Sox2^{creERT2/+};Tbx2^{fl/fl}* (*Sox2-Tbx2^{LOF}*) and *Sox2^{creERT2/+};Hprt^{TBX2/Y}* (*Sox2-TBX2^{GOF}*) cochleae the number of hair cells was preserved (Extended Data Fig. 2a) but they were misaligned in rows of four to five cells of width without a clear separation into one inner and three outer rows. In *Sox2-Tbx2^{LOF}* embryos, expression of the IHC marker SLC17A8 was absent, and of the OHC marker BCL11B and the OHC regulator *Insm1*² expanded to the innermost row of hair cells (Fig. 2a,b, Extended Data Fig. 2b). In contrast, in cochleae of *Sox2-TBX2^{GOF}* embryos the number of BCL11B⁺ OHCs was reduced while SLC17A8⁺ cells were increased paralleling the pattern of forced TBX2 expression (Fig. 2a,b, Extended Data Fig. 1e,f). In both transgenic conditions, a small number of hair cells lacked both SLC17A8 and BCL11B (Fig. 2a,b).

The pattern of supporting cells followed the hair cell changes. In *Sox2-Tbx2^{LOF}* cochleae, pillar cells (marked by NGFR) were shifted to border the innermost hair cell row. Moreover, all supporting

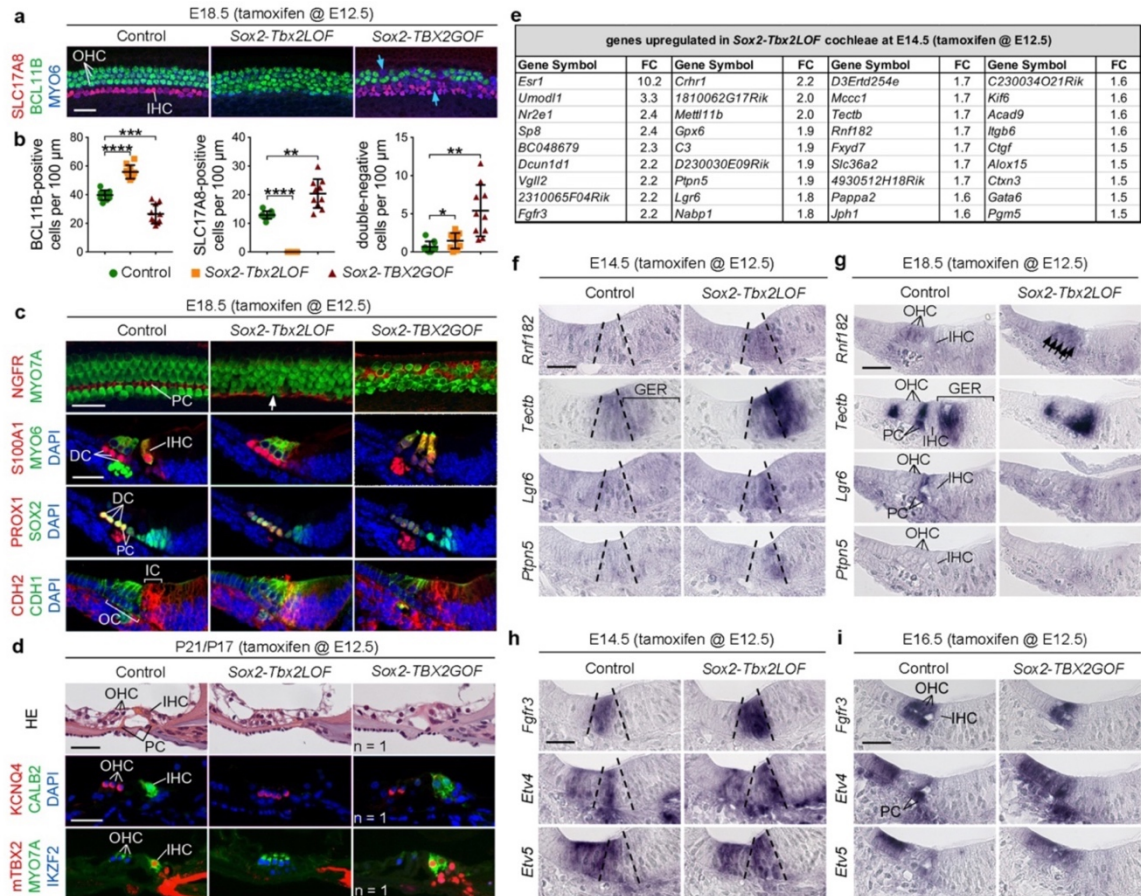


Fig. 2: *Tbx2* specifies the inner compartment of the Organ of Corti. **a**, Co-immunofluorescence analysis of E18.5 cochlear whole-mounts of *Sox2-Tbx2LOF* (n=10 cochleae) and *Sox2-TBX2GOF* embryos (n=10 cochleae) after a single pulse of tamoxifen at E12.5. Expression of SLC17A8 (marks IHCs), BCL11B (marks OHCs) and MYO6 (marks all hair cells) is shown. Blue arrows point to double-negative hair cells (SLC17A8⁺/BCL11B⁺). **b**, Quantification of BCL11B⁺, SLC17A8⁺ and double-negative (only MYO6⁺) hair cells per 100 μm of E18.5 *Sox2-Tbx2LOF*, *Sox2-TBX2GOF* and control organs of Corti (n=10 cochleae) after a single pulse of tamoxifen at E12.5. Mean±standard deviation, unpaired t-test with Welch's correction or Mann-Whitney test. **, p<0,01; ***, p<0,001; ****, p<0.0001. **c**, Immunofluorescence analysis of markers at E18.5: MYO7A/MYO6 in all hair cells, NGFR in pillar cells (PCs, n=6 cochleae), S100A1 in Deiters' cells (DCs) and IHCs, PROX1 in DCs and PCs,

cells underneath the hair cells strongly expressed S100A1 (marks Deiters' cells) and PROX1 (marks Deiters' and pillar cells), indicating a gain of OSCs at the expense of ISCs. In *Sox2-TBX2GOF* mutants, NGFR⁺ pillar cells intermingled with OHC rows. Expression of PROX1 and S100A1 was strongly reduced indicating a gain of ISCs at the expense of OSCs. Hair and supporting cell changes in *Sox2-Tbx2LOF* and *Sox2-TBX2GOF* embryos were accompanied by a medial expansion and reduction, respectively, of the outer compartment marker CDH1

SOX2 in all supporting cells, CDH1 in the outer compartment (OC), CDH2 the inner compartment (IC). Nuclei were counterstained with DAPI. **d**, Histological and immunofluorescence analyses of hair cell markers at P21: MYO7A (all hair cells), KCNQ4 and IKZF2 (OHCs), CALB2 and TBX2 (IHCs). **e**, List of genes with increased expression in E14.5 *Sox2-Tbx2LOF* cochlear ducts as detected by microarray analysis (n=4). **f,g**, Spatial distribution of upregulated genes by RNA *in situ* hybridization on E14.5 (**f**) and E18.5 (**g**) cochlear sections. Arrows point to *Rnf182*-expressing hair cells. **h,i**, Spatial distribution of *Fgf3* and of downstream targets of FGF signaling, *Etv4/5*, in E14.5 *Sox2-Tbx2LOF* (**h**) and E16.5 *Sox2-TBX2GOF* embryos (**i**). Dashed lines in **f,h** show the position of the developing organ of Corti. n=3-4 embryos per analysis. Scale bars: 30 μm. GER, greater epithelial ridge.

(Fig. 2c), pointing to disturbed compartmentalization of the organ of Corti at this stage.

Histological and molecular analysis of mice at P21 and P17, respectively, revealed that the altered patterns of hair cell types observed at E18.5, were preserved in mature *Sox2-Tbx2LOF* and *Sox2-TBX2GOF* cochleae. In *Sox2-Tbx2LOF* mice, all cochlear hair cells presented features of OHCs (smaller size, smaller nucleus, expression of KCNQ4 and SLC26A5). Importantly, these cells also expressed IKZF2, the key regulator of OHC maturation. In contrast, *Sox2-TBX2GOF* cochleae

exhibited an increased number of hair cells with characteristics of IHCs (larger size, large nucleus, expression of SLC17A8 and CALB2) while the number of (IKZF2⁺) OHCs was correspondingly decreased (Fig. 2d, Extended Data Fig. 2c).

The disturbed compartmentalization in *Sox2-Tbx2LOF* mice may result from a mispatterning of prosensory progenitors or from a transdifferentiation of hair and supporting cells that have correctly been specified. To discriminate between these two possibilities, we performed transcriptional profiling by microarray analysis of control and mutant cochlear ducts at E14.5 when hair and supporting cell differentiation has not yet occurred. *Significance Analysis of Microarrays* (SAM) identified 36 upregulated and 90 downregulated genes in the mutant. Among the list of downregulated transcripts, some genes have been described to be expressed in cells of the inner compartment such as *Pvalb*¹³ and *Fgf8*¹⁴, *Fabp7*¹⁵ and *Lfng*¹⁶ (Supplementary table 1). In contrast, some of the upregulated genes were previously identified as markers of the outer compartment (*Crhr1*^{17,18}, *Lgr6*¹⁹, *Ctgf*²⁰ and *Fgfr3*²¹) (Fig. 2e, Supplementary table 2) indicating an expansion of the outer at the expense of the inner compartment at onset of organ of Corti development. This notion was corroborated by *in situ* hybridization analysis of upregulated genes (potential targets of TBX2 repressive activity) in E14.5 and E18.5 *Sox2-Tbx2LOF* cochleae (Fig. 2f,g). *Rnf182*, a gene expressed in OHCs of control animals at E18.5, was ectopically expressed in the entire developing organ of Corti at E14.5. Expression of *Tectb* was strongly enhanced in the inner compartment of the organ of Corti and in the adjacent greater epithelial ridge. *Lgr6*, *Ptpn5* and *Fgfr3* were ectopically expressed in the inner compartment. Since *Lgr6* marks pillar cells starting from E15.5¹⁹, this points to a premature specification of this cell type. Together with loss of CDH2 expression in the inner compartment of the developing organ of Corti at E14.5 (Extended Data Fig. 3), these changes indicate that the inner compartment is not established in the prosensory region of *Sox2-Tbx2LOF* embryos.

We noted increased and/or ectopic expression of some candidate genes in the cochlear epithelium outside the organ of Corti in *Sox2-Tbx2LOF* embryos (Extended Data Fig. 4) pointing to a functional implication of TBX2 expression in the lesser and greater epithelial ridges.

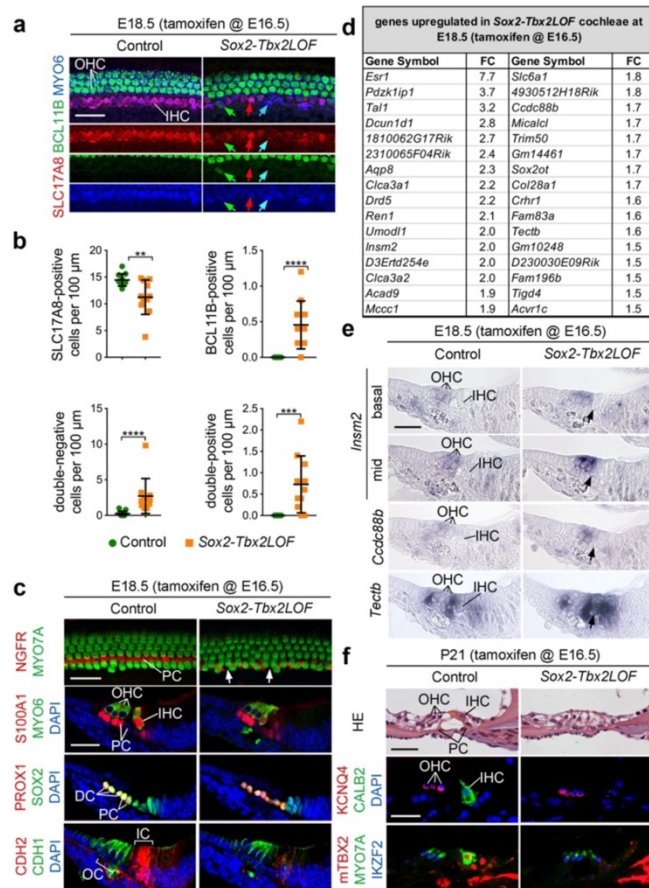


Fig. 3: *Tbx2* maintains IHC and ISC fate by preventing transdifferentiation into OHCs and OSCs, respectively. **a**, Co-immunofluorescence analysis of E18.5 cochlear whole-mounts of *Sox2-Tbx2LOF* embryos (n=11 cochleae) after a single pulse of tamoxifen at E16.5. Red arrow points to a MYO6⁺/SLC17A8⁺ IHC, green arrow to a MYO6⁺/BCL11B⁺ OHC-like and blue arrow to a double-negative hair cell (SLC17A8⁺/BCL11B⁺) in the innermost hair cell row. **b**, Quantification of BCL11B⁺, SLC17A8⁺, double-negative (only MYO6⁺) and double-positive hair cells per 100 μ m in the inner compartment (IC) of E18.5 *Sox2-Tbx2LOF* organs of Corti (n=11 cochleae) after a single pulse of tamoxifen at E16.5. Mean \pm standard deviation, unpaired t-test with Welch's correction or Mann-Whitney-U test. **, p<0,01; ***, p<0,001; ****, p<0.0001. **c**, Immunofluorescence analysis at E18.5: MYO7A/MYO6 (all hair cells), NGFR (pillar cells, PCs, n=6 cochleae), S100A1 (Deiters' cells, DCs and IHCs), PROX1 (DCs and PCs), SOX2 (all supporting cells), CDH1 in the outer compartment (OC), CDH2 in the inner compartment (IC). Nuclei were counterstained with DAPI. **d**, List of genes with increased expression in E18.5 *Sox2-Tbx2LOF* organs of Corti as detected by microarray analysis (n=4). **e**, Validation of some MA candidates by RNA *in situ* hybridization analysis. *Insm2* expression is shown at the basal and medial (mid) turn of the cochlear duct. **f**, Histological and immunofluorescence analyses of hair cell markers at P21: MYO7A (all hair cells), KCNQ4 and IKZF2 (OHCs), CALB2 and TBX2 (IHCs). n=3-4 embryos or n=5 mice per analysis. Scale bars: 30 μ m.

Fgfr3 (fibroblast growth factor receptor 3) was the only deregulated gene, which exhibited a complementary pattern of expression to *Tbx2* in the

developing organ of Corti. *Fgfr3* was expressed in the outer compartment of control cochleae. Its expression expanded into the inner compartment in *Sox2-Tbx2LOF* embryos, and was medially reduced in *Sox2-Tbx2GOF* mutants. Concordantly, expression of *Etv4* and *Etv5*, direct targets of FGF signaling²², was medially expanded upon *Tbx2*-deletion and the *Etv4/5*-negative outer region was lost upon *TBX2*-misexpression (Fig. 2h,i).

Previous work implicated FGF signalling in multiple aspects of cell differentiation in the outer compartment of the organ of Corti^{21,23–27}. Notably, lineage tracing experiments in mouse demonstrated that OHCs, OSCs and pillar cells derive from FGFR3⁺ progenitors²⁸, and deletion or inactivation of *Fgfr3* resulted in disturbed maturation of pillar cells and reduced expression of the OHC-marker SLC26A5^{14,29}. This strongly suggests that *Tbx2* establishes the inner compartment of the organ of Corti by preventing FGFR3-dependent FGF signalling in this region.

TBX2 maintains the fate of differentiating IHCs and ISCs

We next explored whether TBX2 is critical for maintaining the fate of cochlear hair and supporting cells. At E16.5, when these cell types are established at the base of the cochlear duct², they still express SOX2. We therefore administered a single pulse of tamoxifen at E16.5 to *Sox2-TBX2LOF* and *Sox2-TBX2GOF* embryos to analyse for phenotypic changes at E18.5 (Fig. 3a-c). Since we did not obtain *Sox2-TBX2GOF* embryos at this stage, we limited our analysis to the loss-of-function situation.

In *Sox2-TBX2LOF* cochleae, the total number of hair cells was unchanged (Extended Data Fig. 5a). Hair cells in the outer compartment of the organ of Corti were perfectly aligned and expressed the OHC marker BCL11B comparable to control. In contrast, hair cells of the inner compartment were misaligned, showed partly reduced expression of IHC markers SLC17A8 and S100A1, and to some extent ectopic expression of the OHC-marker BCL11B. NGFR⁺ pillar cells were intermingled with the innermost row of hair cells. Although the number of S100A1⁺ Deiters' cells was unchanged, the PROX1⁺ OSC population expanded medially in *Sox2-Tbx2LOF* mutants. Expression of CDH1 was normal but CDH2 was strongly downregulated in the inner compartment (Fig. 3a-c).

Transcriptional profiling of E18.5 *Sox2-Tbx2LOF* cochlear ducts by microarray analysis identified 48 down- and 32 upregulated genes. Among the genes with reduced expression, we found candidates whose

specific or enhanced expression in cells of the inner compartment was previously described: *Fgf8*¹⁴, *Cabp2*³⁰, *Slc17a8*³¹ and *Gabrg3*³² in IHCs, *Fgf20*²³ and *Otol1*³³ in ISCs, and *Npy*²⁸ in inner pillar cells (Supplementary table 3). In the list of upregulated genes, some genes have been described to be expressed in cells of the outer compartment: *Pdzk1ip1*²⁸, *Tal1*¹⁸, *Drd5*³⁴, *Insm2*² and *Crhr1*¹⁷ (Fig. 3d, Supplementary table 4). Only very few candidates were detectable by RNA *in situ* hybridization in control and mutant embryos at E18.5: *Insm2* and *Ccdc88* showed increased expression in OHCs but were not ectopically expressed in the innermost hair cell, contrary to *Tectb*; *Pdzk1ip1*, *Tal1* and *Slc6a1* were expressed in Deiters' cells in both control and mutant (Fig. 3e, Extended Data Fig. 5b). Together, marker analysis and transcriptional profiling suggest that in E18.5 *Sox2-Tbx2LOF* cochleae, hair and supporting cells of the inner compartment have undergone a partial fate shift.

At P21, almost all hair cells expressed OHC-specific markers (IKZF2, SLC26A5, KCNQ4) whereas expression of IHC-specific markers (CALB2, SLC17A8) was not detected (Fig. 3f, Extended Data Fig. 5c) indicating a complete conversion of IHCs to OHCs after an extended time interval. This shows that *Tbx2* is required to maintain the fate of IHCs and ISCs after E16.5 by preventing their transdifferentiation into OHC and OSC, respectively. To address whether FGFR3-mediated signalling contributes to the observed cytodifferentiation defects in *Sox2-Tbx2LOF* embryos, we analysed the expression of some FGF signalling components at E18.5. Hair cells of the inner row lacked expression of *Fgf8* consistent with the loss of an IHC fate. Expression of *Fgfr3* was medially expanded but did not translate into expression of the FGF targets *Etv4/5* that mark pillar cells at this stage (Extended Data Fig. 5d). This precludes transcription-dependent effects of FGFR3 signalling as contributors of hair and supporting cell fate changes in this setting.

TBX2 cell-autonomously maintains IHC fate

To manipulate *Tbx2* function specifically in hair cells, we used an *Atoh1-CreER*^{T2}-mouse line³⁵ that mediates stochastic recombination in differentiating hair cells at low frequency (Extended Data Fig. 6). After administering a single pulse of tamoxifen at E15.5, the total number of MYO6⁺ hair cells and their separation in one inner and three outer rows was preserved in the cochlea of both *Atoh1-CreER*^{T2/+}; *Tbx2*^{fl/fl} (*Atoh1-Tbx2LOF*) and *Atoh1-CreER*^{T2/+}; *Hprt*^{TBX2/+} (*Atoh1-TBX2GOF*) embryos at E18.5 (Fig. 4a, Extended Data Fig. 7a). However, in

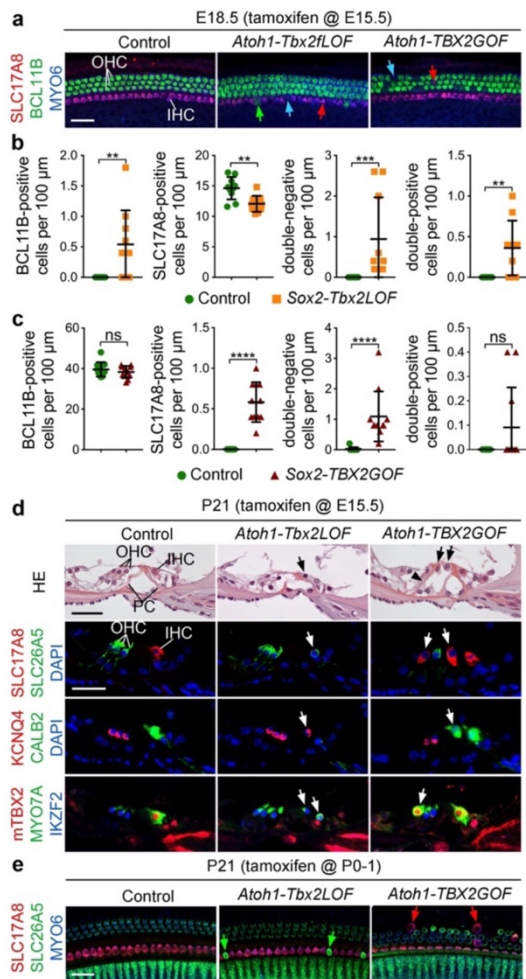


Fig. 4: TBX2 is required and sufficient to induce and maintain the IHC fate. **a**, Co-immunofluorescence analysis of E18.5 cochlear whole-mounts of *Atoh1-Tbx2LOF* (n=10 cochleae) and *Atoh1-TBX2GOF* embryos (n=11 cochleae) after a single pulse of tamoxifen at E15.5. Red arrow points to MYO6⁺/SLC17A8⁺, green arrow to a MYO6⁺/BCL11B⁺ and blue arrow to double-negative hair cell (SLC17A8⁺/BCL11B⁻). **b,c**, Quantification of BCL11B⁺, SLC17A8⁺, double-negative (only MYO6⁺) and double-positive hair cells per 100 μm in the inner compartment of E18.5 *Atoh1-Tbx2LOF* (n=10 cochleae) (**b**) and the outer compartment of *Atoh1-TBX2GOF* (n=11 cochleae) (**c**) organs of Corti after a single pulse of tamoxifen at E15.5. Mean±standard deviation, unpaired t-test or Mann-Whitney-U test. ns, not significant; **, p<0.01; ***, p<0.001; ****, p<0.0001. **d**, Histological and immunofluorescence analysis of hair cell-specific markers at P21: MYO7A (all hair cells), SLC17A8, CALB2 and TBX2 (IHCs), KCNQ4, SLC26A5 and IKZF2 (OHCs). Arrows point to ectopic OHCs and IHCs, respectively. Arrow head points to an ectopic pillar cell. Nuclei were counterstained with DAPI. n=4-7 mice. **e**, Immunofluorescence analyses of *Atoh1-Tbx2LOF* and *Atoh1-TBX2GOF* organs of Corti at P21. Recombination was induced through oral tamoxifen application to breast-feeding dams at P0-1. Green arrows point to ectopic and small SLC26A5⁺ OHCs in the innermost hair cell row of *Atoh1-Tbx2LOF* mice. Red arrows point to ectopic and large SLC17A8⁺ IHCs in the outermost hair cell rows of *Atoh1-TBX2GOF* mice. n=9-10 cochleae. Scale bars: 30 μm.

the innermost hair cell row of *Atoh1-Tbx2LOF* cochleae the number of hair cells expressing the IHC marker SLC17A8 was decreased whereas the number of hair cells expressing the OHC-marker BCL11B, or none or both of these markers was increased (Fig. 4a,b). In *Atoh1-TBX2GOF* embryos, we detected a significantly increased number of SLC17A8⁺ and BCL11B/SLC17A8-double-negative hair cells in the outer compartment of the organ of Corti (Fig. 4a,c). Histological analysis at P21 revealed a normal structural appearance of the organ of Corti in *Atoh1-Tbx2LOF* embryos. However, hair cells located medially from pillar cells, i.e. in the inner row, expressed OHC markers (SLC26A5, KCNQ4) and the regulator of OHC-fate IKZF2 instead of IHC markers (SLC17A8, CALB2). In contrast, in *Atoh1-TBX2GOF* embryos, we found ectopic IHC-like cells and supernumerary pillar cells in the outer compartment of the organ of Corti (Fig. 4d, Extended Data Fig. 7b).

Postnatal inactivation or misexpression of *Tbx2* in cochlear hair cells at P0-1 led to similar changes of IHC and OHC marker expression at P21 (Fig. 4e). This shows that TBX2 confers IHC fate cell-autonomously and independently from positional information.

Conclusion

Together, our findings show TBX2 acts within the organ of Corti in two consecutive but likely independent steps. First, around E14.5, TBX2 patterns the prosensory progenitors and specifies the inner compartment that subsequently gives rise to IHCs and ISCs. After this step, TBX2 cell-autonomously maintains IHCs and ISCs by preventing transdifferentiation into OHCs and OSCs, respectively. We suggest that *Fgfr3* is a critical target of the early patterning function, while the latter role of TBX2 is mediated by repression of regulators of OHC fate such as IKZF2.

Methods

The sample size was not predetermined by statistical methods. The experiments were not blinded due to the obvious phenotype. For all experiments, mutant and control animals were randomly chosen from the litter.

Ethics and animals. All animal work conducted for this study was performed in strict accordance to European and German legislation. The breeding and handling of mouse lines was performed at the central animal laboratory of the Hannover Medical School and approved by the Niedersächsisches Landesamt für Verbraucherschutz und Lebensmittelsicherheit (Permit Number: 33.12-42502-04-19/3081).

All mouse alleles employed in this study have previously been described and were maintained on an NMRI genetic background.

A conditional floxed allele of *Tbx2* [*Tbx2^{tm2.1Vmc}*, synonym: *Tbx2^{lox}*]¹¹ was provided by Vincent Christoffels; an allele with insertion of the human *TBX2* gene at the *Hprt* locus [*Hprt^{tm2(CAG-TBX2-EGFP)Aki}*, synonym: *Hprt^{TBX2}*]¹² was generated in house. The double fluorescent Cre reporter line *Gt(ROSA)26Sor^{tm4(ACTB-tdTomato-EGFP)LoxP}* [*#007576*, synonym: *R26^{mTmG}*]³⁶, the tamoxifen-inducible *Cre-ER^{T2}* driver lines *Sox2^{creERT2}* [*#017593*, *Sox2^{tm1(cre/ERT2)Hoch}*]¹⁰ and *Atoh1-creER^{T2}* [*#007684*, *Tg(Atoh1-cre/Esr1*)14Fsh*]³⁵ were obtained from The Jackson Laboratory. The *Hprt^{TBX2}* strain is available upon request from Andreas Kispert.

Embryos for *Tbx2*/TBX2 expression analyses were derived from matings of NMRI wild-type mice. For generation of loss-of-function mutants *Sox2^{creERT2/+};Tbx2^{lox/lox}* males were mated with *Tbx2^{lox/lox};R26^{mTmG/mTmG}* females to obtain *Sox2^{creERT2/+};Tbx2^{lox/lox};R26^{mTmG/+}* (*Sox2-Tbx2LOF*) mice, and *Atoh1-creER^{T2}+/+;Tbx2^{lox/lox}* males with *Tbx2^{lox/lox};R26^{mTmG/mTmG}* females to obtain *Atoh1-creER^{T2}+/+;Tbx2^{lox/lox};R26^{mTmG/+}* (*Atoh1-Tbx2LOF*) mice. For generation of gain-of-function or misexpression mutants *Sox2^{creERT2/+}* males were mated with *Hprt^{TBX2/TBX2}* females to obtain *Sox2^{creERT2/+};Hprt^{TBX2/Y(+)}* (*Sox2-TBX2GOF*) mice, and *Atoh1-creER^{T2}+/+* males with *Hprt^{TBX2/TBX2}* females to obtain *Atoh1-creER^{T2}+/+;Hprt^{TBX2/Y(+)}* (*Atoh1-TBX2GOF*) mice. *Cre*-negative littermates or *Sox2^{creERT2/+};R26^{mTmG/+}* and *Atoh1-creER^{T2}+/+;R26^{mTmG/+}* served as controls.

For embryonic staging, the discovery day of a vaginal plug was defined as embryonic day (E) 0.5. To induce recombination, 4 mg of tamoxifen (*#T5648*, Sigma-Aldrich) dissolved in corn oil (*#C8267*, Sigma-Aldrich) were orally applied to timed pregnant or breast-feeding dams in a single pulse at E12.5, E15.5, E16.5 or P0-1. From E15.5 onwards, 2 mg of progesterone (*#P8783*, Sigma-Aldrich) were additionally applied. Pregnant females and juvenile mice were euthanized by cervical dislocation, neonates were euthanized by decapitation. Embryos at E14.5, E16.5 and E18.5, neonates at P4 and juveniles at P17/21 were collected for analyses.

Tissue collection and preparation. Embryos were dissected in phosphate-buffered saline (PBS) and decapitated. For organ of Corti whole-mount preparations, cochleae were isolated in PBS and non-sensory epithelia (stria vascularis, Reissner's membrane) were removed. Embryonic heads and cochlear whole-mounts were then fixed overnight in 4% paraformaldehyde (PFA)/PBS (*#A3813*, AppliChem) at 4°C, dehydrated through an ascending methanol series (diluted in PBS) and stored in absolute methanol at -20°C until use.

For collection of older tissue (P21), inner ears were isolated in PBS after decapitation, fixed in 4% PFA overnight and decalcified for 2 days in 0.5 M EDTA/PBS (*#A2937*, AppliChem), pH7.4, at 4°C. Organ of Corti whole-mounts were isolated from inner ears after decalcification and dissected into three pieces (basal, medial, apical). Inner ears and cochlear whole-mounts were then dehydrated and stored in absolute methanol at -20°C until use.

Genotypes were determined by sorting of GFP-expressing tissues and by PCR on genomic DNA prepared from embryonic tissues or ear clips.

Histological analysis. Embryonic heads or postnatal inner ears were embedded in paraffin wax and sectioned to 5-μm. Sections were stained with Hematoxylin (*#GHS332*, Sigma-Aldrich) for 45 seconds, blued in 0.5% sodium-acetate for 1 minute and counterstained with Eosin Y solution (*#HT110132*, Sigma-Aldrich) for 60-90 seconds.

Immunohistochemistry on sections. Detailed information on antibodies, including order number and working concentrations, can be found in Supplementary table 5.

Tissue was embedded in paraffin wax and sectioned to 5-μm, followed by deparaffinization in Roti-Histol (*#6640*, Roth) and rehydration in a descending ethanol/H₂O series. For embryonic sections (E14.5, E16.5, E18.5), epitope retrieval was accomplished with citrate-based antigen unmasking solution (*#H-3300*, Vector Laboratories) for 15 minutes at 100°C. Postnatal tissue sections (P17/21) were subjected to heat-induced antigen retrieval 10 mM Tris-HCl/2 mM EDTA buffer, pH 9.0, for 90 minutes at 80°C. Endogenous peroxidase activity was blocked by incubation in 3% H₂O₂/PBS (*#AP121076.1211*, AppliChem) for 15 minutes at room temperature (RT). All washing steps were performed using 0.1% Tween-20 in PBS (PBST). Samples were blocked with TNB Blocking Buffer (*#FP1012*, PerkinElmer) for 1 hour. For antibodies generated in mice an additional IgG blocking step was performed using the M.O.M. Mouse Ig Blocking Reagent (*#MKB-2213-1*, Vector Laboratories). After blocking, sections were incubated with primary antibodies (diluted in TNB) overnight at 4°C, followed by appropriate secondary and sometimes tertiary antibodies in TNB for 1 hour at RT. Sections were counterstained with DAPI (0.1 μg/ml in PBST, *#6335*, Roth) for 10 minutes and mounted with Immunoselect Antifading Mounting Medium (*#SCR-38447*, Dianova).

For weakly expressed proteins, biotin-labelled secondary antibodies (1 hour at RT) and the Tyramide Signal Amplification Kit (TSA, *#NEL702001KT/NEL701001KT*, PerkinElmer) were used for signal detection. HRP-conjugated streptavidin was diluted in TNB (1:100) and applied to sections for 30 minutes to 1 hour at RT, whereas incubation with TSA reagent was performed for 10 to 15 minutes at RT in accordance with the manufacturer's protocol. For sequential double amplification, a 30 minutes 6% H₂O₂/PBS and an Avidin/Biotin block (15 minutes each, *#SP-2001*, Vector Laboratories) were performed in between the two amplification steps.

For sequential double labelling with two primary antibodies generated in the same host, masking of the first primary antibody was performed using the following unconjugated FAB fragments: goat-anti-rabbit FAB fragment (*#111-007-003*, Dianova), donkey-anti-mouse FAB fragment (*#715-007-003*, Dianova).

Immunohistochemistry on cochlear whole-mount preparations. Cochlear whole-mounts were rehydrated in a descending methanol/PBS series. For the first permeabilization step, whole-mounts were treated with proteinase K (10 μg/ml, *#RP102B*, 7Bioscience) diluted in buffer for 2 minutes at RT. Digestion was stopped by washing in 0.2% glycine/PBS (*#A1067*, AppliChem). For all following permeabilization or washing steps 0.3% Triton X-100 in PBS was used. Endogenous peroxidase activity was blocked by incubation in 3% H₂O₂/PBS for 15 minutes at RT. Samples were blocked with 20% heat-inactivated FCS in PBS-Triton for 1 hour at RT, followed by an overnight incubation with primary antibodies, diluted in blocking solution, at 4°C. Appropriate secondary and sometimes tertiary antibodies were applied to cochlear whole-mounts for 2 hours at RT.

For detection of BCL11B, antigen retrieval was required prior to the blocking step. This was performed using 10 mM sodium citrate, pH 6 with 0.25% Triton X-100 for 30 min at 90°C, followed by cooling down at RT for 30 minutes.

For visualization of NGFR (P75^{NTR}), a biotin-labelled secondary antibody (2 hours at RT) and the TSA Kit were used. Cochlear whole-mounts were incubated with the staining reagent for 30 minutes at RT, followed by washing with PBS-Triton on ice and inactivation of the horseradish peroxidase by incubation in 6% H₂O₂/PBS for 30 minutes at RT.

In some cases, cochlear whole-mount preparations were counterstained with DAPI and mounted with IS mounting medium.

Generation of antisense RNA *in situ* probes. *In vitro* transcription of digoxigenin-labelled-antisense RNA probes from DNA templates was performed using digoxigenin-labelling mix (#11277073910, Sigma) and T7/T3/SP6-RNA-Polymerases (#M0251/11031163001/M0207, NEB/Sigma-Aldrich).

For transcripts, for which no DNA template was available, primers pairs were designed using the MacVector software (version 16.0.8), modified with an additional T7-promoter sequence at the 5' end of the reverse primer, and used for PCR based amplification of DNA templates from genomic DNA or cDNA. Accuracy of all probe templates was confirmed by sequencing. Primer sequences used for amplification of DNA templates are listed in Supplementary table 6.

RNA *in situ* hybridization. *In situ* hybridization analysis was performed on 10- μ m paraffin sections following a standard procedure with digoxigenin-labelled antisense riboprobes³⁷. In brief, sections were deparaffinized, rehydrated in a descending ethanol/water series, and then treated with 10 μ g/ml proteinase K (#RP102B, 7Bioscience) diluted in Tris-HCl buffer solution, pH 7.4, for 7 minutes at 37°C. Followed by a 5-minute incubation in 0.2% glycine/PBS, and re-fixation in 4% PFA/0.2% glutaraldehyde for 20 minutes at RT. Hybridization with digoxigenin-labelled riboprobes was performed overnight at 70°C. After two 30-minute washing steps in saline sodium citrate/formamide at 65°C and a blocking step at RT, sections were incubated with sheep-anti-digoxigenin Fab fragments conjugated with alkaline phosphatase (1:4000, #11093274910, Roche) for 2 hours at RT. Staining reaction was developed using the BM Purple AP substrate precipitating solution (#11442074001, Sigma Aldrich) to localize bound anti-digoxigenin antibody.

Microarray analysis of cochlear ducts. For the E14.5 microarray analysis, whole cochlear ducts were isolated in Leibovitz's L15 Medium (#F1315, Biochrom) and the spiral ganglion was removed. For the E18.5 microarray analysis, cochlear ducts were isolated in Leibovitz's L15 Medium and dissected into two halves. The spiral ligament and the spiral ganglia were removed from the basal half and the remaining sensory tissue was collected for analysis. Immediately after dissection/isolation the tissue was frozen using dry ice and stored at -80°C until use.

For the E14.5 microarray analysis, four independent sex-sorted pools per genotype, each containing 23-27 cochlear ducts, were collected from *Sox2-Tbx2LOF* mutants and cre-negative controls after a single pulse of tamoxifen at E12.5. For the E18.5 microarray analysis four independent sex-sorted pools per genotype, each containing 16-20 organs of Corti from the basal half of the cochlear duct, were collected from *Sox2-Tbx2LOF* mutants and cre-negative controls after a single pulse of tamoxifen at E16.5. After total RNA extraction using the peqGOLD RNAPure reagent (#732-3312, Peqlab) according to the manufacturer's instructions, samples were sent to the Research Core Unit Transcriptomics of Hannover Medical School where they were hybridized to Agilent Whole Mouse Genome Oligo v2 (4x44K) Microarrays (#G4846A, Agilent Technologies) in a dual-colour mode.

Deregulated genes were determined with the software *Significance Analysis of Microarrays* 5.0 (SAM, Stanford University, CA, USA)³⁸. For the analysis normalized expression data was assessed by two class unpaired comparison with *t*-statistics ($n=4$). The value of k for the k -nearest-neighbor algorithm was set to 10 (default), the number of permutations was 100 (default). For the significance cut-off we used a minimum fold change of 1.5 and values for δ (1.39 for E14.5, 1.15 for E18.5) that resulted in an estimated false discovery rate (FDR) of zero.

Image acquisition and analysis. Sections were photographed using the Leica DM5000 microscope with a Leica DFC300FX

digital camera or the Leica DM6000 microscope with a Leica DFC350FX digital camera.

Images of cochlear whole-mounts were acquired using the confocal laser scanning microscope Leica TCS SP8. For overviews the 20x oil magnification was used, whereas the 40x water objective was used for higher magnifications.

Images were processed using Adobe Photoshop CS4.

Quantifications and statistical analysis. Quantification of specific cell types on cochlear whole-mounts at E18.5 occurred in two steps. First, a 500 μ m-long region of the organ of Corti at the mid-basal level of the cochlear duct was defined. Second, MYO6⁺ cells were counted within this area (approx. 260 cells per sample) and each and every hair cell was analysed for expression of BCL11B and/or SLC17A8. Measurements and cell counts were performed using ImageJ (NIH) and Adobe Photoshop CS4 software. At the end cell counts were averaged to a 100 μ m-distance.

Statistical analyses were performed using GraphPad Prism7 and JASP (version 0.13.1). Normal distribution of data was tested using the D'Agostino & Pearson and Shapiro-Wilk normality test (normal distribution if p -values ≥ 0.05) and Q-Q-plots. Equality of variances was assessed by performing the F- and Levene's test (equal variances if p -values ≥ 0.05). For comparison of two groups with normal distribution (parametric) and equal variances we used the unpaired two-tailed *t*-test. For comparison of two groups with normal distribution and unequal variances we used the two-tailed Welch's *t*-test. For comparison of two groups with nonparametric distribution we used the two-tailed Mann-Whitney U test. Results were expressed as mean \pm SD. A p -value < 0.05 was considered statistically significant. For results see Supplementary tables 7-11.

Data availability

All data are available from the corresponding authors upon reasonable request. Microarray data have been deposited in Gene Expression Omnibus under the accession numbers GSE180500 and GSE180501.

References

1. Chessum, L. *et al.* Helios is a key transcriptional regulator of outer hair cell maturation. *Nature* **563**, 696–724 (2018).
2. Wiwatpanit, T. *et al.* Trans-differentiation of outer hair cells into inner hair cells in the absence of INSM1. *Nature* **563**, 691–695 (2018).
3. Dabdoub, A. *et al.* Sox2 signaling in prosensory domain specification and subsequent hair cell differentiation in the developing cochlea. *Proc. Natl. Acad. Sci. U. S. A.* **105**, 18396–401 (2008).
4. Bermingham, N. A. *et al.* Math1: An Essential Gene for the Generation of Inner Ear Hair Cells. *Science* (80-.). **284**, 1837–1841 (1999).
5. Marcotti, W., Johnson, S. L., Holley, M. C. & Kros, C. J. Development of changes in the expression of potassium currents of embryonic, neonatal and mature mouse inner hair cells. *J. Physiol.* **548**, 383–400 (2003).
6. Roberson, D. W. & Rubel, E. W. Cell division in the gerbil cochlea after acoustic trauma. *Am. J. Otol.* **15**, 28–34 (1994).
7. Lorenzen, S. M., Duggan, A., Osipovich, A. B., Magnuson, M. A. & García-Añoveros, J. Insm1 promotes neurogenic proliferation in delaminated otic progenitors. *Mech. Dev.* **138**, 233–245 (2015).
8. Papaioannou, V. E. The T-box gene family: emerging roles in development, stem cells and cancer. *Development* **141**, 3819–3833 (2014).
9. Kaiser, M. *et al.* Regulation of otocyst patterning by Tbx2 and Tbx3 is required for inner ear morphogenesis in the

- mouse. *Development* **148**, (2021).
10. Arnold, K. *et al.* Sox2 + adult stem and progenitor cells are important for tissue regeneration and survival of mice. *Cell Stem Cell* **9**, 317–329 (2011).
 11. Wakker, V. *et al.* Generation of mice with a conditional null allele for Tbx2. *genesis* **48**, 195–199 (2010).
 12. Singh, R. *et al.* Tbx2 and Tbx3 induce atrioventricular myocardial development and endocardial cushion formation. *Cell. Mol. Life Sci.* **69**, 1377–1389 (2012).
 13. Simmons, D. D., Tong, B., Schrader, A. D. & Hornak, A. J. Oncomodulin identifies different hair cell types in the mammalian inner ear. *J. Comp. Neurol.* **518**, 3785–3802 (2010).
 14. Jacques, B. E., Montcouquiol, M. E., Layman, E. M., Lewandoski, M. & Kelley, M. W. Fgf8 induces pillar cell fate and regulates cellular patterning in the mammalian cochlea. *Development* **134**, 3021–3029 (2007).
 15. Saino-Saito, S. *et al.* Localization of fatty acid binding proteins (FABPs) in the cochlea of mice. *Ann. Anat.* **192**, 210–214 (2010).
 16. Basch, M. L. *et al.* Fine-tuning of Notch signaling sets the boundary of the organ of Corti and establishes sensory cell fates. *Elife* **5**, 1–23 (2016).
 17. Vetter, D. E. *et al.* Urocortin-deficient mice show hearing impairment and increased anxiety-like behavior. **31**, 363 (2002).
 18. Maass, J. C. *et al.* Transcriptomic analysis of mouse cochlear supporting cell maturation reveals large-scale changes in Notch responsiveness prior to the onset of hearing. *PLoS One* **11**, 167286 (2016).
 19. Zhang, Y. *et al.* Dynamic expression of Lgr6 in the developing and mature mouse cochlea. *Frontiers in Cellular Neuroscience* vol. 9 165 (2015).
 20. Adams, J. C. Immunocytochemical traits of type IV fibrocytes and their possible relations to cochlear function and pathology. *JARO - J. Assoc. Res. Otolaryngol.* **10**, 369–382 (2009).
 21. Hayashi, T., Cunningham, D. & Bermingham-McDonogh, O. Loss of Fgf3 leads to excess hair cell development in the mouse organ of Corti. *Dev. Dyn.* **236**, 525–533 (2007).
 22. Raible, F. & Brand, M. Tight transcriptional control of the ETS domain factors Erm and Pea3 by Fgf signaling during early zebrafish development. *Mech. Dev.* **107**, 105–117 (2001).
 23. Huh, S.-H., Jones, J., Warchol, M. E. & Ornitz, D. M. Differentiation of the lateral compartment of the cochlea requires a temporally restricted FGF20 signal. *PLoS Biol.* **10**, 1–12 (2012).
 24. Shim, K., Minowada, G., Coling, D. E. & Martin, G. R. Sprouty2, a mouse deafness gene, regulates cell fate decisions in the auditory sensory epithelium by antagonizing FGF signaling. *Dev. Cell* **8**, 553–64 (2005).
 25. Pirvola, U. *et al.* FGFR1 is required for the development of the auditory sensory epithelium. *Neuron* **35**, 671–680 (2002).
 26. Mansour, S. L., Li, C. & Urness, L. D. Genetic rescue of Muenke syndrome model hearing loss reveals prolonged FGF-dependent plasticity in cochlear supporting cell fates. *Genes Dev.* **27**, 2320–2331 (2013).
 27. Ono, K. *et al.* FGFR1-Frs2/3 Signalling Maintains Sensory Progenitors during Inner Ear Hair Cell Formation. *PLoS Genet.* **10**, e1004118 (2014).
 28. Kolla, L. *et al.* Characterization of the development of the mouse cochlear epithelium at the single cell level. *Nat. Commun.* **11**, 2389 (2020).
 29. Puligilla, C. *et al.* Disruption of fibroblast growth factor receptor 3 signaling results in defects in cellular differentiation, neuronal patterning, and hearing impairment. *Dev. Dyn.* **236**, 1905–1917 (2007).
 30. Picher, M. M. *et al.* Ca²⁺-binding protein 2 inhibits Ca²⁺-channel inactivation in mouse inner hair cells. *Proc. Natl. Acad. Sci. U. S. A.* **114**, E1717–E1726 (2017).
 31. Seal, R. P. *et al.* Sensorineural Deafness and Seizures in Mice Lacking Vesicular Glutamate Transporter 3. *Neuron* **57**, 263–275 (2008).
 32. Girotto, G. *et al.* Expression and replication studies to identify new candidate genes involved in normal hearing function. *PLoS One* **9**, e85352 (2014).
 33. Deans, M. R., Peterson, J. M. & Wong, G. W. Mammalian otolin: A multimeric glycoprotein specific to the inner ear that interacts with otoconial matrix protein otoconin-90 and cerebellin-1. *PLoS One* **5**, 1–15 (2010).
 34. Maison, S. F. *et al.* Dopaminergic signaling in the cochlea: receptor expression patterns and deletion phenotypes. *J. Neurosci.* **32**, 344–355 (2012).
 35. Machold, R. & Fishell, G. Math1 is expressed in temporally discrete pools of cerebellar rhombic-lip neural progenitors. *Neuron* **48**, 17–24 (2005).
 36. Muzumdar, M. D., Tasic, B., Miyamichi, K., Li, L. & Luo, L. A global double-fluorescent Cre reporter mouse. *genesis* **45**, 593–605 (2007).
 37. Moorman, A. F. M., Houweling, A. C., de Boer, P. A. J. & Christoffels, V. M. Sensitive nonradioactive detection of mRNA in tissue sections: novel application of the whole-mount in situ hybridization protocol. *J. Histochem. Cytochem.* **49**, 1–8 (2001).
 38. Tusher, V. G., Tibshirani, R. & Chu, G. Significance analysis of microarrays applied to the ionizing radiation response. *Proc. Natl. Acad. Sci.* **98**, 5116–5121 (2001).

Acknowledgements

The monoclonal antibody against CDH2 (clone: MNCD2) developed by Takeichi, M. / Matsunami, H. was obtained from the Developmental Studies Hybridoma Bank, created by the NICHD of the NIH and maintained at The University of Iowa, Department of Biology, Iowa City, IA 52242. We thank the Research Core Unit Transcriptomics of Hannover Medical School for microarray analysis, and Achim Gossler for critical reading of the manuscript. This work was supported by the German Research Council (Deutsche Forschungsgemeinschaft) [DFG TR1325/1-1 to M.-O.T.]

Author contributions

Conceptualization: A.K., M.-O.T.; Formal analysis: M.K., A.K., M.-O.T.; Investigation: M.K., T.H.L., M.-O.T.; Resources: V.M.C.; Data curation: M.K., M.-O.T.; Writing - original draft: M.K., A.K., M.-O.T.; Writing - review & editing: M.K., T.H.L., V.M.C., A.K., M.-O.T.; Visualization: M.K.; Supervision: A.K., M.-O.T.; Project administration: M.-O.T.; Funding acquisition: M.-O.T.

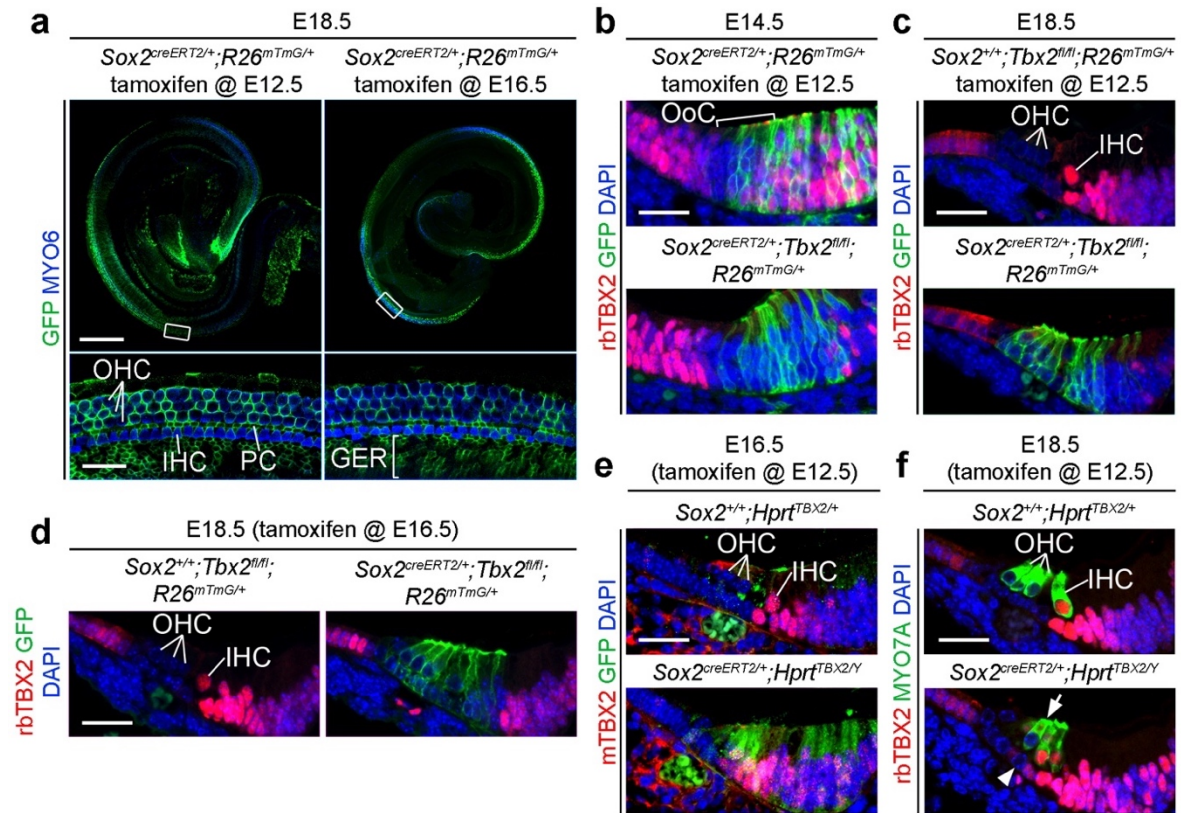
Corresponding author

Correspondence to Andreas Kispert or Mark-Oliver Trowe

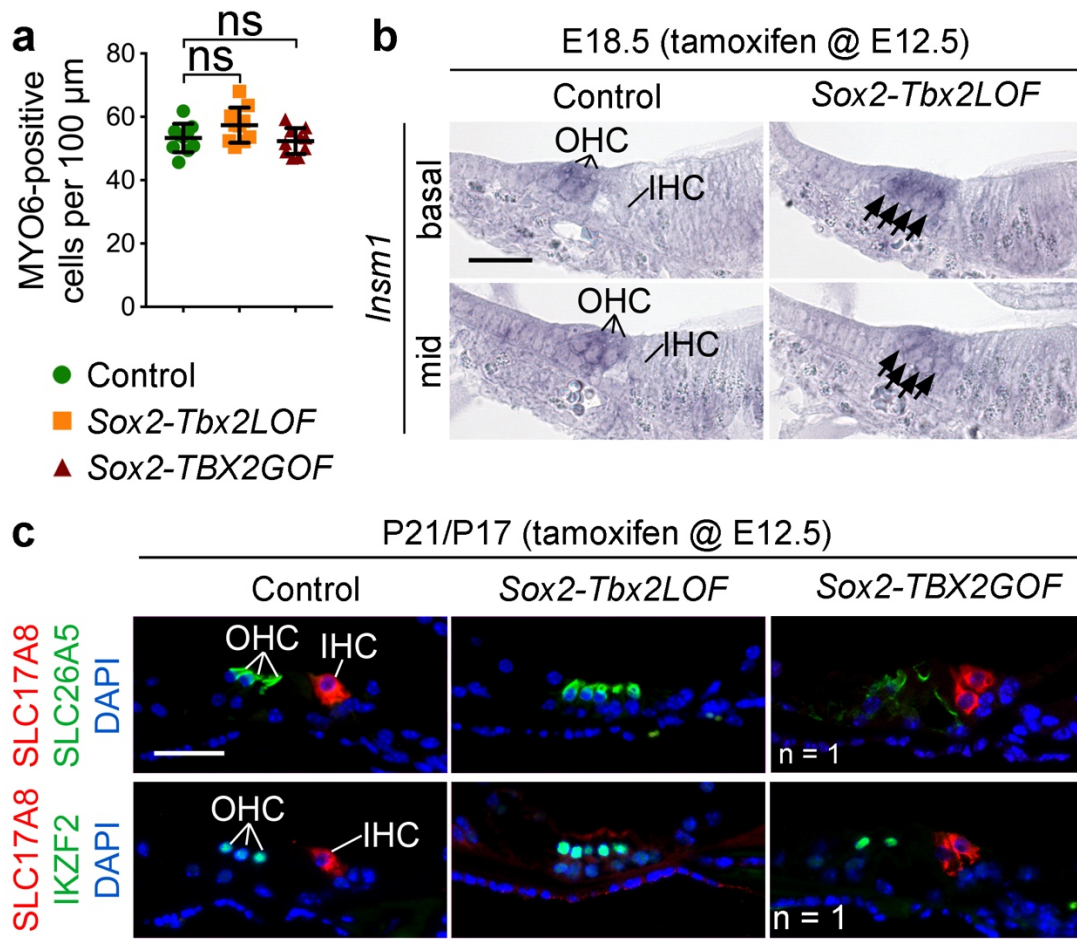
Competing interests

All other authors declare no competing interests.

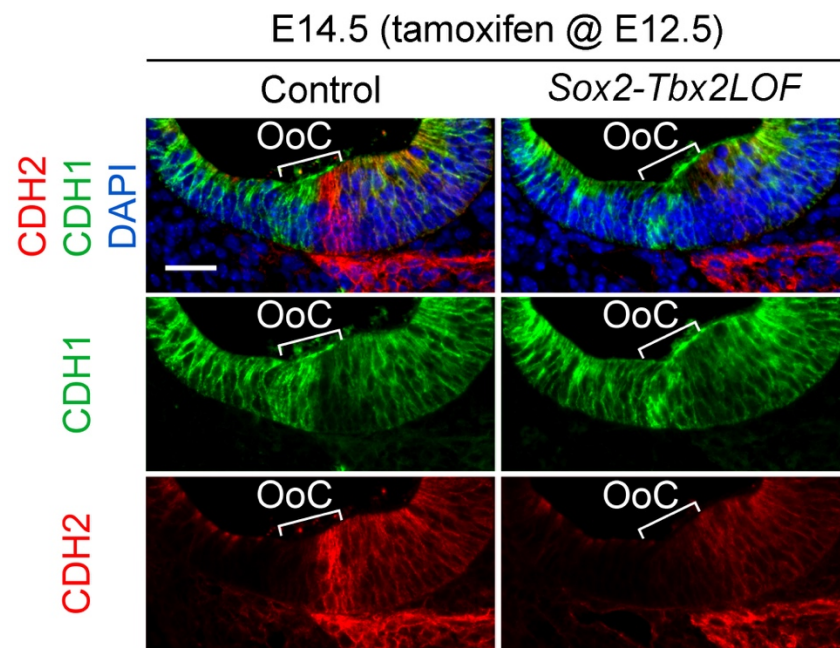
Extended Data



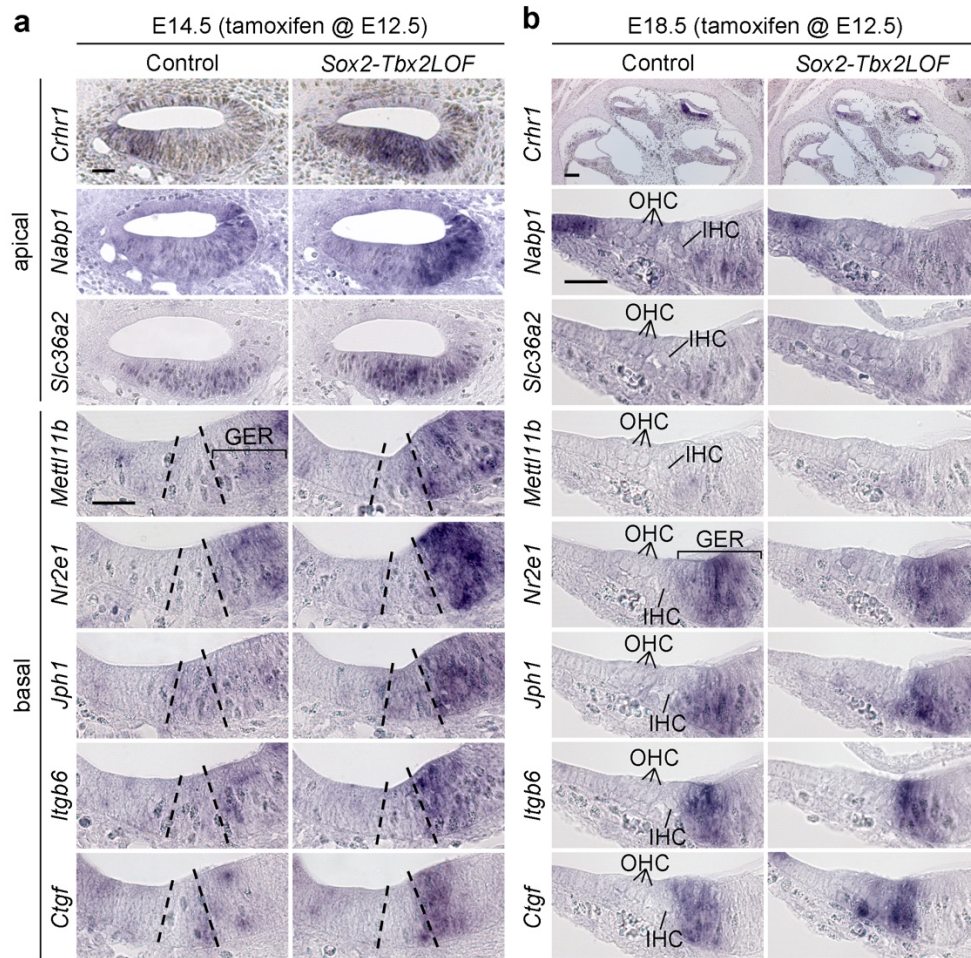
Extended Data Fig. 1: Efficient manipulation of TBX2 expression in the prosensory region of the cochlea using the *Sox2^{creERT2}* mouse line. Immunofluorescence analyses of cochlear whole-mount preparations (a) and cross-sections of the cochlea at the mid-basal level (b-f). **a**, Analysis of GFP expression in E18.5 *Sox2^{creERT2/+};R26^{mTmG/+}* embryos (n≥5) after a single pulse of tamoxifen at E12.5 or E16.5 shows that the *Sox2^{creERT2}* line leads to efficient recombination in IHCs and OHCs (MYO6⁺) and cells of the adjacent greater epithelial ridge (GER). **b,c**, Analysis of TBX2 expression in *Sox2^{creERT2/+};Tbx2^{fl/fl}* and control (*Sox2^{creERT2/+};R26^{mTmG/+}*) cochleae (n≥3) at E14.5 (b) and E18.5 (c) after a single pulse of tamoxifen at E12.5. Expression of TBX2 is completely lost in recombined (GFP⁺) cells of the developing organ of Corti (OoC) and cells of the adjacent GER. **d**, Analysis of TBX2 expression in *Sox2^{creERT2/+};Tbx2^{fl/fl}* and control (*Sox2^{+/+};Tbx2^{fl/fl};R26^{mTmG/+}*) cochleae (n=3) at E18.5 after a single pulse of tamoxifen at E16.5. Expression of TBX2 is completely lost in recombined (GFP⁺) hair and supporting cells of the organ of Corti. **e,f**, Analysis of GFP expression at E16.5 and of TBX2 expression at E18.5 in *Sox2^{creERT2/+};Hprt^{TBX2/Y}* and control (*Sox2^{+/+};Hprt^{TBX2/Y}*) cochleae (n=4) after a single pulse of tamoxifen at E12.5. Note that ectopic TBX2 expression does not occur in all hair cells (MYO7A⁺, arrow) and underlying supporting cells (arrow head). Nuclei were counterstained with DAPI. Scale bars: 250 μm (overview in a), 30 μm. mTBX2, mouse-anti-TBX2 antibody; PC, pillar cell; rbTBX2, rabbit-anti-TBX2 antibody.



Extended Data Fig. 2: Increased number of OHCs at the expense of IHCs upon inactivation of *Tbx2* at E12.5. **a**, Quantification of the total number of hair cells (MYO6⁺) per 100 μm at the mid-basal level of cochlear whole-mount preparations of E18.5 *Sox2-Tbx2LOF*, *Sox2-TBX2GOF* and control embryos (n=10) after a single pulse of tamoxifen at E12.5. Mean \pm standard deviation, unpaired t-test. ns, not significant. **b**, RNA *in situ* hybridization analysis of *Insm1* expression in E18.5 *Sox2-Tbx2LOF* cochleae compared to controls (n \geq 3). In the control, *Insm1* is weakly expressed in the three OHCs but not in IHCs at the basal as well as medial (mid) level of the cochlear duct. Upon *Tbx2* inactivation, the number of *Insm1*-expressing cells increased (arrows). **c**, Immunofluorescence analysis of expression of SLC17A8 (marks IHCs), SLC26A5 and IKZF2 (mark OHCs) on cochlear cross sections of P21 *Sox2-Tbx2LOF* (n=4) and *Sox2-TBX2GOF* (n=1) mutants compared to controls. Nuclei are counterstained with DAPI. Scale bars: 30 μm .

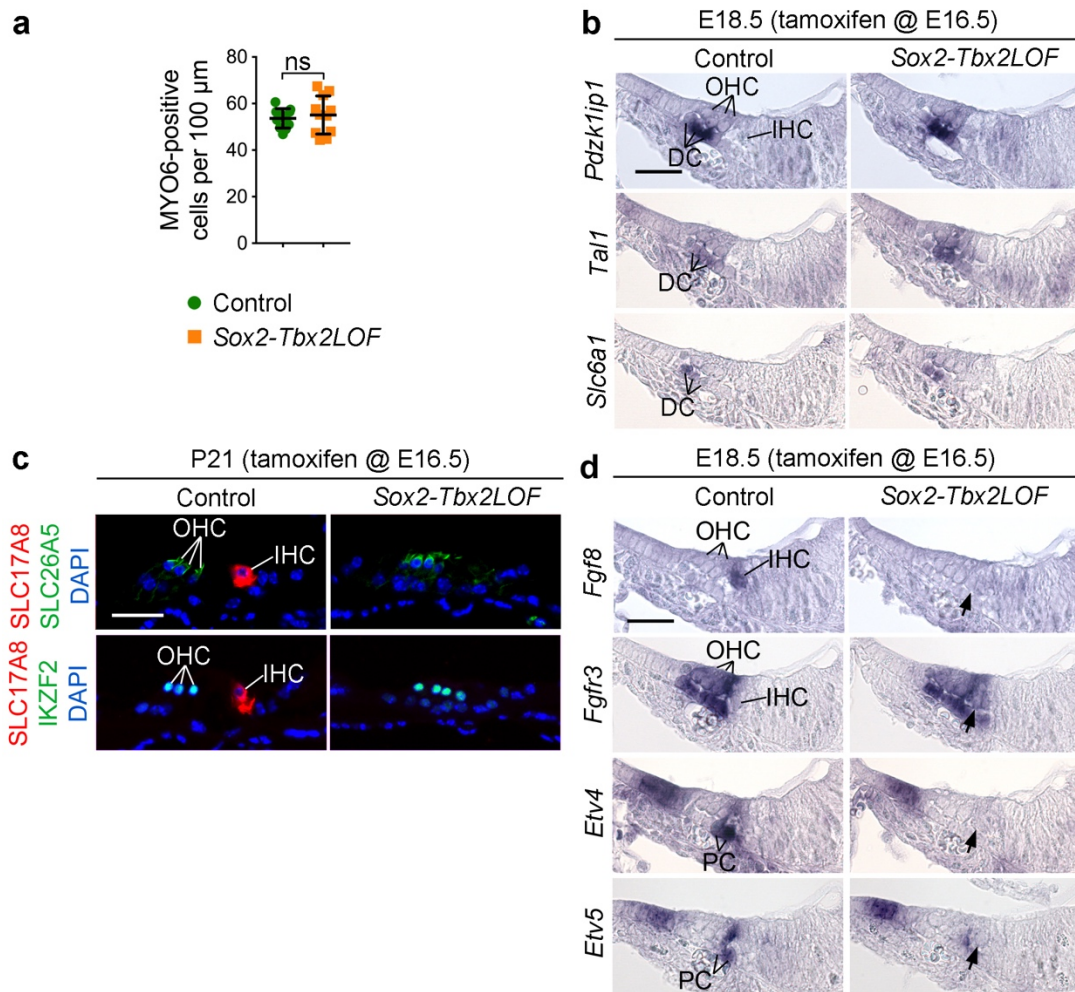


Extended Data Fig. 3: The inner compartment of the organ of Corti is not established upon inactivation of *Tbx2* at E12.5. Immunofluorescence analysis of CDH1 and CDH2 expression in the developing organ of Corti (OoC) of E14.5 *Sox2-Tbx2*^{LOF} and control embryos after a single pulse of tamoxifen at E12.5. The strong CDH2 expression, which marks the inner compartment of the developing OoC, is absent in *Tbx2*-deficient cochleae. Nuclei are counterstained with DAPI. Scale bar: 30 μ m.

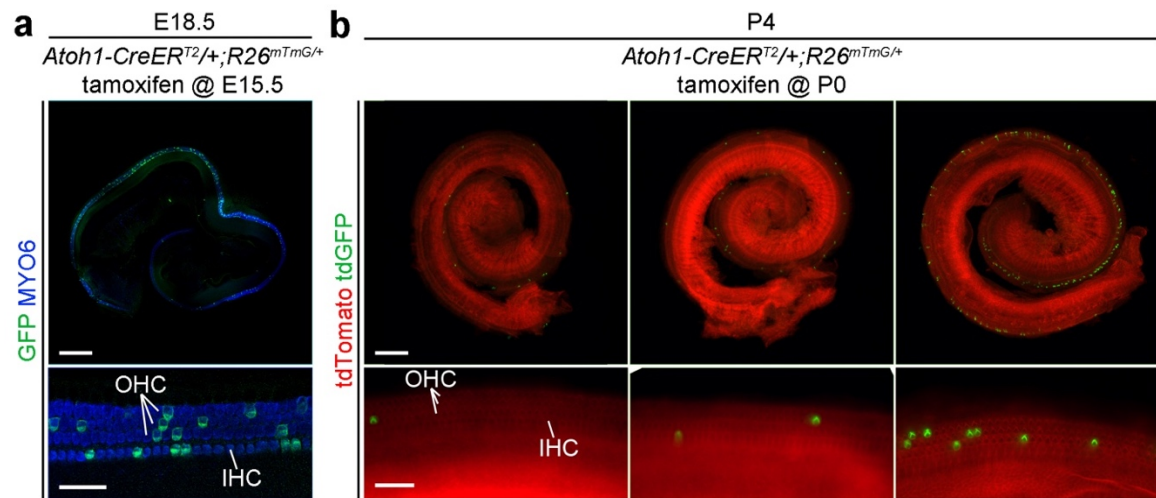


Extended Data Fig. 4: The patterning of the cochlear epithelium is affected upon early *Tbx2* inactivation.

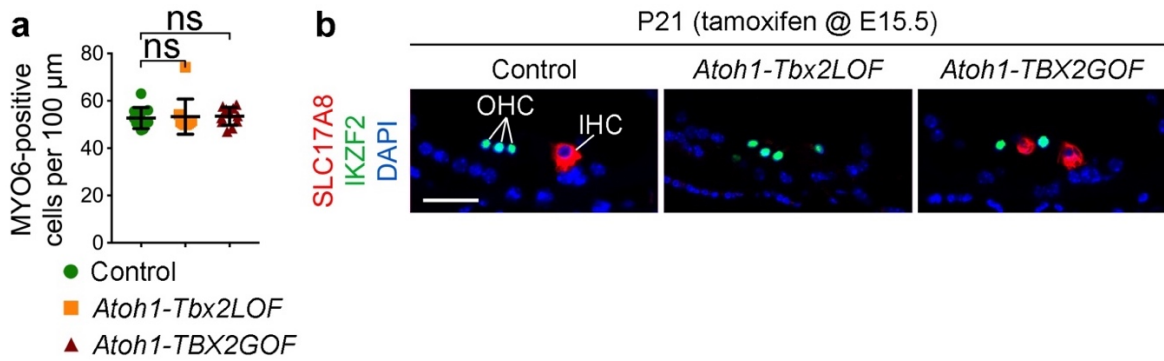
a,b, RNA *in situ* hybridization analysis of transcripts significantly upregulated in a microarray analysis of E14.5 *Sox2-Tbx2LOF* cochlear ducts after a single pulse of tamoxifen at E12.5. Spatial distribution is shown at E14.5 (**a**) and E18.5 (**b**). Expression of *Crhr1*, *Nabp1* and *Slc36a2* is upregulated in the most apical turn of *Tbx2*-deficient cochleae at E14.5, whereas *Mettl11b*, *Nr2e1*, *Jph1*, *Itgb6* and *Ctgf* are upregulated or ectopically expressed in the greater epithelial ridge (GER) in the basal turn. At E18.5, *Crhr1* expression is restricted to the apical turn and *Nabp1* is expressed in cells of the outer sulcus in control and *Sox2-Tbx2LOF* embryos. *Slc36a2* and *Mettl11b* are not expressed at E18.5, whereas *Nr2e1*, *Jph1*, *Itgb6* and *Ctgf* are still expressed in the GER. Dashed lines mark the outer borders of the developing organ of Corti (OoC). Scale bars: 100 μ m (for *Crhr1* in **b**), 30 μ m.



Extended Data Fig. 5: Increased number of OHCs and a complete loss of IHCs upon late inactivation of *Tbx2* at E16.5. **a**, Quantification of the total number of hair cells (MYO6⁺) per 100 μm at the mid-basal level of cochlear whole-mount preparations of E18.5 *Sox2-Tbx2LOF* and control embryos (n=11) after a single pulse of tamoxifen at E16.5. Mean \pm standard deviation, unpaired t-test with Welch's correction. ns, not significant. **b**, RNA *in situ* hybridization analysis of transcripts significantly upregulated in E18.5 *Sox2-Tbx2LOF* cochlear ducts after a single pulse of tamoxifen at E16.5. *Pdzk1ip1*, *Tal1* and *Slc6a1* are expressed in a subset of Deiters' cells (DCs) in control and *Sox2-Tbx2LOF* cochleae. **c**, Immunofluorescence analysis of SLC17A8 (marks IHCs), SLC26A5 and IKZF2 (mark OHCs) expression on cochlear cross sections of P21 *Sox2-Tbx2LOF* (n=5) mice compared to controls. Nuclei are counterstained with DAPI. **d**, RNA *in situ* hybridization analysis of FGF signaling components in *Sox2-Tbx2LOF* cochleae at E18.5. Expression of *Fgf8* in the innermost hair cell and that of *Etv4* and *Etv5* in pillar cells (PCs) is lost or strongly downregulated upon late *Tbx2*-inactivation. Expression of *Fgfr3*, which marks DCs and PCs, is expanded medially in *Sox2-Tbx2LOF* cochleae. Arrow marks the innermost hair cell. Scale bars: 30 μm .



Extended Data Fig. 6: The *Atoh1-CreER^{T2}* mouse line allows hair cell-specific manipulation of TBX2 expression. **a**, Immunofluorescence analysis of GFP expression in E18.5 *Atoh1-CreER^{T2}/+;R26^{mTmG/+}* cochlear whole-mount preparations (n=5) after a single pulse of tamoxifen at E15.5 shows that the *Atoh1-CreER^{T2}* line induces recombination in single hair cells (MYO6⁺). **b**, Analysis of native tdGFP and tdTomato expression in *Atoh1-CreER^{T2}/+;R26^{mTmG/+}* cochleae (n=10) at P4. Oral application of tamoxifen to the feeding dam one day after birth (P0-1) leads to variable numbers of GFP⁺ hair cells in an apical-to-basal gradient. Scale bar: 250 μ m (overviews in **a** and **b**), 30 μ m.



Extended Data Fig. 7: Manipulation of *Tbx2* leads to shifts of hair cell fates at P21. **a**, Quantification of the total number of hair cells (MYO6⁺) per 100 μm at the mid-basal level of cochlear whole-mount preparations of E18.5 *Atoh1-Tbx2LOF* (n=10) *Atoh1-TBX2GOF* (n=11) and control embryos after a single pulse of tamoxifen at E15.5. Mean \pm standard deviation, Mann-Whitney or unpaired t-test. ns, not significant. **b**, Immunofluorescence analysis of SLC17A8 (marks IHCs) and IKZF2 (mark OHCs) expression on cochlear cross sections of P21 *Atoh1-Tbx2LOF* (n=4) and *Atoh1-TBX2GOF* (n=7) mutants compared to controls. Nuclei are counterstained with DAPI. Scale bar: 30 μm .

TBX2 specifies and maintains inner hair and supporting cell fate in the Organ of Corti

Supplementary Information Guide

Title and Summary

Supplementary table 1. List of genes with significant downregulation in cochlear ducts of E14.5 *Sox2^{creERT2/+};Tbx2^{fl/fl}* embryos after a single pulse of tamoxifen at E12.5. 90 genes are significantly downregulated in E14.5 *Sox2^{creERT2/+};Tbx2^{fl/fl}* cochlear ducts compared to *cre*-negative controls.

Supplementary table 2. List of genes with significant upregulation in cochlear ducts of E14.5 *Sox2^{creERT2/+};Tbx2^{fl/fl}* mutants after a single pulse of tamoxifen at E12.5. 36 genes are significantly upregulated in E14.5 *Sox2^{creERT2/+};Tbx2^{fl/fl}* cochlear ducts compared to *cre*-negative controls.

Supplementary table 3. List of genes with significantly decreased expression in cochlear ducts of E18.5 *Sox2^{creERT2/+};Tbx2^{fl/fl}* mutants after a single pulse of tamoxifen at E16.5. 48 genes are significantly downregulated in E14.5 *Sox2^{creERT2/+};Tbx2^{fl/fl}* cochlear ducts compared to *cre*-negative controls.

Supplementary table 4. List of genes with significantly increased expression in cochlear ducts of E18.5 *Sox2^{creERT2/+};Tbx2^{fl/fl}* mutants after a single pulse of tamoxifen at E16.5. 32 genes are significantly upregulated in E14.5 *Sox2^{creERT2/+};Tbx2^{fl/fl}* cochlear ducts compared to *cre*-negative controls.

Supplementary table 5. List of antibodies used in this study.

Supplementary table 6. List of primers used for amplification of DNA fragments as templates for *in vitro* transcription of antisense RNA probes.

Supplementary table 7. Quantification of hair cell numbers in E18.5 *Sox2^{creERT2/+};Tbx2^{fl/fl}* loss-of-function mutants (*Sox2-Tbx2LOF*) compared to controls after a single pulse of tamoxifen at E12.5. Complete loss of SLC17A8⁺ (VGLUT3⁺) IHCs and increased number of BCL11B⁺ OHCs in E18.5 *Sox2^{creERT2/+};Tbx2^{fl/fl}* cochlear ducts compared to controls.

Supplementary table 8. Quantification of hair cell numbers in E18.5 *Sox2^{creERT2/+};Hprt^{TBX2/Y}* gain-of-function mutants (*Sox2-TBX2GOF*) compared to controls after a single pulse of tamoxifen at E12.5. Increased number of SLC17A8⁺ (VGLUT3⁺) IHCs and reduced number of BCL11B⁺ OHCs in E18.5 *Sox2^{creERT2/+};Hprt^{TBX2/Y}* cochlear ducts compared to controls.

Supplementary table 9. Quantification of hair cell numbers in E18.5 *Sox2^{creERT2/+};Tbx2^{fl/fl}* loss-of-function mutants (*Sox2-Tbx2LOF*) compared to controls after a single pulse of tamoxifen at E16.5. Reduced number of SLC17A8⁺ (VGLUT3⁺) IHCs and increased number of BCL11B⁺, SLC17A8⁺/BCL11B⁺ and SLC17A8⁺/BCL11B⁻ hair cells in the inner compartment of E18.5 *Sox2^{creERT2/+};Tbx2^{fl/fl}* cochlear ducts compared to controls.

Supplementary table 10. Quantification of hair cell numbers in E18.5 *Atoh1-CreER^{T2/+};Tbx2^{fl/fl}* loss-of-function mutants (*Atoh1-Tbx2LOF*) compared to controls after a single pulse of tamoxifen at E15.5. Reduced number of SLC17A8⁺ (VGLUT3⁺) IHCs and increased number of BCL11B⁺, SLC17A8⁺/BCL11B⁺ and SLC17A8⁺/BCL11B⁻ hair cells in the inner compartment of E18.5 *Atoh1-CreER^{T2/+};Tbx2^{fl/fl}* cochlear ducts compared to controls.

Supplementary table 11. Quantification of hair cell numbers in E18.5 *Atoh1-CreER^{T2/+};Hprt^{TBX2/+ (Y)}* gain-of-function mutants (*Atoh1-TBX2GOF*) compared to controls after a single pulse of tamoxifen at E15.5. Increased number of SLC17A8⁺ (VGLUT3⁺) and SLC17A8⁺/BCL11B⁻ hair cells in the outer compartment of E18.5 *Atoh1-CreER^{T2/+};Tbx2^{fl/fl}* cochlear ducts compared to controls.

Supplementary Table Legends

Supplementary table 1. List of genes with significant downregulation in cochlear ducts of E14.5 *Sox2^{creERT2/+};Tbx2^{fl/fl}* embryos after a single pulse of tamoxifen at E12.5. 4 different pools of control and mutant material were used for the microarray analysis. Genes are sorted accordingly to their Fold Change (FC). For genes marked by an asterisk mRNA or protein expression data are available in the literature (reference). E, embryonic day; P, postnatat day.

Supplementary table 2. List of genes with significant upregualtion in cochlear ducts of E14.5 *Sox2^{creERT2/+};Tbx2^{fl/fl}* mutants after a single pulse of tamoxifen at E12.5. 4 different pools of control and mutant material were used for the microarray analysis. Genes are sorted accordingly to their Fold Change (FC). For genes marked by an asterisk mRNA or protein expression data are available in the literature (reference). E, embryonic day; P, postnatat day.

Supplementary table 3. List of genes with significantly decreased expression in cochlear ducts of E18.5 *Sox2^{creERT2/+};Tbx2^{fl/fl}* mutants after a single pulse of tamoxifen at E16.5. 4 different pools of control and mutant material were used for the microarray analysis. Genes are sorted accordingly to their Fold Change (FC). For genes marked by an asterisk mRNA or protein expression data are available in the literature (reference). E, embryonic day; P, postnatat day.

Supplementary table 4. List of genes with significantly increased expression in cochlear ducts of E18.5 *Sox2^{creERT2/+};Tbx2^{fl/fl}* mutants after a single pulse of tamoxifen at E16.5. 32 genes are significantly upregulated in E14.5 *Sox2^{creERT2/+};Tbx2^{fl/fl}* cochlear ducts compared to *Cre*-negative controls.

Supplementary table 5. List of antibodies used in this study. List of primary and secondary antibodies with relevant information like dilution, order and lot number and company.

Supplementary table 6. List of primers used for amplification of DNA fragments as templates for *in vitro* transcription of antisense RNA probes. List of forward and reverse primers used for amplification of DNA template fragments. A T7-promoter sequence (TAATACGACTCACTATAGGG) was added to the 5' end of the reverse primer. Additional information like length of the DNA template and source of DNA for PCR are listed in the table.

Supplementary table 7. Quantification of hair cell numbers in E18.5 *Sox2^{creERT2/+};Tbx2^{fl/fl}* loss-of-function mutants (*Sox2-Tbx2LOF*) compared to controls after a single pulse of tamoxifen at E12.5. Cell numbers were counted at the mid-basal level of each organ of Corti in an area of 500 μm . Subsequently, cell counts were averaged to an area of 100 μm . Normal distribution of data was analyzed by the D'Agostino & Pearson and Shapiro-Wilk normality test (normal distribution if p-values ≥ 0.05). Equality of variances was assessed by performing the F- and Levene's test (equal variances if p-values ≥ 0.05). The appropriate statistical test (green boxes) was selected based on calculated parameters.

Supplementary table 8. Quantification of hair cell numbers in E18.5 *Sox2^{creERT2/+};Hprt^{TBX2/Y}* gain-of-function mutants (*Sox2-TBX2GOF*) compared to controls after a single pulse of tamoxifen at E12.5. Cell numbers were counted at the mid-basal level of each organ of Corti in an area of 500 μm . Subsequently, cell counts were averaged to an area of 100 μm . Normal distribution of data was analyzed by the D'Agostino & Pearson and Shapiro-Wilk normality test (normal distribution if p-values ≥ 0.05). Equality of variances was assessed by performing the F- and Levene's test (equal variances if p-values ≥ 0.05). The appropriate statistical test (green boxes) was selected based on calculated parameters.

Supplementary table 9. Quantification of hair cell numbers in E18.5 *Sox2^{creERT2/+};Tbx2^{fl/fl}* loss-of-function mutants (*Sox2-Tbx2LOF*) compared to controls after a single pulse of tamoxifen at E16.5. Cell numbers were counted at the mid-basal level of each organ of Corti in an area of 500 μm . Subsequently, cell counts were averaged to an area of 100 μm . Normal distribution of data was analyzed by the D'Agostino & Pearson and Shapiro-Wilk normality test (normal distribution if p-values ≥ 0.05). Equality of variances was assessed by performing the F- and Levene's test (equal variances if p-values ≥ 0.05). The appropriate statistical test (green boxes) was selected based on calculated parameters.

Supplementary table 10. Quantification of hair cell numbers in E18.5 *Atoh1-CreERT2/+;Tbx2^{fl/fl}* loss-of-function mutants (*Atoh1-Tbx2LOF*) compared to controls after a single pulse of tamoxifen at E15.5. Cell numbers were counted at the mid-basal level of each organ of Corti in an area of 500 μm . Subsequently, cell counts were averaged to an area of 100 μm . Normal distribution of data was analyzed by the D'Agostino & Pearson and Shapiro-Wilk normality test (normal distribution if p-values ≥ 0.05). Equality of variances was assessed by performing the F- and Levene's test (equal variances if p-values ≥ 0.05). The appropriate statistical test (green boxes) was selected based on calculated parameters.

Supplementary table 11. Quantification of hair cell numbers in E18.5 *Atoh1-CreER^{T2}/+;Hprt^{TBX2/+ (Y)}* gain-of-function mutants (*Atoh1-TBX2GOF*) compared to controls after a single pulse of tamoxifen at E15.5. Cell numbers were counted at the mid-basal level of each organ of Corti in an area of 500 μm . Subsequently, cell counts were averaged to an area of 100 μm . Normal distribution of data was analyzed by the D'Agostino & Pearson and Shapiro-Wilk normality test (normal distribution if p-values ≥ 0.05). Equality of variances was assessed by performing the F- and Levene's test (equal variances if p-values ≥ 0.05). The appropriate statistical test (green boxes) was selected based on calculated parameters

Concluding remarks and future perspectives

The formation of a functional inner ear depends on two major events. First, the induction of spatially restricted gene expression domains in the early otocyst that trigger the formation of the vestibular system at the dorsal and of the cochlear duct at the ventral side. Second, the precise differentiation and diversification of hair and supporting cells within the sensory end organs.

This thesis demonstrates that the T-box gene *Tbx2* is required for both events. Shortly after otocyst formation, *Tbx2* mediates the restriction of the neurogenic domain to the anterior-ventral aspect of the otocyst. Subsequently, it promotes cochlear elongation and refines the morphogenesis of vestibular structures. From the onset of prosensory cell differentiation, *Tbx2*/TBX2 is differentially expressed in the developing organ of Corti. Here, *Tbx2* specifies and maintains inner hair and supporting cell identity.

In contrast, *Tbx3* contributes to inner ear morphogenesis only in a minor fashion by promoting the formation of the posterior semicircular canal. However, the severe morphological phenotype of *Tbx2/3cDKO* mutants shows that *Tbx2* and *Tbx3* act redundantly in inner ear morphogenesis.

Since murine and human TBX2 proteins share about 96% of identity, and inner ear anatomy, physiology and molecular biology is highly comparable between mice and men, the results of this thesis are likely to be transferable to humans¹³⁷. In fact, the functions of *Tbx2* in early patterning of the otocyst and in differentiation of IHCs can explain why some patients with microdeletions on chromosome 17 which encompass *TBX2*, suffer from sensorineural hearing loss^{148,149}.

New insights into the regulatory network promoting otic neurogenesis

The first subproject of this thesis provides novel insights into the regulation of otic neurogenesis in mice. Molecular analyses of *Tbx2cKO* and *Tbx2/3cDKO* mutants demonstrated that the posterior expansion of the neurogenic domain (*Neurog1*, *Neurod1*, *Dll1*) is accompanied by ectopic FGF signalling (*Etv4*, *Etv5*, *Fgf8*) and loss of *Tbx1* expression. Analyses in chicken showed that FGF signalling, especially FGF8, is a potent inducer of the neuronal competence factor *Sox3*, which was ectopically expressed in *Tbx2*-deficient otocysts^{39,43,159}. Pharmacological inhibition of FGF signalling in organ culture restricted the *Neurog1*-positive domain to the anterior-ventral aspect of *Tbx2/3cDKO* otocysts. These results suggest that TBX2 represses a *Fgf8-Sox3/Sox2-Neurog1* regulatory

module in mammals. Since *Tbx2* is expressed in chicken otocysts, it cannot be ruled out that *Tbx2* function has diverged in chicken and mice¹³⁶. Alternatively, TBX2 might repress FGF signalling through a yet unknown factor that is only present in mammals. To discriminate between these two possibilities, a detailed analysis of *Tbx2* expression in chicken otocysts should be performed, followed by a phenotypic and molecular analysis of chicken inner ears deficient for *Tbx2*. Mis/overexpression of *Fgf8* in murine otocysts using viral vectors and organ culture experiments might shed additional light onto the conservation of the regulatory axis.

In addition to ectopic FGF signalling, *Tbx2*-deficient otocysts were characterized by downregulation of the neuronal suppressor gene *Tbx1* in the ventral region. Inactivation of *Tbx1* results in posterior-ventral expansion of the neurogenic domain accompanied by expanded *Fgf3* expression³⁶. We showed that in contrast to *Tbx2*-deficient embryos the expression domains of *Etv4/5* and *Fgf3* did not overlap in *Tbx1KO* otocysts, and that the *Fgf8-Sox3* regulatory module was not ectopically expressed. These results indicate that FGF8-mediated signalling acts upstream of *Tbx1*. Future work may address this regulatory axis in greater detail by *Fgf8* mis/overexpression experiments in early otocysts.

Ectopic upregulation of FGF signalling in the ventral half of *Tbx2/3cKO* otocyst was accompanied by loss of BMP signalling (*Id2*, *Id3*). Previous studies showed that the expression of some T-box genes (*Tbx2*, *Tbx3*, *Tbx5*) depends on this signalling pathway^{160–162}. Coexpression of *Id2/Id3* and *Tbx1* in the posterior otocyst implies that BMP signalling is required for maintenance of *Tbx1* expression in the developing inner ear. In other contexts, BMP and FGF signalling was shown to act antagonistically¹⁶³. Hence, we suggest that de-repression of FGF signalling in *Tbx2*-deficient otocysts leads to inhibition of BMP signalling and its downstream target *Tbx1*. Analysis of *Tbx1* expression in BMP-deficient and of *Id2/Id3* expression in *Fgf8* mis/overexpression models may further validate this hypothesis.

***Tbx2* is a crucial regulator of inner hair and supporting cell identity**

The second subproject of this thesis identified *Tbx2* as a crucial regulator of inner hair and supporting cell differentiation. Inactivation and misexpression of *Tbx2* in the prosensory domain resulted in a complete loss and increased number of IHCs at the expense of OHCs, respectively. A similar phenotype was observed in underlying supporting cells. Thus, *Tbx2* is required for specification of cells in the inner compartment of the organ of Corti, where this transcription factor is expressed from the onset of differentiation. Spatial expression analysis of upregulated candidates from a microarray analysis of loss-of-function mutants,

identified *Fgfr3* as the only gene with a pattern of expression complementary to that of *Tbx2* in normal conditions. Since *Fgfr3*-positive cells were shown to give rise to OHCs, Deiters' cells and pillar cells, expansion of *Fgfr3* expression in loss-of-function mutants and reduction of the *Fgfr3*-positive domain in gain-of-function mutants is likely to cause the initial mispatterning of the developing prosensory domain¹¹⁷. There are two genetic ways to test this hypothesis. First, misexpression of a constitutively active variant of *Fgfr3* under the control of the *Sox2^{creERT2}*-driver line should lead to expansion of the outer compartment at the expense of the inner compartment of the organ of Corti. Second, inactivation of both *Tbx2* and *Fgfr3* in the prosensory domain should rescue the phenotype of *Tbx2*-deficient cochleae and re-establish the normal compartmentalization of the organ of Corti. However, the second experiment might be difficult to evaluate since the dose of *Fgfr3* rather than its expression domain is affected.

Hair cell-specific inactivation or misexpression of *Tbx2* after the onset of differentiation resulted in conversion of IHCs into OHCs and *vice versa* demonstrating that TBX2 is also required for maintenance of IHC fate, at least until shortly after birth. It would be interesting to inactivate or misexpress *Tbx2* at later postnatal stages for example using the *vGlut3-P2A-iCreER*-line (recombination in IHCs) or the *prestin-CreERT2*-line (recombination in OHCs) and examine if TBX2 is required to maintain and sufficient to induce IHC identity upon full maturation.

Inactivation of *Insm1* leads to an increased number of IHCs in the outer compartment of the organ of Corti at the expense of OHCs indicating that IHC fate is the default state and that it needs to be actively repressed to promote OHCs development¹²⁵. Initial expression of *Tbx2* throughout the prosensory domain and its progressive exclusion from OHCs supports this assumption. However, our data also demonstrate that IHC fate needs to be actively maintained by TBX2 possibly by repression of OHC fate. Together, the increased number of *Insm1*- and IKZF2-positive OHCs at the expense of IHCs in *Tbx2*-deficient cochleae and the ectopic *Tbx2*-positive IHCs in the outer compartment of the organ of Corti in *Insm1* mutants, indicate that the transcription factors involved in diversification of IHCs vs OHCs act antagonistically. A chromatin immunoprecipitation (ChIP) assay or Cleavage Under Targets and Tagmentation (CUT&Tag) technology followed by a sequencing reaction present experimental approaches to test whether TBX2 binds to regulatory regions in *Insm1* and *Ikzf2* and *vice versa* in the future.

In *Ikzf2/Helios*-deficient cochleae, some OHC-specific genes (e.g. *Slc26a5*, *Ocm*) are downregulated at P8 but reach normal levels by P16 while the expression of other genes

(e.g. *Ppp1r17*) is not restored¹²⁶. These results indicate that Helios regulates an OHC-specific gene set but that other factors compensate for the loss of this factor¹²⁶. In contrast, *SLC26A5* is stably expressed in *Tbx2*-deficient cochleae until P21. These contradicting observations could be due to the earlier inactivation of *Tbx2* (P0-1) compared to *Ikzf2* (P4). Alternatively, TBX2 might induce and suppress the complete IHC and OHC program, respectively. To address this possibility, *Tbx2* should be inactivated or misexpressed at later time points using the *vGlut3-P2A-iCreER*-line or the *prestin-CreER^{T2}*-line followed by single cell RNA sequencing to determine which genes are regulated by this T-box transcription factor. This approach should provide a deeper insight into the molecular function of TBX2 and might uncover additional regulators of hair cell diversification.

The therapeutic potential of TBX2

Sensorineural hearing loss is an increasing pandemic in our society mainly due to overexposure to loud noises, viral infections and ototoxic drugs.

The results of this thesis open avenues for novel therapeutic approaches with respect to congenital and acquired forms of sensorineural hearing loss. Costa et al. successfully converted mouse embryonic stem cells (ESCs) into the hair cell lineage using a “cocktail” of transcription factor genes including *Atoh1*¹⁶⁴. Transduction of these “induced hair cells” with *Tbx2* might direct their differentiation into IHCs. These targeted cells could then be used to test new pharmacological compounds for IHC-specific ototoxicity (drug screening) or for their potential to induce regenerative responses *in vitro*. Cell culture approaches could also be used to analyse IHC-specific tropism of different viruses and therefore their potential as viral vectors.

References

1. Lin, F. R. & Albert, M. Hearing Loss and Dementia – Who’s Listening? *Aging Ment. Health* **18**, 671 (2014).
2. WHO - Deafness and hearing loss. (2021). Available at: <https://www.who.int/news-room/fact-sheets/detail/deafness-and-hearing-loss>.
3. Delmaghani, S. & El-Amraoui, A. Inner Ear Gene Therapies Take Off: Current Promises and Future Challenges. *J. Clin. Med.* **9**, 2309 (2020).
4. Liberman, M. C. Noise-induced and age-related hearing loss: new perspectives and potential therapies. *F1000Research* **6**, 927 (2017).
5. Raviv, D., Dror, A. A. & Avraham, K. B. Hearing loss: a common disorder caused by many rare alleles. *Ann. N. Y. Acad. Sci.* **1214**, 168–179 (2010).
6. Bommakanti, K., Iyer, J. S. & Stankovic, K. M. Cochlear histopathology in human genetic hearing loss: State of the science and future prospects. *Hear. Res.* **382**, 107785 (2019).
7. Atkinson, P. J., Huarcaya Najarro, E., Sayyid, Z. N. & Cheng, A. G. Sensory hair cell development and regeneration: similarities and differences. *Development* **142**, 1561–1571 (2015).
8. Wagner, E. L. & Shin, J.-B. Mechanisms of Hair Cell Damage and Repair. *Trends Neurosci.* **42**, 414–424 (2019).
9. Kral, A., Dorman, M. F. & Wilson, B. S. Neuronal Development of Hearing and Language: Cochlear Implants and Critical Periods. *Annu. Rev. Neurosci.* **42**, 47–65 (2019).
10. Lesica, N. A. Why do hearing aids fail to restore normal auditory perception? *Trends Neurosci.* **41**, 174 (2018).
11. Donkelaar, H. J. Ten *et al.* An Updated Terminology for the Internal Ear with Combined Anatomical and Clinical Terms. *J. Phonetics Audiol.* **6**, 1–13 (2020).
12. Munnamalai, V. & Fekete, D. M. The acquisition of positional information across the radial axis of the cochlea. *Dev. Dyn.* **249**, 281–297 (2020).
13. Zheng, J. *et al.* Prestin is the motor protein of cochlear outer hair cells. *Nature* **405**, 149–155 (2000).
14. Pujol, R., Lenoir, M., Ladrech, S., Tribillac, F. & Rebillard, G. Correlation Between the Length of Outer Hair Cells and the Frequency Coding of the Cochlea. *Audit. Physiol. Percept.* 45–52 (1992). doi:10.1016/B978-0-08-041847-6.50011-3
15. Anniko, M. & Wikström, S.-O. Pattern formation of the otic placode and morphogenesis of the otocyst. *Am. J. Otolaryngol.* **5**, 373–381 (1984).
16. Sher, A. E. The embryonic and postnatal development of the inner ear of the mouse. *Acta Otolaryngol. Suppl.* **285**, 1–77 (1971).
17. Torres, M. & Giraldez, F. The development of the vertebrate inner ear. *Mech. Dev.* **71**, 5–21 (1998).
18. Nishikori, T., Hatta, T., Kawauchi, H. & Otani, H. Apoptosis during inner ear development in human and mouse embryos: an analysis by computer-assisted three-dimensional reconstruction. *Anat. Embryol. (Berl.)* **200**, 19–26 (1999).
19. León, Y., Sánchez-Galiano, S. & Gorospe, I. Programmed cell death in the development of the vertebrate inner ear. *Apoptosis* **9**, 255–264 (2004).
20. Ceconi, F. *et al.* Apaf1-dependent programmed cell death is required for inner ear morphogenesis and growth. *Development* **131**, 2125–2135 (2004).
21. Martin, P. & Swanson, G. J. Descriptive and Experimental Analysis of the Epithelial Remodellings That Control Semicircular Canal Formation in the Developing Mouse Inner Ear. *Dev. Biol.* **159**, 549–558 (1993).
22. Driver, E. C., Northrop, A. & Kelley, M. W. Cell migration, intercalation and growth regulate mammalian cochlear extension. *Development* **144**, 3766–3776 (2017).
23. Kopecky, B. J., Jahan, I. & Fritzsche, B. Correct Timing of Proliferation and Differentiation is Necessary for Normal Inner Ear Development and Auditory Hair Cell Viability. *Dev. Dyn.* **242**, 132–147 (2013).
24. Lang, H., Bever, M. M. & Fekete, D. M. Cell Proliferation and Cell Death in the Developing Chick Inner Ear : Spatial and Temporal Patterns. *J. Comp. Neurol.* **417**, 205–220 (2000).
25. Bok, J. *et al.* Transient retinoic acid signaling confers anterior-posterior polarity to the inner ear. *PNAS* **108**, 161–6 (2011).
26. Wu, D. K., Nunes, F. D. & Choo, D. Axial specification for sensory organs versus non-sensory structures of the chicken inner ear. *Development* **125**, 11–20 (1998).
27. Frohman, M. A., Martin, G. R., Cordes, S. P., Halamek, L. P. & Barsh, G. S. Altered rhombomere-specific gene expression and hyoid bone differentiation in the mouse segmentation mutant, kreisler (kr). *Development* **117**, 925–36 (1993).

28. McKay, I. J., Lewis, J. & Lumsden, A. The role of FGF-3 in early inner ear development: an analysis in normal and kreisler mutant mice. *Dev. Biol.* **174**, 370–378 (1996).
29. Lufkin, T., Dierich, A., LeMeur, M., Mark, M. & Chambon, P. Disruption of the Hox-1.6 homeobox gene results in defects in a region corresponding to its rostral domain of expression. *Cell* **66**, 1105–19 (1991).
30. Deol, M. S. The abnormalities of the inner ear in kreisler mice. *J. Embryol. Exp. Morphol.* **12**, 475–490 (1964).
31. Riccomagno, M. M., Takada, S. & Epstein, D. J. Wnt-dependent regulation of inner ear morphogenesis is balanced by the opposing and supporting roles of Shh. *Genes Dev.* **19**, 1612–1623 (2005).
32. Riccomagno, M. M., Martinu, L., Mulheisen, M., Wu, D. K. & Epstein, D. J. Specification of the mammalian cochlea is dependent on Sonic hedgehog. *Genes Dev.* **16**, 2365–2378 (2002).
33. Bok, J., Bronner-Fraser, M. & Wu, D. K. Role of the hindbrain in dorsoventral but not anteroposterior axial specification of the inner ear. *Development* **132**, 2115–24 (2005).
34. Sirbu, I. O., Gresh, L., Barra, J. & Duester, G. Shifting boundaries of retinoic acid activity control hindbrain segmental gene expression. *Development* **132**, 2611–2622 (2005).
35. Nichols, D. H. *et al.* Lmx1a is required for segregation of sensory epithelia and normal ear histogenesis and morphogenesis. *Cell Tissue Res.* **334**, 339–358 (2008).
36. Raft, S., Nowotschin, S., Liao, J. & Morrow, B. E. Suppression of neural fate and control of inner ear morphogenesis by Tbx1. *Development* **131**, 1801–1812 (2004).
37. Morsli, H., Choo, D., Ryan, A., Johnson, R. & Wu, D. K. Development of the mouse inner ear and origin of its sensory organs. *J. Neurosci.* **18**, 3327–3335 (1998).
38. Cole, L. K. *et al.* Sensory organ generation in the chicken inner ear: Contributions of bone morphogenetic protein 4, Serrate1, and lunatic fringe. *J. Comp. Neurol.* **424**, 509–520 (2000).
39. Alsina, B. *et al.* FGF signaling is required for determination of otic neuroblasts in the chick embryo. *Dev. Biol.* **267**, 119–134 (2004).
40. Vázquez-Echeverría, C., Dominguez-Frutos, E., Charnay, P., Schimmang, T. & Pujades, C. Analysis of mouse kreisler mutants reveals new roles of hindbrain-derived signals in the establishment of the otic neurogenic domain. *Dev. Biol.* **322**, 167–178 (2008).
41. Vitelli, F. *et al.* TBX1 is required for inner ear morphogenesis. *Hum. Mol. Genet.* **12**, 2041–2048 (2003).
42. Yntema, C. L. Experiments on the origin of the sensory ganglia of the facial nerve in the chick. *J. Comp. Neurol.* **81**, 147–167 (1944).
43. Abelló, G. *et al.* Independent regulation of Sox3 and Lmx1b by FGF and BMP signaling influences the neurogenic and non-neurogenic domains in the chick otic placode. *Dev. Biol.* **339**, 166–178 (2010).
44. Bok, J. *et al.* Opposing gradients of Gli repressor and activators mediate Shh signaling along the dorsoventral axis of the inner ear. *Development* **134**, 1713–1722 (2007).
45. Dai, P. *et al.* Sonic Hedgehog-induced Activation of the Gli1 Promoter Is Mediated by GLI3 *. *J. Biol. Chem.* **274**, 8143–8152 (1999).
46. Goodrich, L. V., Johnson, R. L., Milenkovic, L., McMahon, J. A. & Scott, M. P. Conservation of the hedgehog/patched signaling pathway from flies to mice: induction of a mouse patched gene by Hedgehog. *Genes Dev.* **10**, 301–12 (1996).
47. Brown, A. S. & Epstein, D. J. Otic ablation of smoothened reveals direct and indirect requirements for Hedgehog signaling in inner ear development. *Development* **138**, 3967–3976 (2011).
48. Dudley, A. T. & Robertson, E. J. Overlapping expression domains of bone morphogenetic protein family members potentially account for limited tissue defects in BMP7 deficient embryos. *Dev. Dyn.* **208**, 349–62 (1997).
49. Lee, K. J., Mendelsohn, M. & Jessell, T. M. Neuronal patterning by BMPs: a requirement for GDF7 in the generation of a discrete class of commissural interneurons in the mouse spinal cord. *Genes Dev.* **12**, 3394–407 (1998).
50. Chang, W. *et al.* Bmp4 is essential for the formation of the vestibular apparatus that detects angular head movements. *PLoS Genet.* **4**, e1000050 (2008).
51. Ohta, S., Mansour, S. L. & Schoenwolf, G. C. BMP/SMAD signaling regulates the cell behaviors that drive the initial dorsal-specific regional morphogenesis of the otocyst. *Dev. Biol.* **347**, 369–381 (2010).
52. Ohta, S., Wang, B., Mansour, S. L. & Schoenwolf, G. C. BMP regulates regional gene expression in the dorsal otocyst through canonical and non-canonical intracellular pathways. *Development* **143**, 2228–2237 (2016).
53. Hatch, E. P., Noyes, C. A., Wang, X., Wright, T. J. & Mansour, S. L. Fgf3 is required for dorsal patterning and morphogenesis of the inner ear epithelium. *Development* **134**, 3615–25 (2007).
54. Wright, T. J. & Mansour, S. L. Fgf3 and Fgf10 are required for mouse otic placode induction. *Development* **130**, 3379–3390 (2003).
55. Pirvola, U. *et al.* FGF/FGFR-2(IIIb) signaling is essential for inner ear morphogenesis. *J. Neurosci.* **20**, 6125–6134 (2000).

56. Urness, L. D. *et al.* Spatial and temporal inhibition of FGFR2b ligands reveals continuous requirements and novel targets in mouse inner ear morphogenesis. *Development* **145**, dev170142 (2018).
57. Mansour, S. L., Goddard, J. M. & Capecchi, M. R. Mice homozygous for a targeted disruption of the proto-oncogene int-2 have developmental defects in the tail and inner ear. *Development* **117**, 13–28 (1993).
58. Pauley, S. *et al.* Expression and function of FGF10 in mammalian inner ear development. *Dev. Dyn.* **227**, 203–215 (2003).
59. Frohman, M. A., Martin, G. R., Cordes, S. P., Halamek, L. P. & Barsh, G. S. Altered rhombomere-specific gene expression and hyoid bone differentiation in the mouse segmentation mutant, kreisler (kr). *Development* **117**, 925–936 (1993).
60. Choo, D. *et al.* Molecular mechanisms underlying inner ear patterning defects in kreisler mutants. *Dev. Biol.* **289**, 308–317 (2006).
61. Alsina, B. & Whitfield, T. T. Sculpting the labyrinth: Morphogenesis of the developing inner ear. *Semin. Cell Dev. Biol.* **65**, 47–59 (2017).
62. Fekete, D. M., Homburger, S. A., Waring, M. T., Riedl, A. E. & Garcia, L. F. Involvement of programmed cell death in morphogenesis of the vertebrate inner ear. *Development* **124**, 2451–61 (1997).
63. Chacon-Heszele, M. F., Ren, D., Reynolds, A. B., Chi, F. & Chen, P. Regulation of cochlear convergent extension by the vertebrate planar cell polarity pathway is dependent on p120-catenin. *Development* **139**, 968–978 (2012).
64. Wang, J. *et al.* Regulation of polarized extension and planar cell polarity in the cochlea by the vertebrate PCP pathway. *Nat. Genet.* **37**, 980–985 (2005).
65. McKenzie, E., Krupin, A. & Kelley, M. W. Cellular Growth and Rearrangement during the Development of the Mammalian Organ of Corti. *Dev. Dyn.* **229**, 802–812 (2004).
66. Anagnostopoulos, A. V. A compendium of mouse knockouts with inner ear defects. *Trends Genet.* **18**, 21–38 (2002).
67. Merlo, G. R. *et al.* The Dlx5 homeobox gene is essential for vestibular morphogenesis in the mouse embryo through a BMP4-mediated pathway. *Dev. Biol.* **248**, 157–169 (2002).
68. Acampora, D. *et al.* Craniofacial, vestibular and bone defects in mice lacking the Distal-less-related gene Dlx5. *Development* **126**, 3795–809 (1999).
69. Hadrys, T., Braun, T., Rinkwitz-Brandt, S., Arnold, H.-H. & Bober, E. Nkx5-1 controls semicircular canal formation in the mouse inner ear. *Development* **125**, 33–99 (1998).
70. Wang, W., Chan, E. K., Baron, S., Van de Water, T. & Lufkin, T. Hmx2 homeobox gene control of murine vestibular morphogenesis. *Development* **128**, 5017–5029 (2001).
71. Lin, Z., Cantos, R., Patente, M. & Wu, D. K. Gbx2 is required for the morphogenesis of the mouse inner ear: a downstream candidate of hindbrain signaling. *Development* **132**, 2309–18 (2005).
72. Urness, L. D., Wang, X., Shibata, S., Ohyama, T. & Mansour, S. L. Fgf10 is required for specification of non-sensory regions of the cochlear epithelium. *Dev. Biol.* **400**, 59–71 (2015).
73. Morsli, H. *et al.* Otx1 and Otx2 activities are required for the normal development of the mouse inner ear. *Development* **126**, 2335–43 (1999).
74. Burton, Q., Cole, L. K., Mulheisen, M., Chang, W. & Wu, D. K. The role of Pax2 in mouse inner ear development. *Dev. Biol.* **272**, 161–175 (2004).
75. Torres, M., Gómez-Pardo, E. & Gruss, P. Pax2 contributes to inner ear patterning and optic nerve trajectory. *Development* **122**, 3381–3391 (1996).
76. Arnold, J. S. *et al.* Tissue-specific roles of Tbx1 in the development of the outer, middle and inner ear, defective in 22q11DS patients. *Hum. Mol. Genet.* **15**, 1629–1639 (2006).
77. Jerome, L. A. & Papaioannou, V. E. DiGeorge syndrome phenotype in mice mutant for the T-box gene, Tbx1. *Nat. Genet.* **27**, 286–91 (2001).
78. Xu, H. *et al.* Tbx1 regulates population, proliferation and cell fate determination of otic epithelial cells. *Dev. Biol.* **302**, 670–682 (2007).
79. Moraes, F., Nóvoa, A., Jerome-Majewska, L. A., Papaioannou, V. E. & Mallo, M. Tbx1 is required for proper neural crest migration and to stabilize spatial patterns during middle and inner ear development. *Mech. Dev.* **122**, 199–212 (2005).
80. Koo, S. K. *et al.* Lmx1a maintains proper neurogenic, sensory, and non-sensory domains in the mammalian inner ear. *Dev. Biol.* **333**, 14–25 (2009).
81. Steffes, G. *et al.* Mutanlallemand (mtl) and Belly Spot and Deafness (bsd) Are Two New Mutations of Lmx1a Causing Severe Cochlear and Vestibular Defects. *PLoS One* **7**, 1–19 (2012).
82. Ohyama, T. & Groves, A. K. Generation of Pax2-Cre mice by modification of a Pax2 bacterial artificial chromosome. *genesis* **38**, 195–9 (2004).
83. Evsen, L., Sugahara, S., Uchikawa, M., Kondoh, H. & Wu, D. K. Progression of Neurogenesis in the Inner Ear Requires Inhibition of Sox2 Transcription by Neurogenin1 and Neurod1. *J. Neurosci.* **33**, 3879–3890 (2013).

84. Neves, J., Uchikawa, M., Bigas, A. & Giraldez, F. The prosensory function of Sox2 in the chicken inner ear relies on the direct regulation of Atoh1. *PLoS One* **7**, e30871 (2012).
85. Neves, J., Parada, C., Chamizo, M. & Giraldez, F. Jagged 1 regulates the restriction of Sox2 expression in the developing chicken inner ear: a mechanism for sensory organ specification. *Development* **138**, 735–744 (2011).
86. Puligilla, C., Dabdoub, A., Brenowitz, S. D. & Kelley, M. W. Sox2 induces neuronal formation in the developing mammalian cochlea. *J. Neurosci.* **30**, 714–722 (2010).
87. Steevens, A. R., Sookiasian, D. L., Glatzer, J. C. & Kiernan, A. E. SOX2 is required for inner ear neurogenesis. *Sci. Rep.* **7**, 1–11 (2017).
88. Ma, Q., Chen, Z., Barrantes, I. D. B., De La Pompa, J. L. & Anderson, D. J. Neurogenin1 Is Essential for the Determination of Neuronal Precursors for Proximal Cranial Sensory Ganglia. *Neuron* **20**, 469–482 (1998).
89. Liu, M. *et al.* Essential role of BETA2/NeuroD1 in development of the vestibular and auditory systems. *Genes Dev.* **14**, 2839–2854 (2000).
90. Brooker, R., Hozumi, K. & Lewis, J. Notch ligands with contrasting functions: Jagged1 and Delta1 in the mouse inner ear. *Development* **133**, 1277–1286 (2006).
91. Daudet, N., Ariza-McNaughton, L. & Lewis, J. Notch signalling is needed to maintain, but not to initiate, the formation of prosensory patches in the chick inner ear. *Development* **134**, 2369–2378 (2007).
92. Krüger, M., Schmid, T., Krüger, S., Bober, E. & Braun, T. Functional redundancy of NSCL-1 and NeuroD during development of the petrosal and vestibulocochlear ganglia. *Eur. J. Neurosci.* **24**, 1581–1590 (2006).
93. Deng, M., Yang, H., Xie, X., Liang, G. & Gan, L. Comparative expression analysis of POU4F1, POU4F2 and ISL1 in developing mouse cochleovestibular ganglion neurons. *Gene Expr. Patterns* **15**, 31–37 (2014).
94. Raft, S. *et al.* Cross-regulation of Ngn1 and Math1 coordinates the production of neurons and sensory hair cells during inner ear development. *Development* **134**, 4405–4415 (2007).
95. Xu, H., Chen, L. & Baldini, A. In vivo genetic ablation of the periotic mesoderm affects cell proliferation survival and differentiation in the cochlea. *Dev. Biol.* **310**, 329–340 (2007).
96. Dabdoub, A. *et al.* Sox2 signaling in prosensory domain specification and subsequent hair cell differentiation in the developing cochlea. *Proc. Natl. Acad. Sci. U. S. A.* **105**, 18396–401 (2008).
97. Kiernan, A. E. *et al.* Sox2 is required for sensory organ development in the mammalian inner ear. *Nature* **434**, 1031–1035 (2005).
98. Chen, P. & Segil, N. p27Kip1 links cell proliferation to morphogenesis in the developing organ of Corti. *Development* **126**, 1581–1590 (1999).
99. Lee, Y.-S., Liu, F. & Segil, N. A morphogenetic wave of p27Kip1 transcription directs cell cycle exit during organ of Corti development. *Development* **133**, 2817–2826 (2006).
100. Chen, P., Johnson, J. E., Zoghbi, H. Y. & Segil, N. The role of Math1 in inner ear development: Uncoupling the establishment of the sensory primordium from hair cell fate determination. *Development* **129**, 2495–2505 (2002).
101. Lanford, P. J., Shailam, R., Norton, C. R., Gridley, T. & Kelley, M. W. Expression of Math1 and HES5 in the cochleae of wildtype and Jag2 mutant mice. *JARO* **1**, 161–171 (2000).
102. Tateya, T. *et al.* Three-dimensional live imaging of Atoh1 reveals the dynamics of hair cell induction and organization in the developing cochlea. *Development* **146**, (2019).
103. Driver, E. C., Sillers, L., Coate, T. M., Rose, M. F. & Kelley, M. W. The Atoh1-lineage gives rise to hair cells and supporting cells within the mammalian cochlea. *Dev. Biol.* **376**, 86–98 (2013).
104. Woods, C., Montcouquiol, M. & Kelley, M. W. Math1 regulates development of the sensory epithelium in the mammalian cochlea. *Nat. Neurosci.* **7**, 1310–8 (2004).
105. Zheng, J. L. & Gao, W.-Q. Overexpression of Math1 induces robust production of extra hair cells in postnatal rat inner ears. *Nat. Neurosci.* **3**, 580–586 (2000).
106. Bermingham, N. A. *et al.* Math1: An Essential Gene for the Generation of Inner Ear Hair Cells. *Science* (80-.). **284**, 1837–1841 (1999).
107. Cai, T., Seymour, M. L., Zhang, H., Pereira, F. A. & Groves, A. K. Conditional Deletion of Atoh1 Reveals Distinct Critical Periods for Survival and Function of Hair Cells in the Organ of Corti. *J. Neurosci.* **33**, 10110–10122 (2013).
108. Lanford, P. J. *et al.* Notch signalling pathway mediates hair cell development in mammalian cochlea. *Nat. Genet.* **21**, 289–92 (1999).
109. Morrison, A., Hodgetts, C., Gossler, A., Hrabé de Angelis, M. & Lewis, J. Expression of Delta1 and Serrate1 (Jagged1) in the mouse inner ear. *Mech. Dev.* **84**, 169–72 (1999).
110. Kiernan, A. E., Cordes, R., Kopan, R., Gossler, A. & Gridley, T. The Notch ligands DLL1 and JAG2 act synergistically to regulate hair cell development in the mammalian inner ear. *Development* **132**, 4353–4362 (2005).

111. Abdolazimi, Y., Stojanova, Z. & Segil, N. Selection of cell fate in the organ of Corti involves the integration of Hes/Hey signaling at the Atoh1 promoter. *Development* **143**, 841–850 (2016).
112. Doetzlhofer, A. *et al.* Hey2 Regulation by FGF Provides a Notch-Independent Mechanism for Maintaining Pillar Cell Fate in the Organ of Corti. *Dev. Cell* **16**, 58–69 (2009).
113. Li, S. *et al.* Hey2 functions in parallel with Hes1 and Hes5 for mammalian auditory sensory organ development. *BMC Dev. Biol.* **8**, 1–13 (2008).
114. Zine, A. *et al.* Hes1 and Hes5 activities are required for the normal development of the hair cells in the mammalian inner ear. *J. Neurosci.* **21**, 4712–4720 (2001).
115. Hayashi, T., Cunningham, D. & Bermingham-McDonogh, O. Loss of Fgfr3 leads to excess hair cell development in the mouse organ of Corti. *Dev. Dyn.* **236**, 525–533 (2007).
116. Jacques, B. E., Montcouquiol, M. E., Layman, E. M., Lewandoski, M. & Kelley, M. W. Fgf8 induces pillar cell fate and regulates cellular patterning in the mammalian cochlea. *Development* **134**, 3021–3029 (2007).
117. Kolla, L. *et al.* Characterization of the development of the mouse cochlear epithelium at the single cell level. *Nat. Commun.* **11**, 2389 (2020).
118. Shim, K., Minowada, G., Coling, D. E. & Martin, G. R. Sprouty2, a mouse deafness gene, regulates cell fate decisions in the auditory sensory epithelium by antagonizing FGF signaling. *Dev. Cell* **8**, 553–64 (2005).
119. Pannier, S. *et al.* Activating Fgfr3 Y367C mutation causes hearing loss and inner ear defect in a mouse model of chondrodysplasia. *Biochim. Biophys. Acta* **1792**, 140–147 (2009).
120. Mansour, S. L. *et al.* Hearing loss in a mouse model of Muenke syndrome. *Hum. Mol. Genet.* **18**, 43–50 (2009).
121. Mansour, S. L., Li, C. & Urness, L. D. Genetic rescue of Muenke syndrome model hearing loss reveals prolonged FGF-dependent plasticity in cochlear supporting cell fates. *Genes Dev.* **27**, 2320–2331 (2013).
122. Puligilla, C. *et al.* Disruption of fibroblast growth factor receptor 3 signaling results in defects in cellular differentiation, neuronal patterning, and hearing impairment. *Dev. Dyn.* **236**, 1905–1917 (2007).
123. Mueller, K. L., Jacques, B. E. & Kelley, M. W. Fibroblast growth factor signaling regulates pillar cell development in the organ of Corti. *J. Neurosci.* **22**, 9368–9377 (2002).
124. Lorenzen, S. M., Duggan, A., Osipovich, A. B., Magnuson, M. A. & García-Añoveros, J. Insm1 promotes neurogenic proliferation in delaminated otic progenitors. *Mech. Dev.* **138**, 233–245 (2015).
125. Wiwatpanit, T. *et al.* Trans-differentiation of outer hair cells into inner hair cells in the absence of INSM1. *Nature* **563**, 691–695 (2018).
126. Chessum, L. *et al.* Helios is a key transcriptional regulator of outer hair cell maturation. *Nature* **563**, 696–724 (2018).
127. Frasch, M. *T-box Genes in Development*. (Academic Press (imprint of Elsevier), 2017).
128. Papaioannou, V. E. The T-box gene family: emerging roles in development, stem cells and cancer. *Development* **141**, 3819–3833 (2014).
129. Naiche, L. A., Harrelson, Z., Kelly, R. G. & Papaioannou, V. E. T-Box Genes in Vertebrate Development. *Annu. Rev. Genet.* **39**, 219–239 (2005).
130. Trowe, M.-O., Maier, H., Schweizer, M. & Kispert, A. Deafness in mice lacking the T-box transcription factor Tbx18 in otic fibrocytes. *Development* **135**, 1725–1734 (2008).
131. Tian, C. & Johnson, K. R. TBX1 is required for normal stria vascularis and semicircular canal development. *Dev. Biol.* **457**, 91–103 (2020).
132. Braunstein, E. M., Monks, D. C., Aggarwal, V. S., Arnold, J. S. & Morrow, B. E. Tbx1 and Brn4 regulate retinoic acid metabolic genes during cochlear morphogenesis. *BMC Dev. Biol.* **9**, 31 (2009).
133. Chapman, D. L. *et al.* Expression of the T-box family genes, Tbx1-Tbx5, during early mouse development. *Dev. Dyn.* **206**, 379–390 (1996).
134. Bollag, R. J. *et al.* An ancient family of embryonically expressed mouse genes sharing a conserved protein motif with the T locus. *Nature* **8**, 340–344 (1994).
135. Mesbah, K. *et al.* Identification of a Tbx1/Tbx2/Tbx3 genetic pathway governing pharyngeal and arterial pole morphogenesis. *Hum. Mol. Genet.* **21**, 1217–1229 (2012).
136. Gibson-Brown, J. J., I. Agulnik, S., Silver, L. M. & Papaioannou, V. E. Expression of T-box genes Tbx2-Tbx5 during chick organogenesis. *Mech. Dev.* **74**, 165–169 (1998).
137. Law, D. J., Gebuhr, T., Garvey, N., Agulnik, S. I. & Silver, L. M. Identification, characterization, and localization to Chromosome 17q21-22 of the human TBX2 homolog, member of a conserved developmental gene family. *Mamm. Genome* **6**, 793–797 (1995).
138. Lingbeek, M. E., Jacobs, J. J. L. & Van Lohuizen, M. The T-box repressors TBX2 and TBX3 specifically regulate the tumor suppressor gene p14ARF via a variant T-site in the initiator. *J. Biol. Chem.* **277**, 26120–26127 (2002).
139. Lüdtke, T. H.-W. *et al.* Tbx2 Controls Lung Growth by Direct Repression of the Cell Cycle Inhibitor

- Genes *Cdkn1a* and *Cdkn1b*. *PLoS Genet.* **9**, e1003189 (2013).
140. Wang, B. *et al.* The T Box Transcription Factor TBX2 Promotes Epithelial-Mesenchymal Transition and Invasion of Normal and Malignant Breast Epithelial Cells. *PLoS One* **7**, e41355 (2012).
 141. Cho, G.-S., Park, D.-S., Choi, S.-C. & Han, J.-K. Tbx2 regulates anterior neural specification by repressing FGF signaling pathway. *Dev. Biol.* **421**, 183–193 (2017).
 142. Jacobs, J. J. L. *et al.* Senescence bypass screen identifies TBX2, which represses *Cdkn2a* (p19(ARF)) and is amplified in a subset of human breast cancers. *Nat. Genet.* **26**, 291–299 (2000).
 143. Rodriguez, M., Aladowicz, E., Lanfrancone, L. & Goding, C. R. Tbx3 represses E-cadherin expression and enhances melanoma invasiveness. *Cancer Res.* **68**, 7872–7881 (2008).
 144. Davenport, T. G., Jerome-Majewska, L. A. & Papaioannou, V. E. Mammary gland, limb and yolk sac defects in mice lacking Tbx3, the gene mutated in human ulnar mammary syndrome. *Development* **130**, 2263–2273 (2003).
 145. Harrelson, Z. *et al.* Tbx2 is essential for patterning the atrioventricular canal and for morphogenesis of the outflow tract during heart development. *Development* **131**, 5041–5052 (2004).
 146. Bamshad, M. *et al.* Mutations in human TBX3 alter limb, apocrine and genital development in ulnar-mammary syndrome. *Nat. Genet.* **16**, 311–315 (1997).
 147. Liu, N. *et al.* Functional variants in TBX2 are associated with a syndromic cardiovascular and skeletal developmental disorder. *Hum. Mol. Genet.* **27**, 2454–2465 (2018).
 148. Nimmakayalu, M. *et al.* Microdeletion of 17q22q23.2 Encompassing TBX2 and TBX4 in a Patient With Congenital Microcephaly, Thyroid Duct Cyst, Sensorineural Hearing Loss, and Pulmonary Hypertension. *Am. J. Med. Genet.* 418–423 (2010). doi:10.1002/ajmg.a.33827
 149. Ballif, B. C. *et al.* Identification of a recurrent microdeletion at 17q23.1q23.2 flanked by segmental duplications associated with heart defects and limb abnormalities. *Am. J. Hum. Genet.* **86**, 454–61 (2010).
 150. Christoffels, V. M. *et al.* T-box transcription factor Tbx2 represses differentiation and formation of the cardiac chambers. *Dev. Dyn.* **229**, 763–770 (2004).
 151. Behesti, H., Papaioannou, V. E. & Sowden, J. C. Loss of Tbx2 delays optic vesicle invagination leading to small optic cups. *Dev. Biol.* **333**, 360–372 (2009).
 152. Singh, R. *et al.* Tbx2 and Tbx3 induce atrioventricular myocardial development and endocardial cushion formation. *Cell. Mol. Life Sci.* **69**, 1377–1389 (2012).
 153. Aydoğdu, N. *et al.* TBX2 and TBX3 act downstream of canonical WNT signaling in patterning and differentiation of the mouse ureteric mesenchyme. *Development* **145**, (2018).
 154. Kaiser, M. Funktionelle Analyse der T-Box Transkriptionsfaktoren Tbx2 und Tbx3 in der Entwicklung des murinen Innenohrs. (Gottfried Wilhelm Leibniz Universität Hannover, 2013).
 155. Kaiser, M. Funktionelle Analyse der T-Box Transkriptionsfaktoren Tbx2 und Tbx3 in der Morphogenese des Innenohrs der Maus. (Medizinischen Hochschule Hannover, 2015).
 156. Wojahn, I. Phänotypische Charakterisierung der Innenohrentwicklung bei Tbx2 und Tbx3 mutanten Mäusen. (Gottfried Wilhelm Leibniz Universität in Hannover, 2013).
 157. Arnold, K. *et al.* Sox2 + adult stem and progenitor cells are important for tissue regeneration and survival of mice. *Cell Stem Cell* **9**, 317–329 (2011).
 158. Machold, R. & Fishell, G. Math1 is expressed in temporally discrete pools of cerebellar rhombic-lip neural progenitors. *Neuron* **48**, 17–24 (2005).
 159. Adamska, M. *et al.* FGFs control the patterning of the inner ear but are not able to induce the full ear program. *Mech. Dev.* **109**, 303–313 (2001).
 160. Tümpel, S. *et al.* Regulation of Tbx3 Expression by Anteroposterior Signalling in Vertebrate Limb Development. *Dev. Biol.* **250**, 251–262 (2002).
 161. Klaus, A., Saga, Y., Taketo, M. M., Tzahor, E. & Birchmeier, W. Distinct roles of Wnt/ β -catenin and Bmp signaling during early cardiogenesis. *Proc. Natl. Acad. Sci.* **104**, 18531–18536 (2007).
 162. Suzuki, T., Takeuchi, J., Koshiba-Takeuchi, K. & Ogura, T. Tbx Genes Specify Posterior Digit Identity through Shh and BMP Signaling. *Dev. Cell* **6**, 43–53 (2004).
 163. Schliermann, A. & Nickel, J. Unraveling the Connection between Fibroblast Growth Factor and Bone Morphogenetic Protein Signaling. *Int. J. Mol. Sci.* **19**, (2018).
 164. Costa, A. *et al.* Generation of sensory hair cells by genetic programming with a combination of transcription factors. *Development* **142**, 1948–1959 (2015).

Acknowledgement

First of all, I want to thank Prof. Dr. Andreas Kispert for his never-ending trust in my abilities as a scientist and for the opportunity to continue working in his lab on this amazing project after my bachelor and master theses. Also, for his critical input and discussions, and for the encouraging words during the difficult phases of my work. And of course, for his expertise and help in writing the two manuscripts.

I want to thank my supervisor Dr. Mark-Oliver Trowe for this amazing project, for all the patience and the time he invested in my training and for all the reminders “Sure, you can” each time I said “I can’t”. For all the schemes he drew to make certain connections clear to me and for all the encouragements. He is the best teacher and supervisor one can wish for!

I would like to thank Prof. Dr. Doris Steinemann and Prof. Dr. Hans Gerd Nothwang for the kind acceptance to be the examiners of my thesis, Prof. Dr. Hansjörg Küster for accepting the duty as the chair of my disputation and Prof. Dr. Anaclet Ngezahayo for taking on this task at a very short notice.

I would like to thank Prof. Dr. Achim Gossler for his support and the composure during the worst of times for the institute and all the members. And a special thank you for the editing of the second manuscript.

I would like to thank Dr. Carsten Rudat, Dr. Lena Tveriakhina and Dr. Irina Wojahn for their help with editing my thesis and for all the encouraging conversations which helped a lot in keeping me going!

I would like to thank all the members of the lab and the department for all the help and support they gave me in the past six years. And a special thank you to my girls (Irina, Jenny, Lena and Fairouz) for all the funny times in and outside the lab and for being my cheerleaders during the difficult times.

Last but not least, I would like to thank my family, especially my mom, for their constant support and unconditional love. Without you, I would never have come this far!

THANK YOU

Appendix

Curriculum Vitae

Personal information

Name: Marina Kaiser
 Date of birth: 01.03.1987
 Place of birth: Magnitogorsk
 Citizenship: German
 Email: marinakaiser3@gmx.de

School education

1994 – 1998 Mittelschule, Magnitogorsk
 1998 – 1999 Andreas Fack Regelschule, Kaltennordheim
 2000 – 2001 Werratschule, Bad Salzungen
 2001 – 2004 Robert-Koch-Realschule, Langenhagen (Sekundarabschluss I)
 2004 – 2007 Gymnasium Langenhagen (Abitur)

Professional education

2007 – 2010 Hannover Medical School, Hannover, Germany
Medical-technical laboratory assistant (technician)
 Main subjects: histology/cytology, clinical chemistry, hematology, microbiology

University studies

2010 – 2013 Gottfried Wilhelm Leibniz Universität Hannover, Hannover, Germany
Bachelor of Science (B. Sc.) in Biology
 Thesis topic: “Functional analysis of the T-box transcription factors *Tbx2* and *Tbx3* in the development of the inner ear in mice”

2013 – 2015 Hannover Medical School, Hannover, Germany
Master of Science (M.Sc.), Master of Biomedicine
 Thesis topic: “Functional Analysis of the T-box transcription factors *Tbx2* and *Tbx3* in the morphogenesis of the murine inner ear”

2015 – present Hannover Medical School, Hannover, Germany
PhD student in Developmental and Molecular Biology

List of publications

Kaiser, M., Wojahn, I., Rudat, C., Lüdtke, T. H., Christoffels, V. M., Moon, A., Kispert, A., & Trowe, M.-O. (2021). Regulation of otocyst patterning by *Tbx2* and *Tbx3* is required for inner ear morphogenesis in the mouse. *Development*, 148(8).

<https://doi.org/10.1242/dev.195651>

Tsay, H. C., Yuan, Q., Balakrishnan, A., **Kaiser, M.**, Möbus, S., Kozdrowska, E., Farid, M., Tegtmeyer, P. K., Borst, K., Vondran, F. W. R., Kalinke, U., Kispert, A., Manns, M. P., Ott, M., & Sharma, A. D. (2019). Hepatocyte-specific suppression of microRNA-221-3p mitigates liver fibrosis. *The Journal of Hepatology*, 70(4), 722–734.

<https://doi.org/10.1016/j.jhep.2018.12.016>

Weiss, A., Bohnenpoll, T., Kurz, J., Blank, P., Airik, R., Lüdtke, T. H., Kleppa, M., Deuper, L., **Kaiser, M.**, Mamo, T. M., Costa, R., Hahn, T., Trowe, M., & Kispert, A. (2019). Delayed onset of smooth muscle cell differentiation leads to hydroureter formation in mice with conditional loss of the zinc finger transcription factor gene *Gata2* in the ureteric mesenchyme. *The Journal of Pathology*, 248(4), 452–463.

<https://doi.org/10.1002/path.5270>

Aydoğdu, N., Rudat, C., Trowe, M.-O., **Kaiser, M.**, Lüdtke, T. H., Taketo, M. M., Christoffels, V. M., Moon, A., & Kispert, A. (2018). TBX2 and TBX3 act downstream of canonical WNT signaling in patterning and differentiation of the mouse ureteric mesenchyme. *Development*, 145(23).

<https://doi.org/10.1242/dev.171827>